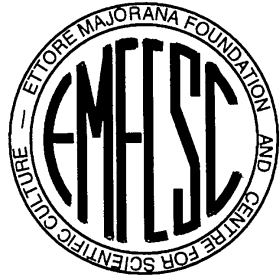


# Radio detection of extensive air showers

## Precision measurements of the properties of cosmic rays



«ETTORE MAJORANA» FOUNDATION AND CENTRE FOR SCIENTIFIC CULTURE

INTERNATIONAL SCHOOL OF COSMIC-RAY ASTROPHYSICS  
«MAURICE M. SHAPIRO»

*22<sup>nd</sup> Course: “From cosmic particles to gravitational waves: now and to come”*  
*30 July – 7 August 2022*

PRESIDENT AND DIRECTOR OF THE CENTRE: PROFESSOR A. ZICHICHI

DIRECTORS OF THE COURSE: PROFESSORS J.P. WEFEL, T. STANEV, J.R. HÖRANDEL



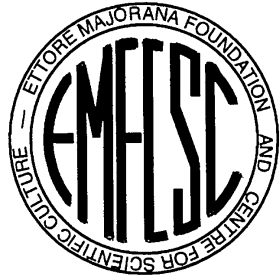
Nikhef





# Radio detection of extensive air showers

## Precision measurements of the properties of cosmic rays



«ETTORE MAJORANA» FOUNDATION AND CENTRE FOR SCIENTIFIC CULTURE

INTERNATIONAL SCHOOL OF COSMIC-RAY ASTROPHYSICS  
«MAURICE M. SHAPIRO»

*22<sup>nd</sup> Course: “From cosmic particles to gravitational waves: now and to come”*  
*30 July – 7 August 2022*

PRESIDENT AND DIRECTOR OF THE CENTRE: PROFESSOR A. ZICHICHI

DIRECTORS OF THE COURSE: PROFESSORS J.P. WEFEL, T. STANEV, J.R. HÖRANDEL



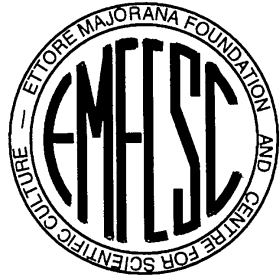
Nikhef





# Radio detection of extensive air showers

## Precision measurements of the properties of cosmic rays



«ETTORE MAJORANA» FOUNDATION AND CENTRE FOR SCIENTIFIC CULTURE

INTERNATIONAL SCHOOL OF COSMIC-RAY ASTROPHYSICS  
«MAURICE M. SHAPIRO»

*22<sup>nd</sup> Course: “From cosmic particles to gravitational waves: now and to come”*  
*30 July – 7 August 2022*

PRESIDENT AND DIRECTOR OF THE CENTRE: PROFESSOR A. ZICHICHI

DIRECTORS OF THE COURSE: PROFESSORS J.P. WEFEL, T. STANEV, J.R. HÖRANDEL



Nikhef

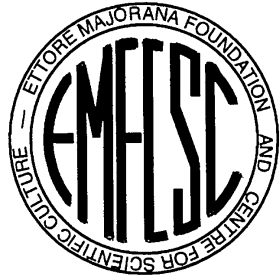


**characterize cosmic rays:**  
**-direction**  
**-energy**  
**-mass**  
**@100% duty cycle**



# Radio detection of extensive air showers

## Precision measurements of the properties of cosmic rays



«ETTORE MAJORANA» FOUNDATION AND CENTRE FOR SCIENTIFIC CULTURE

INTERNATIONAL SCHOOL OF COSMIC-RAY ASTROPHYSICS  
«MAURICE M. SHAPIRO»

*22<sup>nd</sup> Course: “From cosmic particles to gravitational waves: now and to come”*  
*30 July – 7 August 2022*

PRESIDENT AND DIRECTOR OF THE CENTRE: PROFESSOR A. ZICHICHI

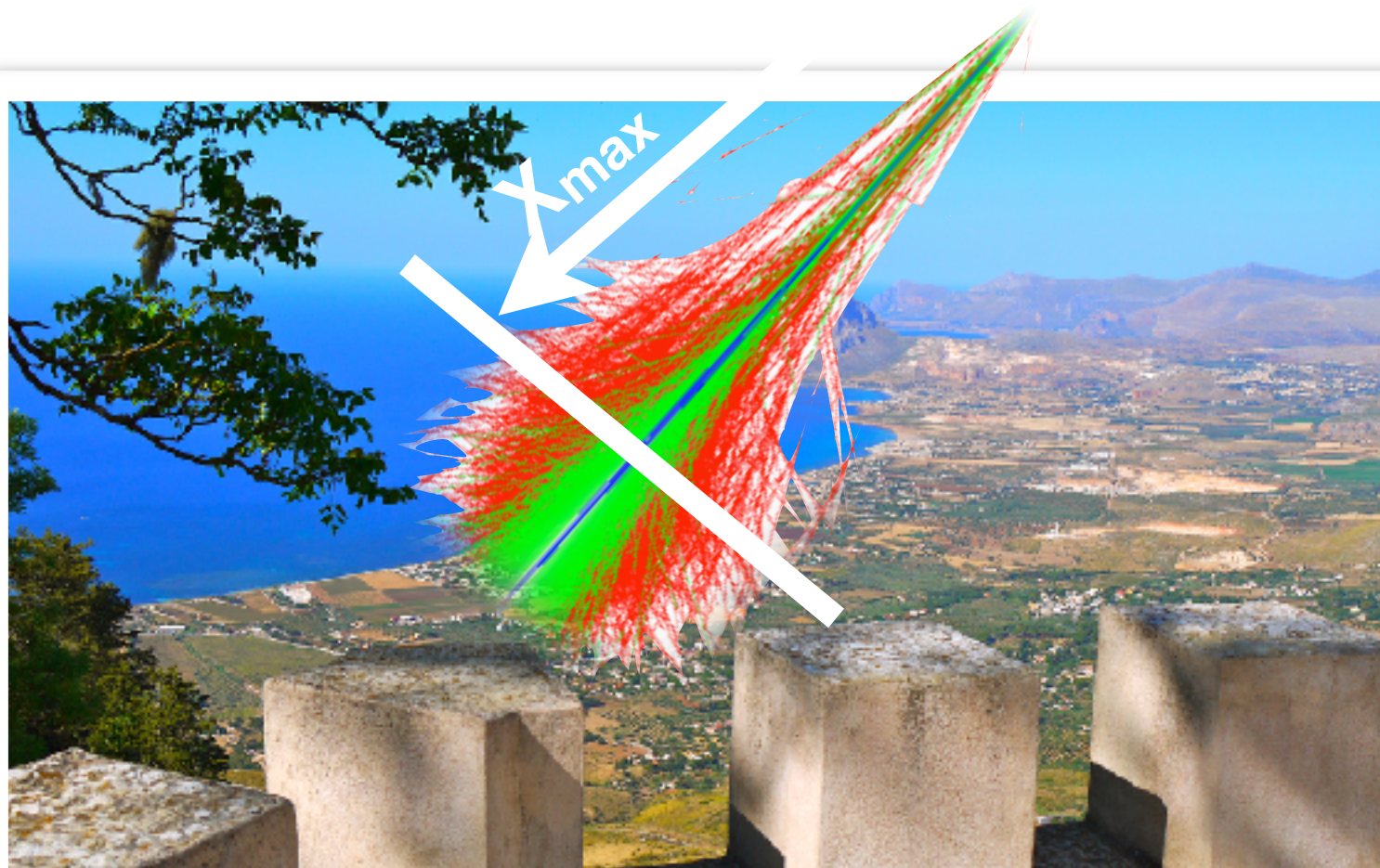
DIRECTORS OF THE COURSE: PROFESSORS J.P. WEFEL, T. STANEV, J.R. HÖRANDEL



Nikhef



VUB

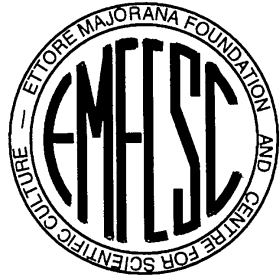


**characterize cosmic rays:**  
**-direction**  
**-energy**  
**-mass**  
**@100% duty cycle**



# Radio detection of extensive air showers

## Precision measurements of the properties of cosmic rays



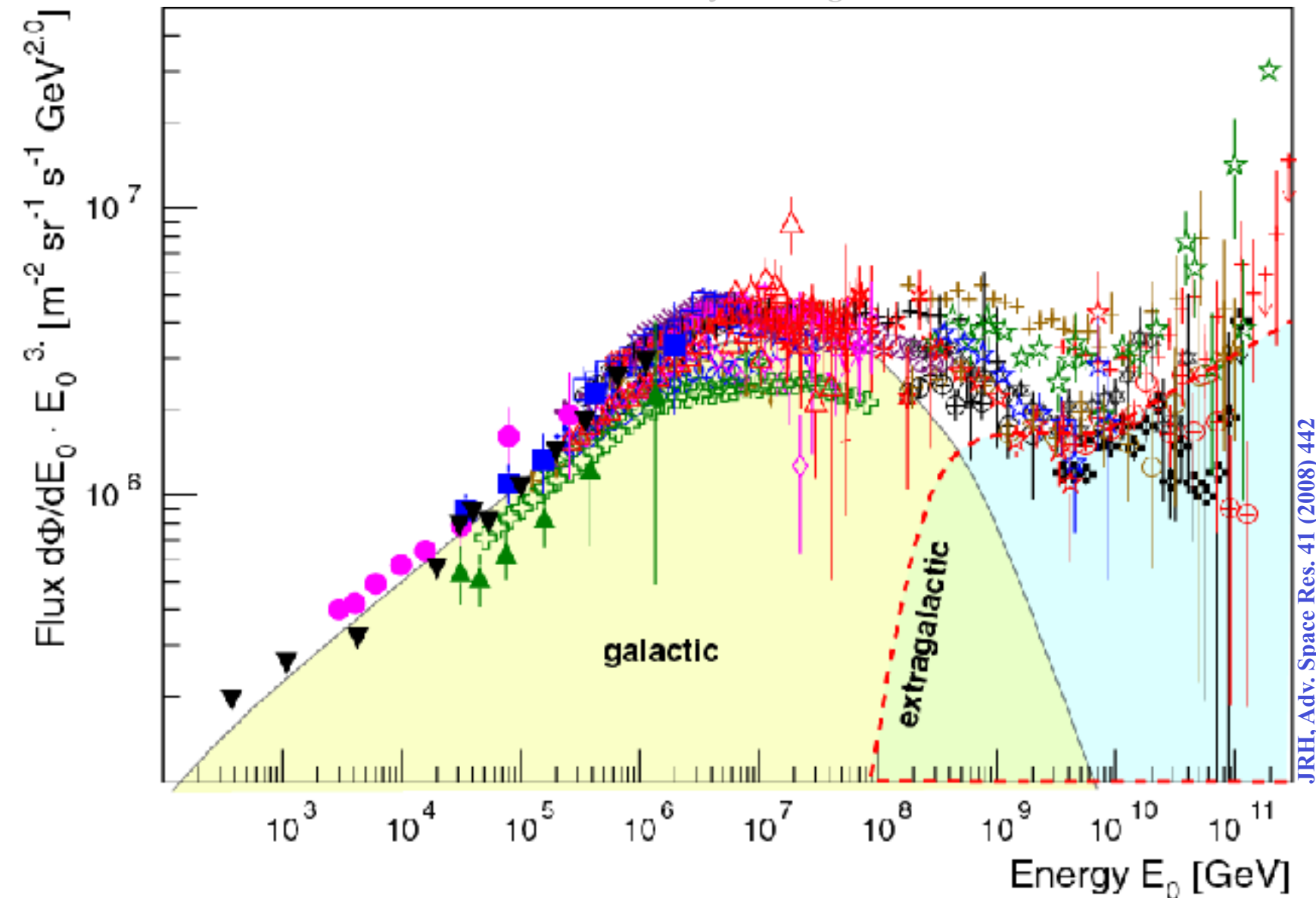
«ETTORE MAJORANA» FOUNDATION AND CENTRE FOR SCIENTIFIC CULTURE

INTERNATIONAL SCHOOL OF COSMIC-RAY ASTROPHYSICS  
«MAURICE M. SHAPIRO»



Nikhef

22<sup>nd</sup> Course: “From cosmic particles to gravitational waves: now and to come”  
30 July – 7 August 2022



**characterize cosmic rays:**  
-direction  
-energy  
-mass  
@100% duty cycle



# Radio detection of extensive air showers

## Precision measurements of the properties of cosmic rays



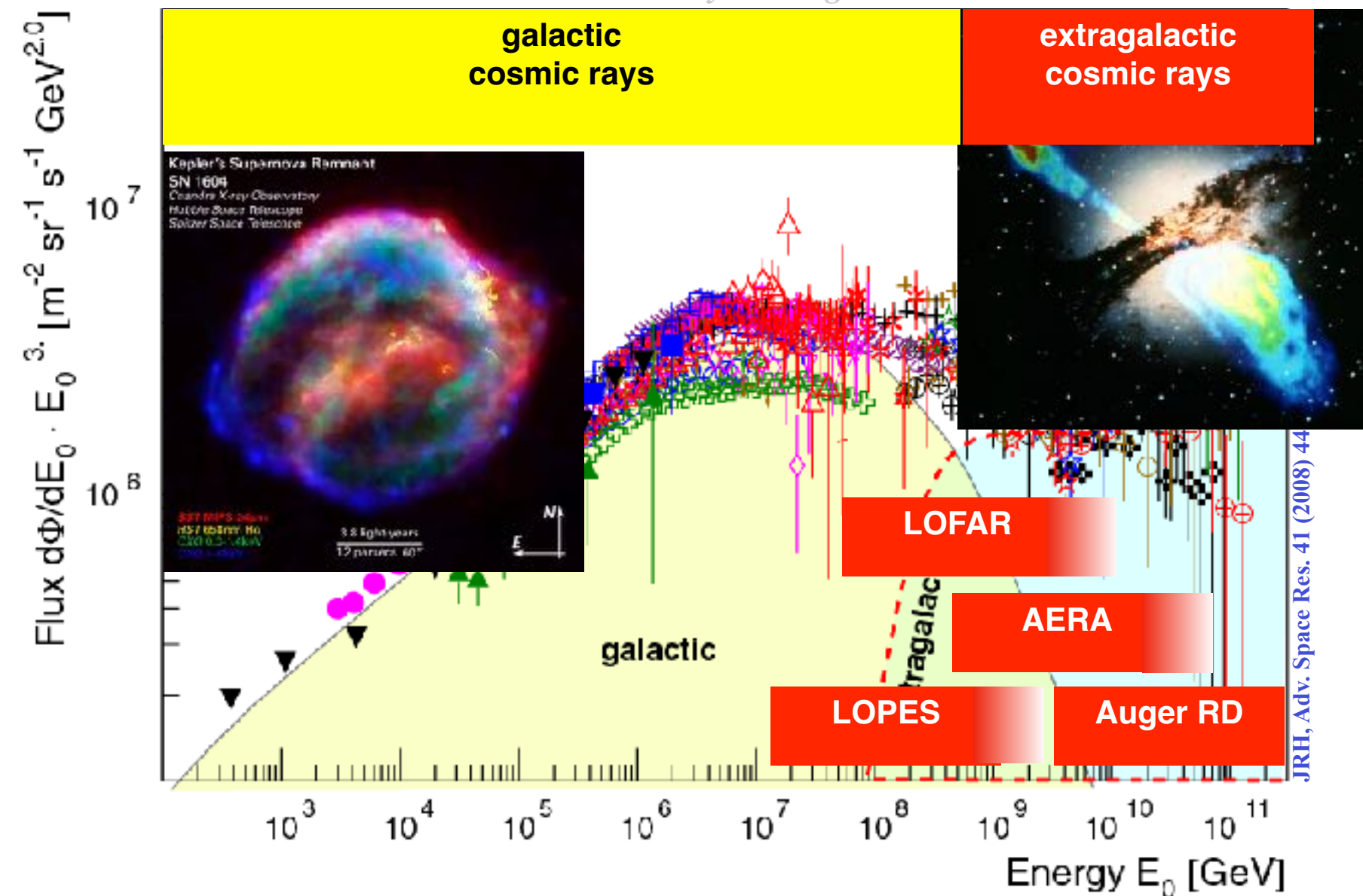
«ETTORE MAJORANA» FOUNDATION AND CENTRE FOR SCIENTIFIC CULTURE

INTERNATIONAL SCHOOL OF COSMIC-RAY ASTROPHYSICS  
«MAURICE M. SHAPIRO»



Nikhef

22<sup>nd</sup> Course: “From cosmic particles to gravitational waves: now and to come”  
30 July – 7 August 2022



**characterize cosmic rays:**  
-direction  
-energy  
-mass  
@100% duty cycle



# First radio detection of air showers 1965

Blackett's Field ~1967

Porter MSc

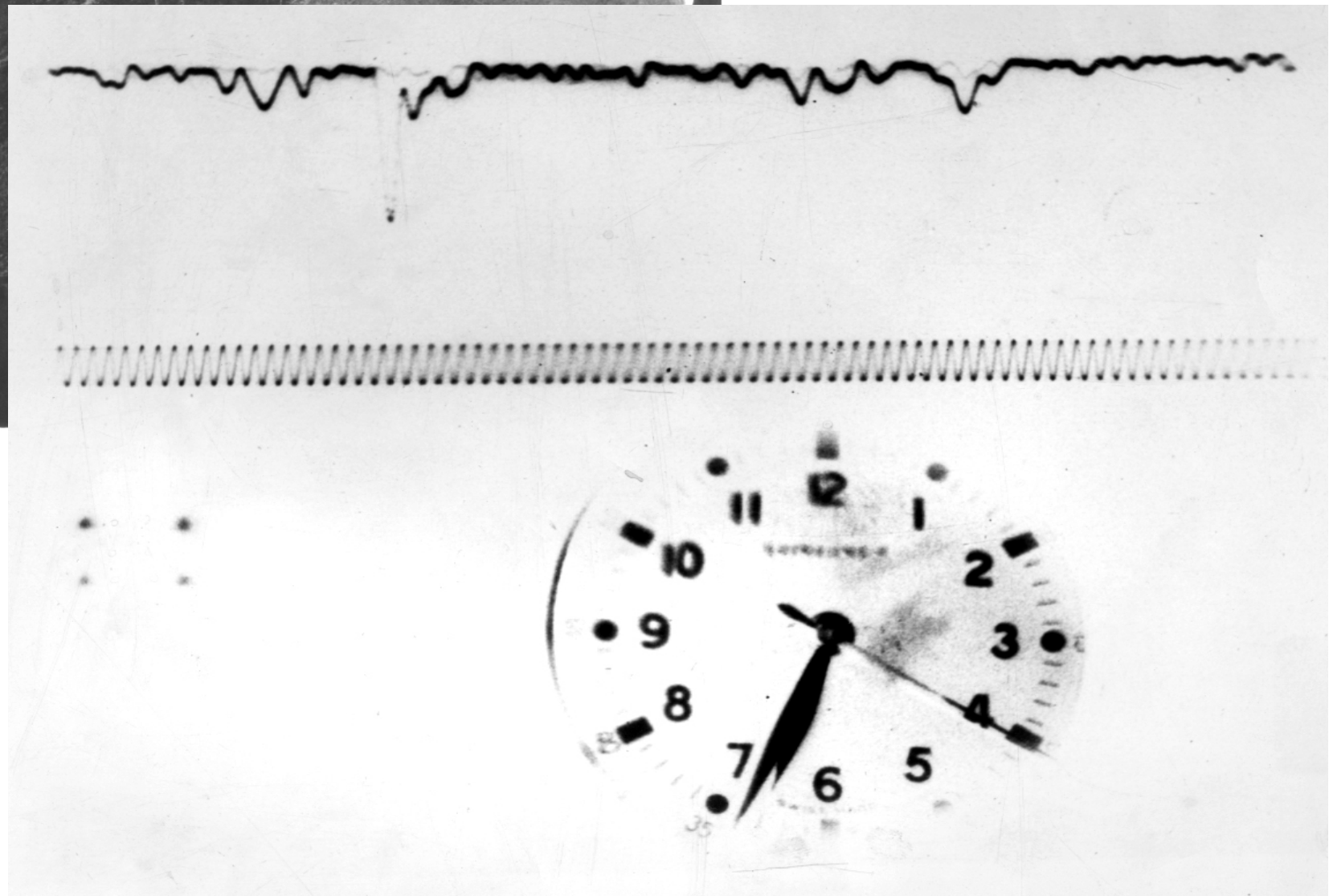
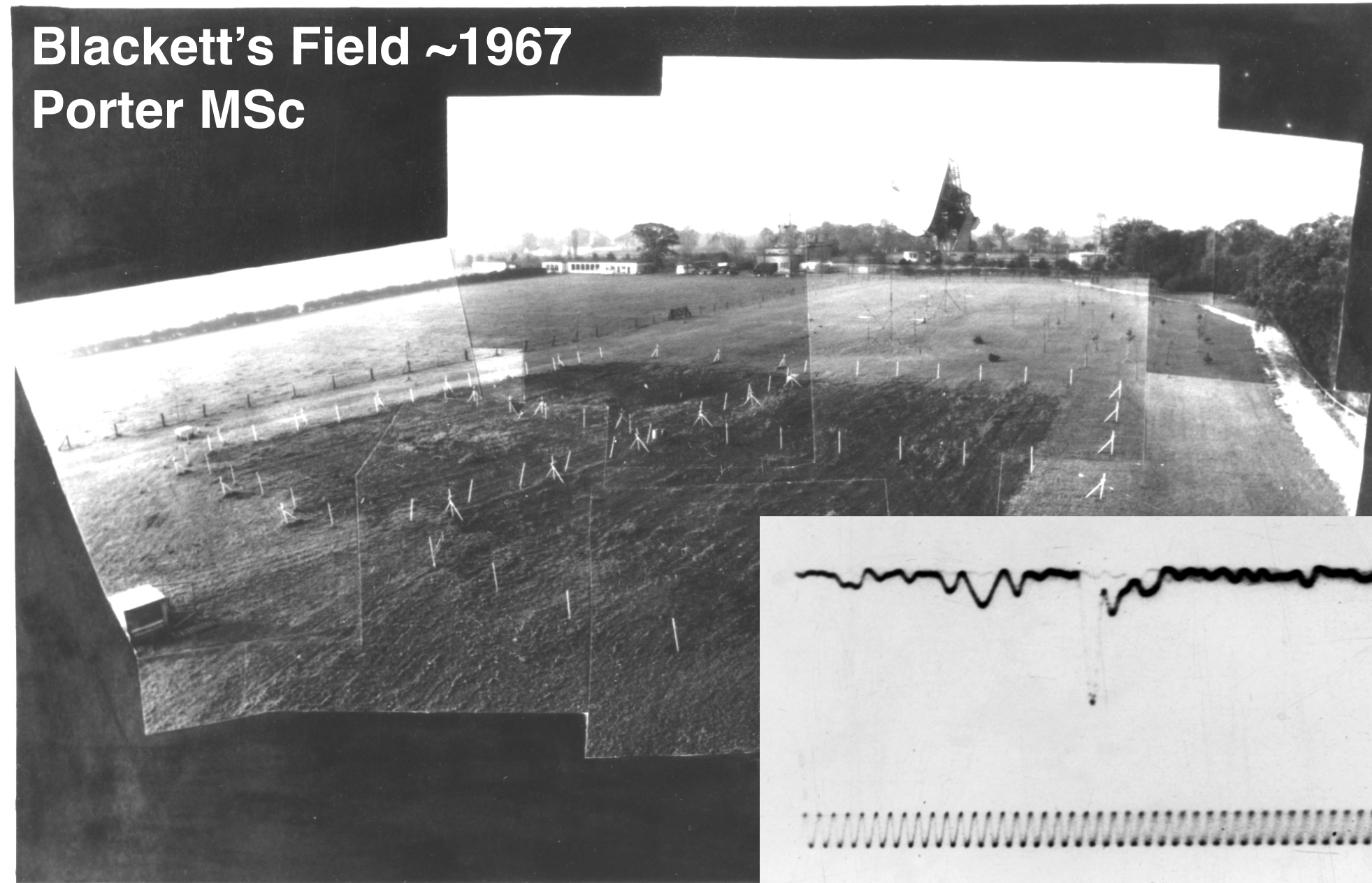




# First radio detection of air showers 1965

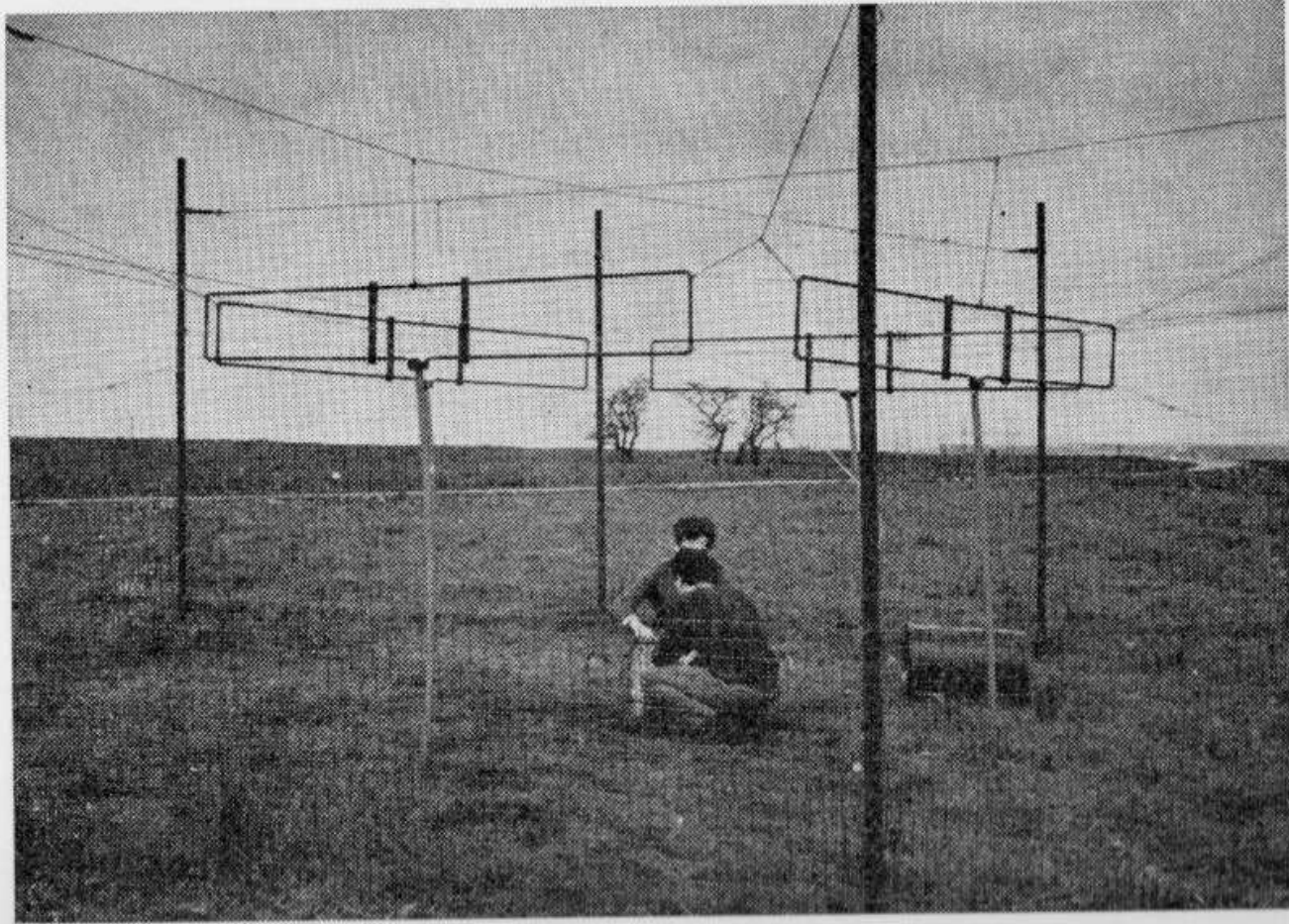
Blackett's Field ~1967

Porter MSc



Jelley et al Nature 1965  
R. A. Porter MSc Thesis 1967



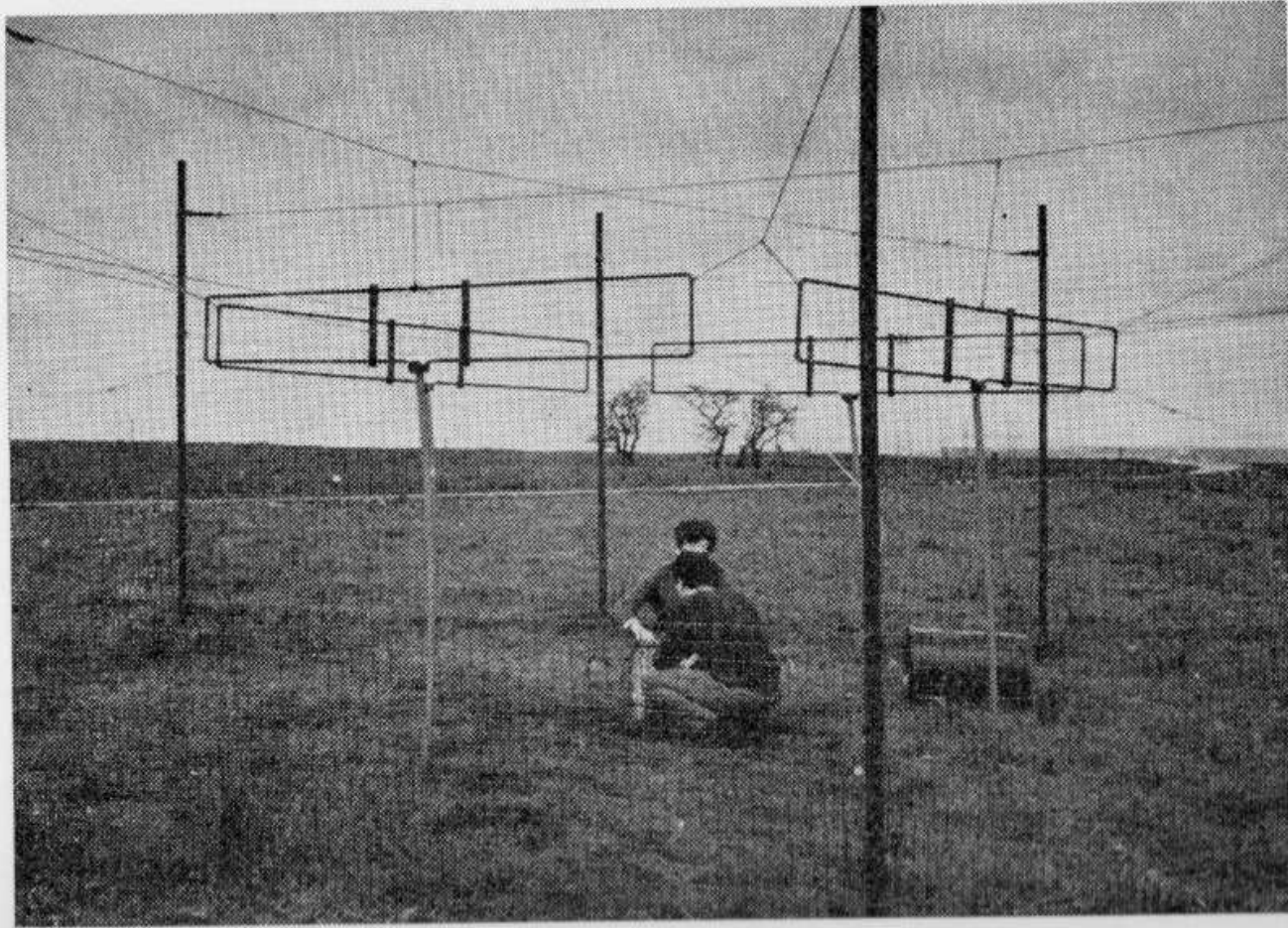


Recent receiving antennas (44 MHz) forming part of the Haverah Park Extensive Air Shower Array.



# Haverah Park (Leeds)

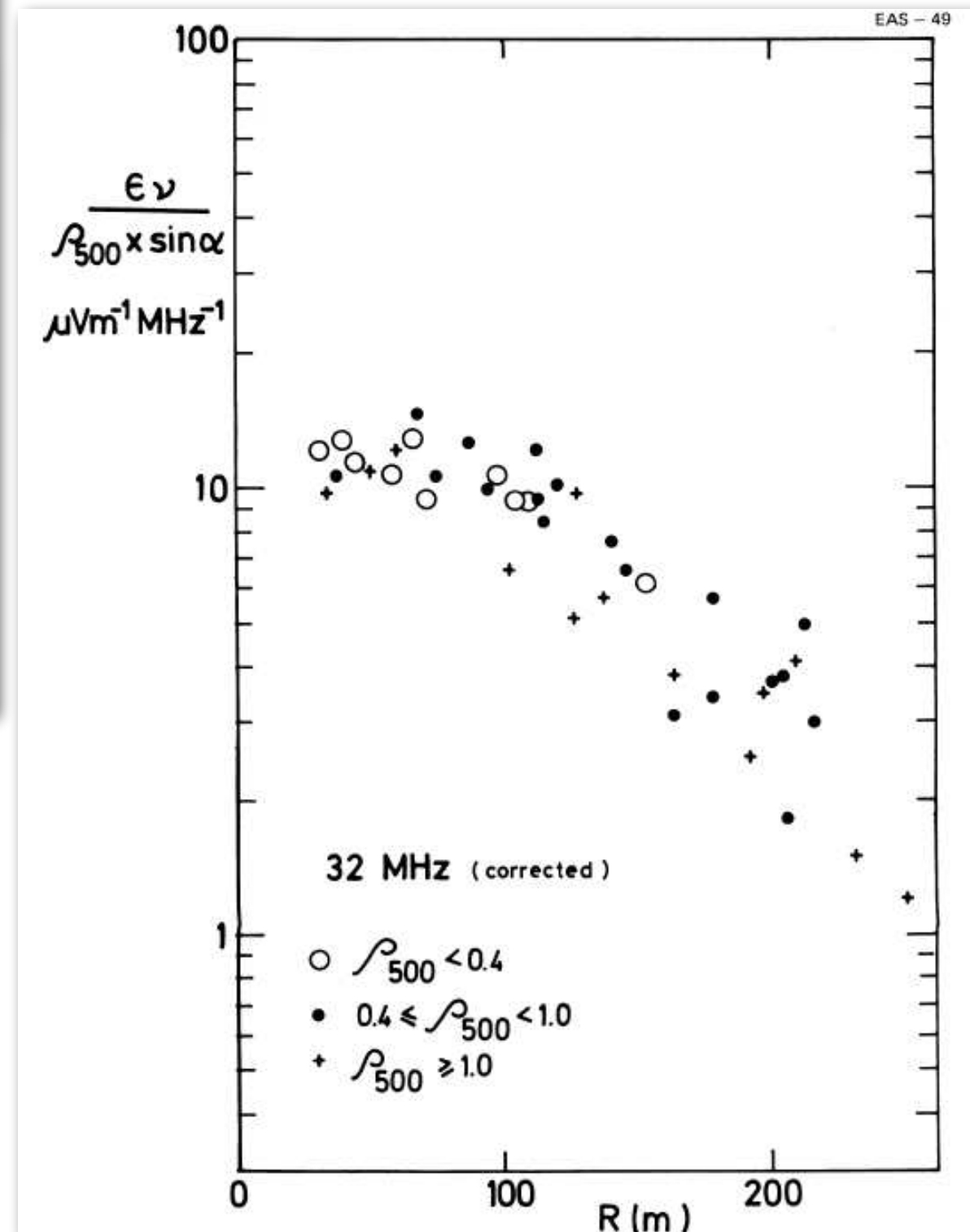
Allan 1971



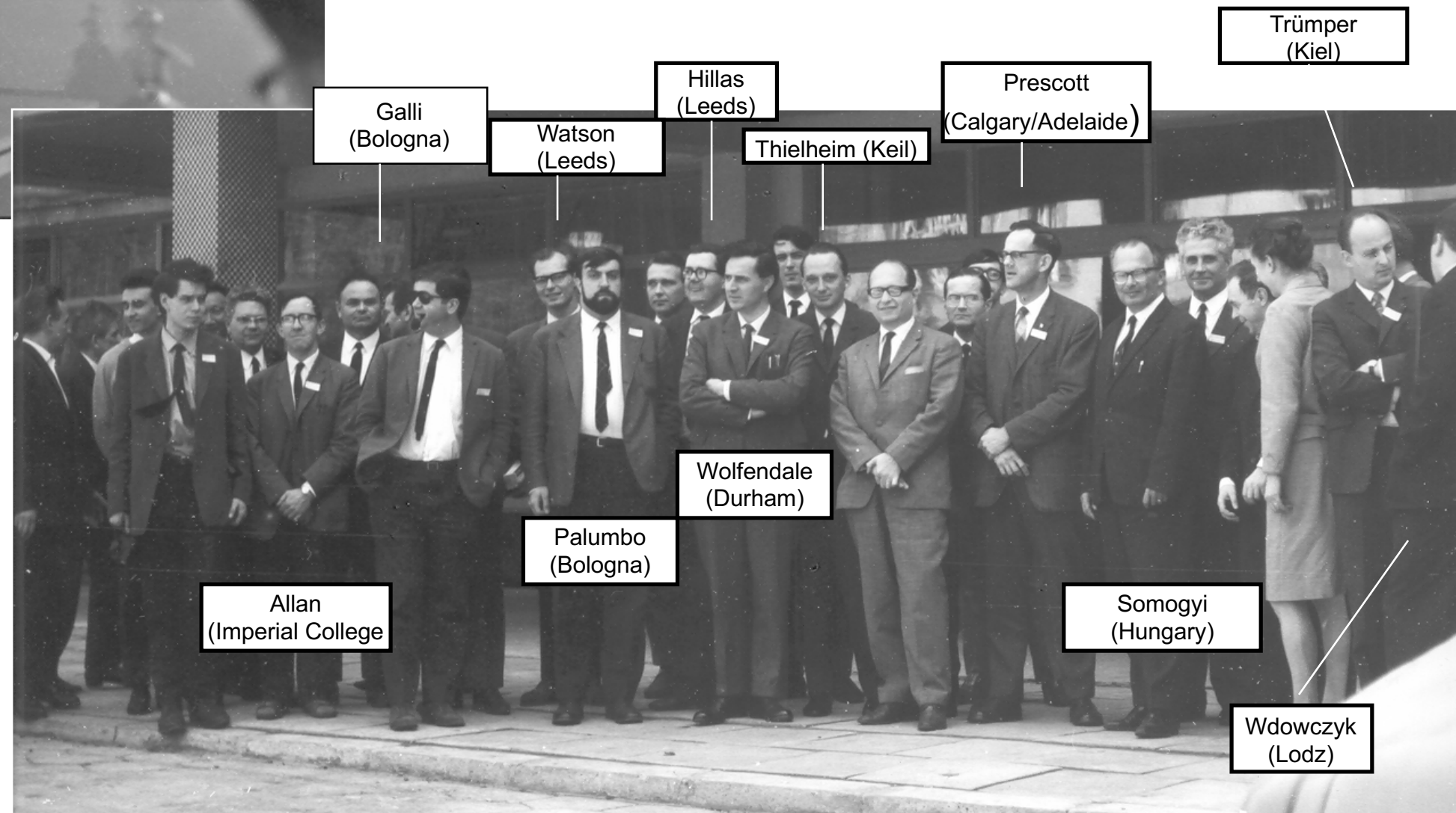
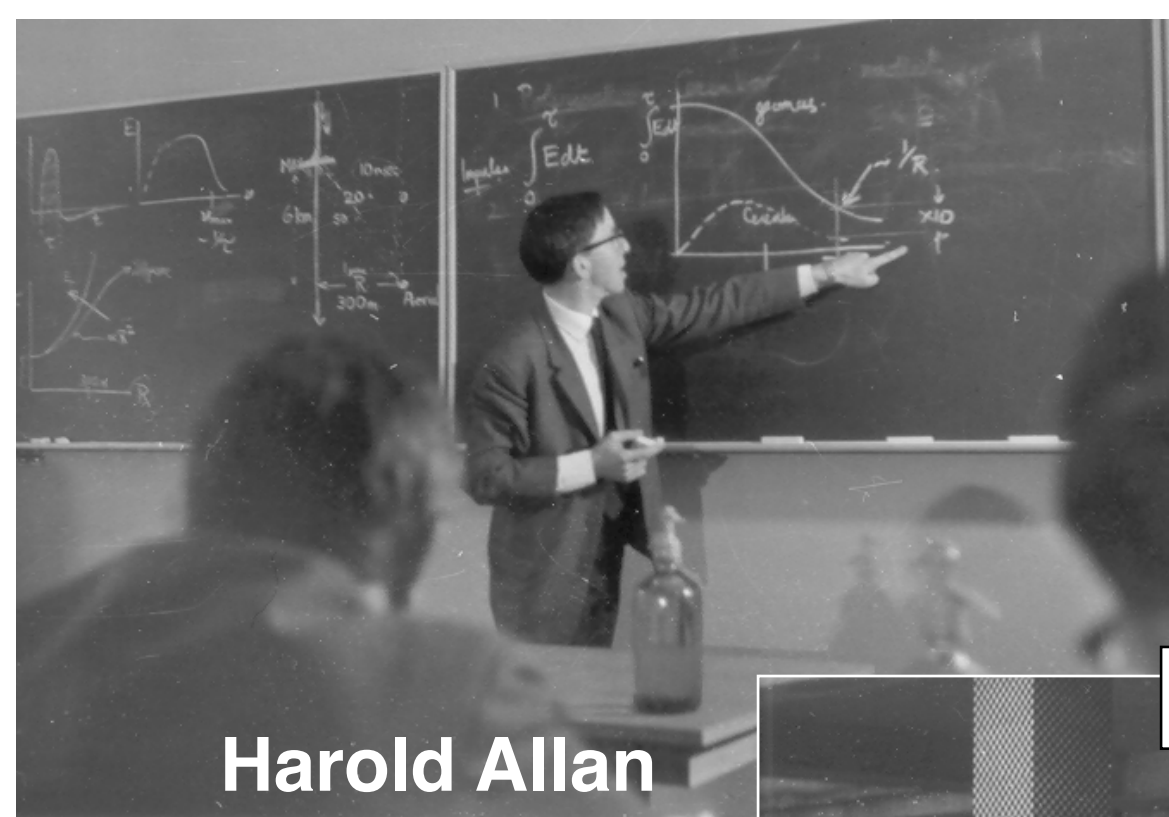
Recent receiving antennas (44 MHz) forming part of the Haverah Park Extensive Air Shower Array.

$$\epsilon_\nu = 2 \left( \frac{E_p}{10^{17}} \right) \left( \frac{\sin \alpha \cos \theta}{\sin 45 \cos 30} \right) \exp \left( \frac{-r}{r_0} \right) \left( \frac{\nu}{50} \right)^{-1} \mu\text{V/m/MHz}$$

$r_0 = 110$  m at  $\nu = 55$  MHz.  $\alpha$ =angle to B,  $\theta$ =Zenith angle







## First European Symposium on High Energy Interactions and Extensive Air Shower: Lodz, Poland April 1968

The renaissance of radio detection of cosmic rays

TIM HUEGE<sup>1</sup>

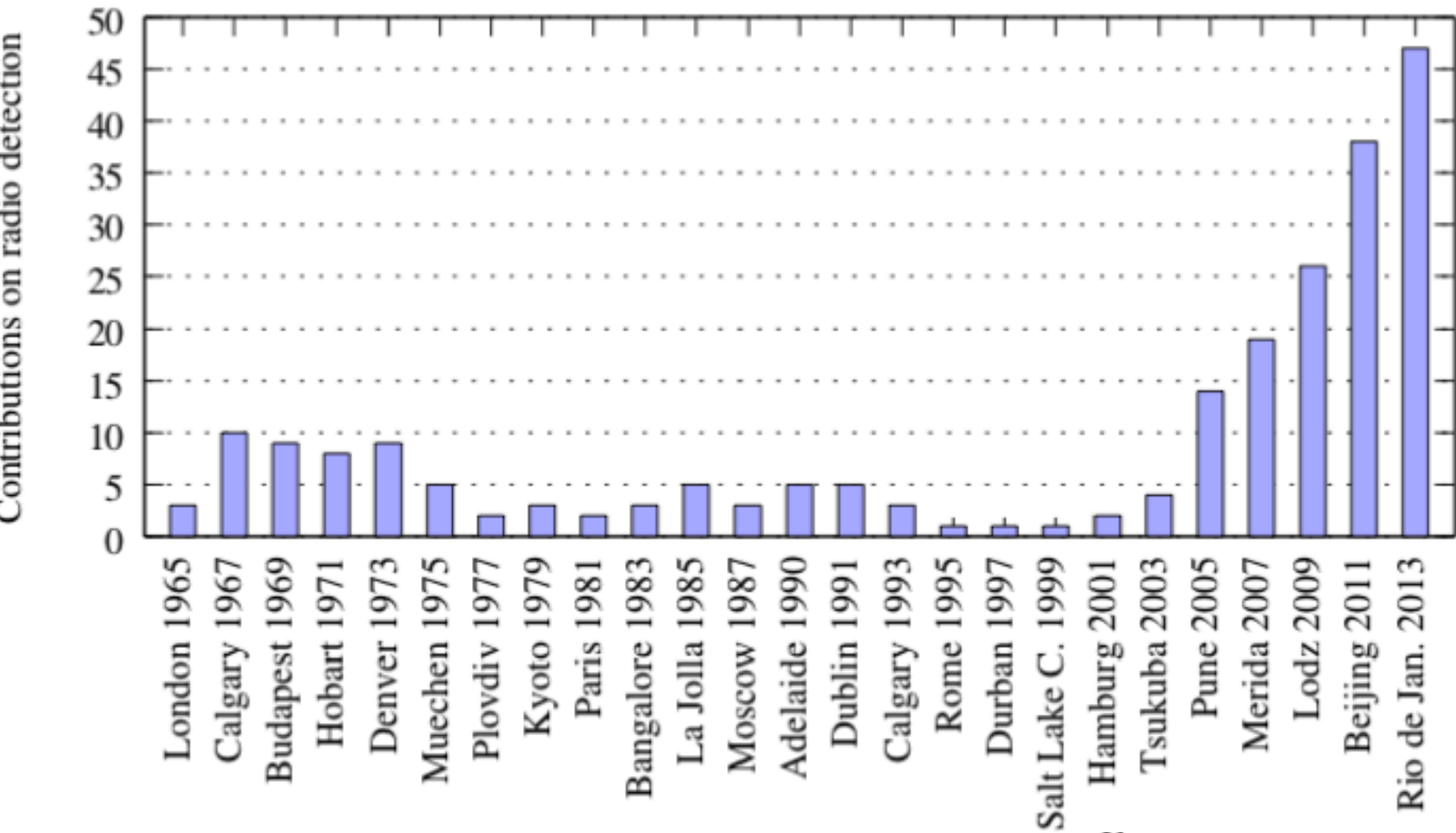


**Figure 1:** Number of contributions related to radio detection of cosmic rays or neutrinos to the ICRCs since 1965. The field has grown very impressively since the modern activities started around 2003. Data up to 2007 were taken from [11].



The renaissance of radio detection of cosmic rays

TIM HUEGE<sup>1</sup>

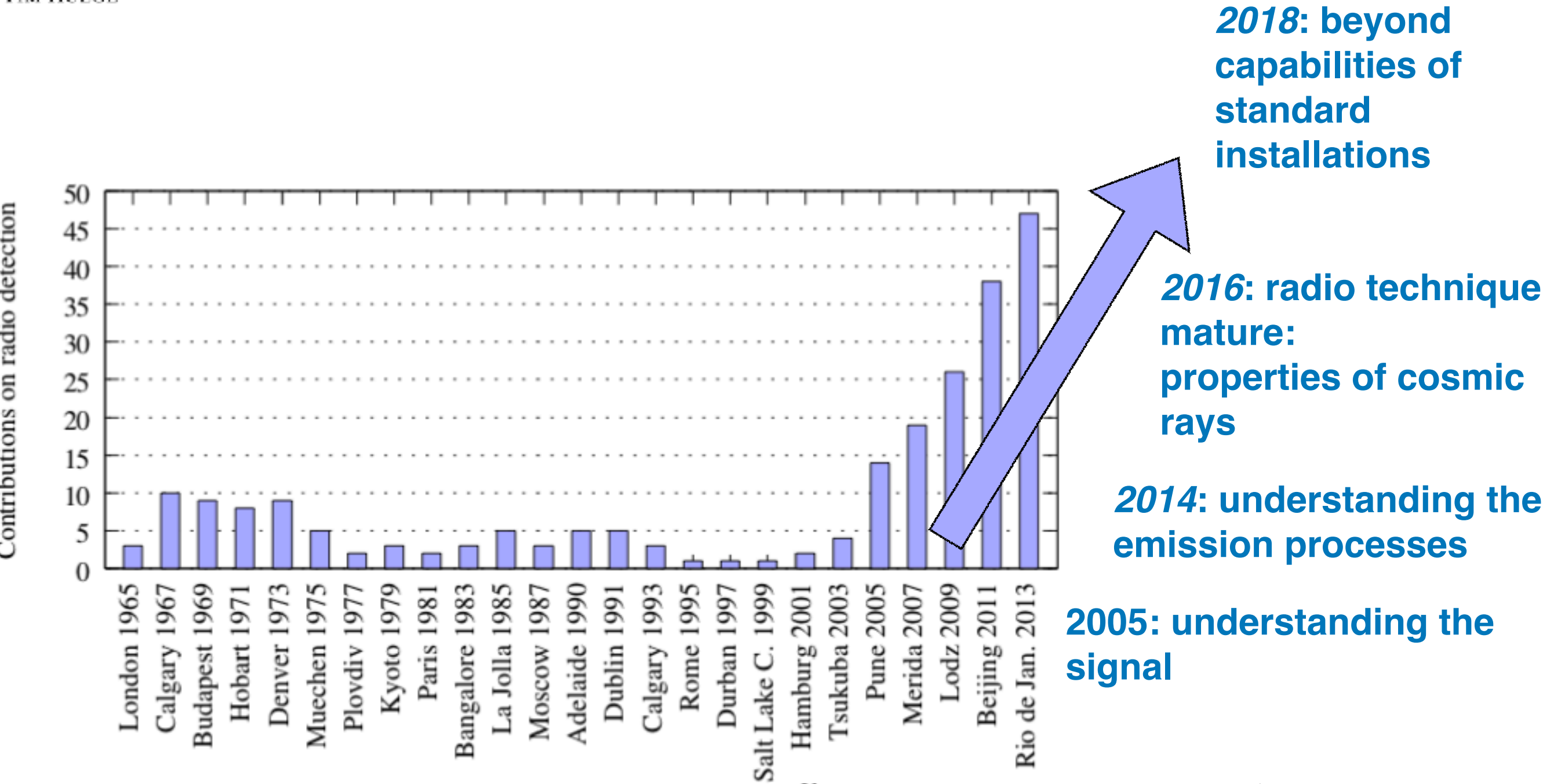
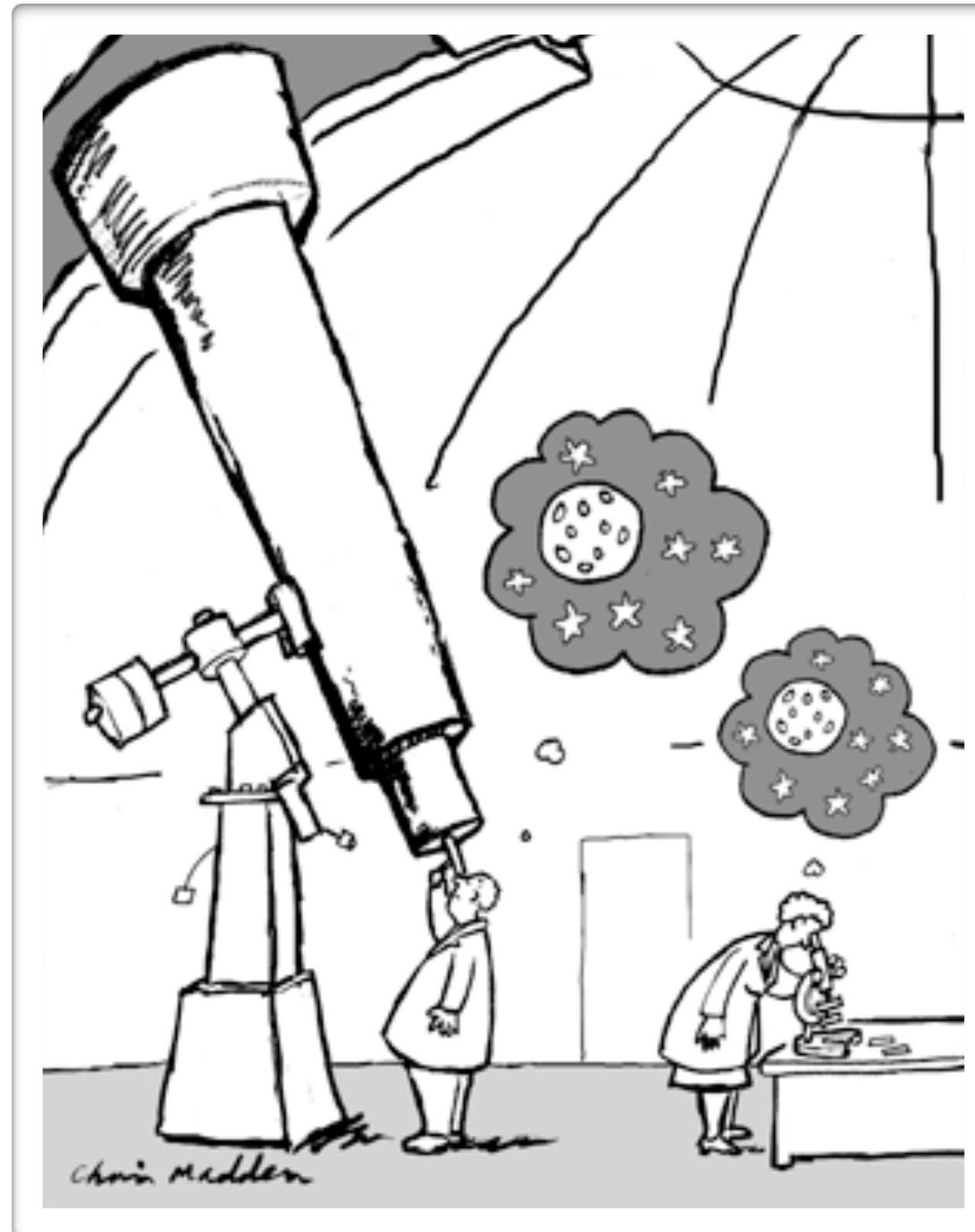


**Figure 1:** Number of contributions related to radio detection of cosmic rays or neutrinos to the ICRCs since 1965. The field has grown very impressively since the modern activities started around 2003. Data up to 2007 were taken from [11].

# Radio Detectors





# Radio detection of extensive air showers around the world

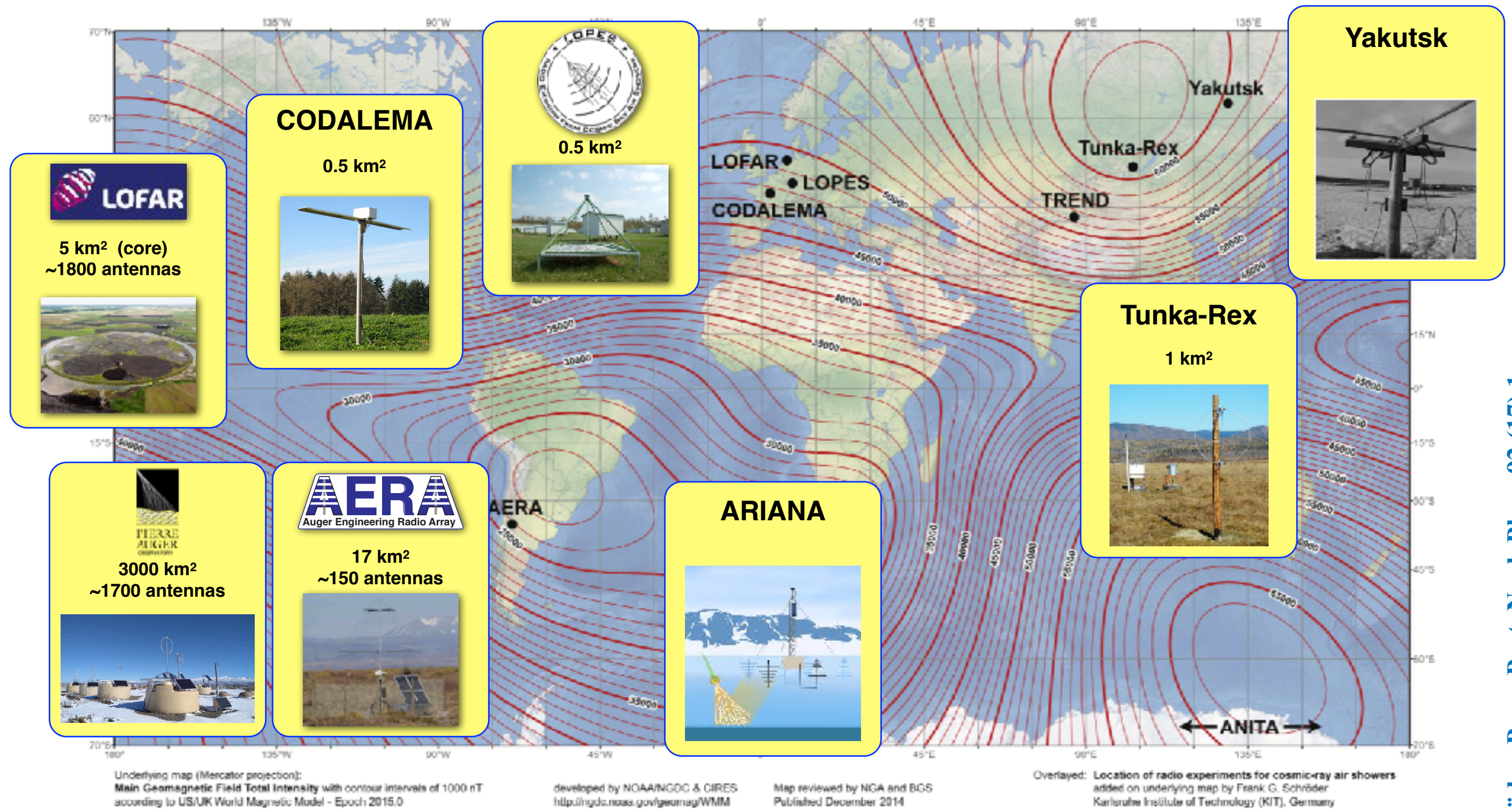


**Fig. 21.** Map of the total geomagnetic field strengths (world magnetic model [207]) and the location of various radio experiments detecting cosmic-ray air showers.





LOFAR

scintillators

30 - 80 MHz

core  
23 stations ~5 km<sup>2</sup>

International LOFAR Telescope (ILT)

120 - 240 MHz

30- 80 MHz

each (dutch) station:  
96 low-band antennas  
high-band antennas (2x24 tiles) 120-240 MHz

M. van Haarlem et al., A&A 556 (2013) A2



LORA  
LOFAR Radboud Array  
scintillator detectors

### Superterp:

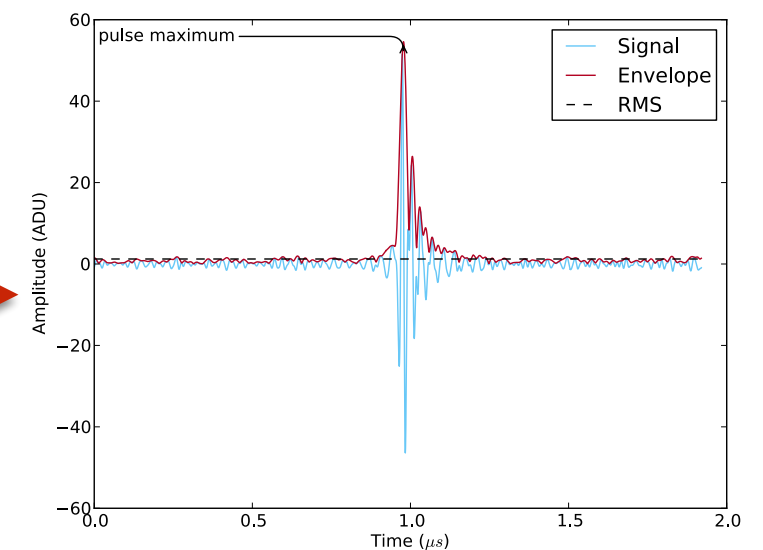
- \* diameter  $\sim 300$  m
- \* 20 LORA detectors
- \* 6 LBA stations  
(= 6 x 48 antennas)
- \* more LBA stations  
around superterp

trigger: 13 of 20  
detectors

buffer

2 ms read-out

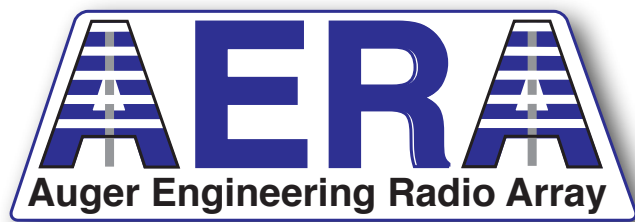
offline analysis  
P. Schellart et al., A&A 560, 98 (2013)



Low Band Antennas (LBA)  
30 - 80 MHz

Selection this analysis:  
4+ LBA stations

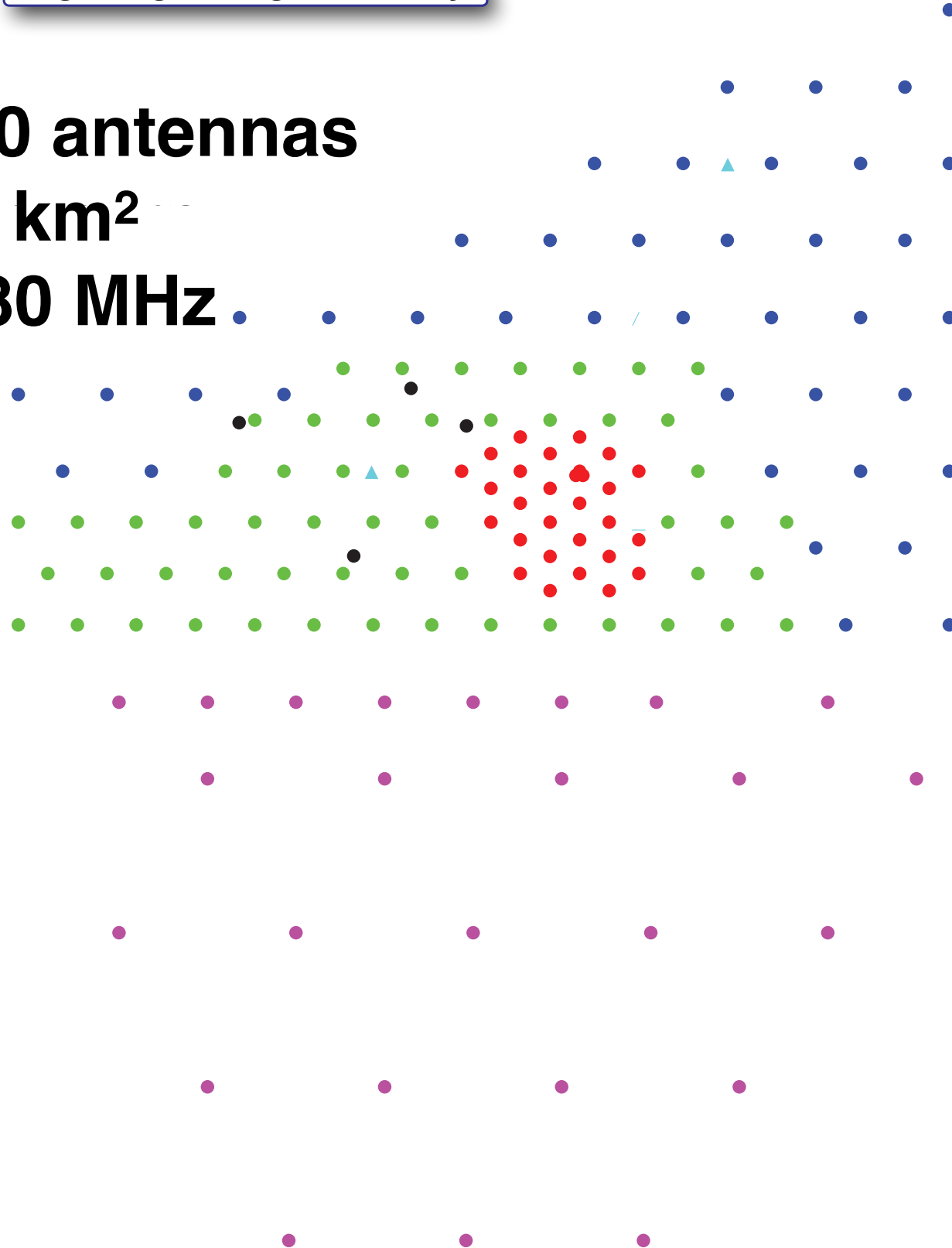




**~150 antennas**

**~17 km<sup>2</sup>**

**30-80 MHz**



**LOFAR core**

**23 stations ~5 km<sup>2</sup>**

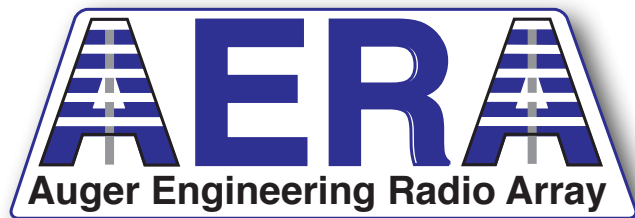


>2000 antennas

1 km



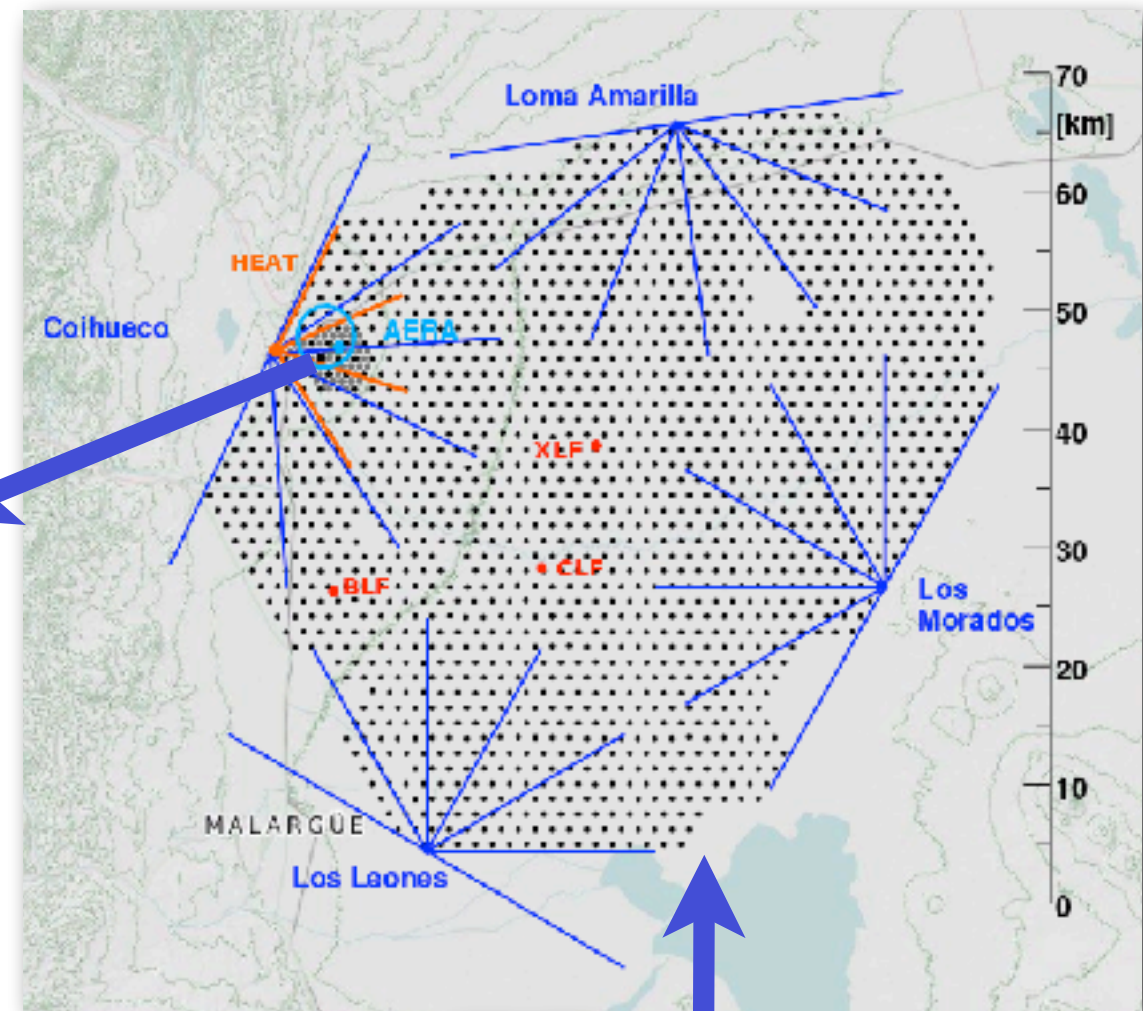
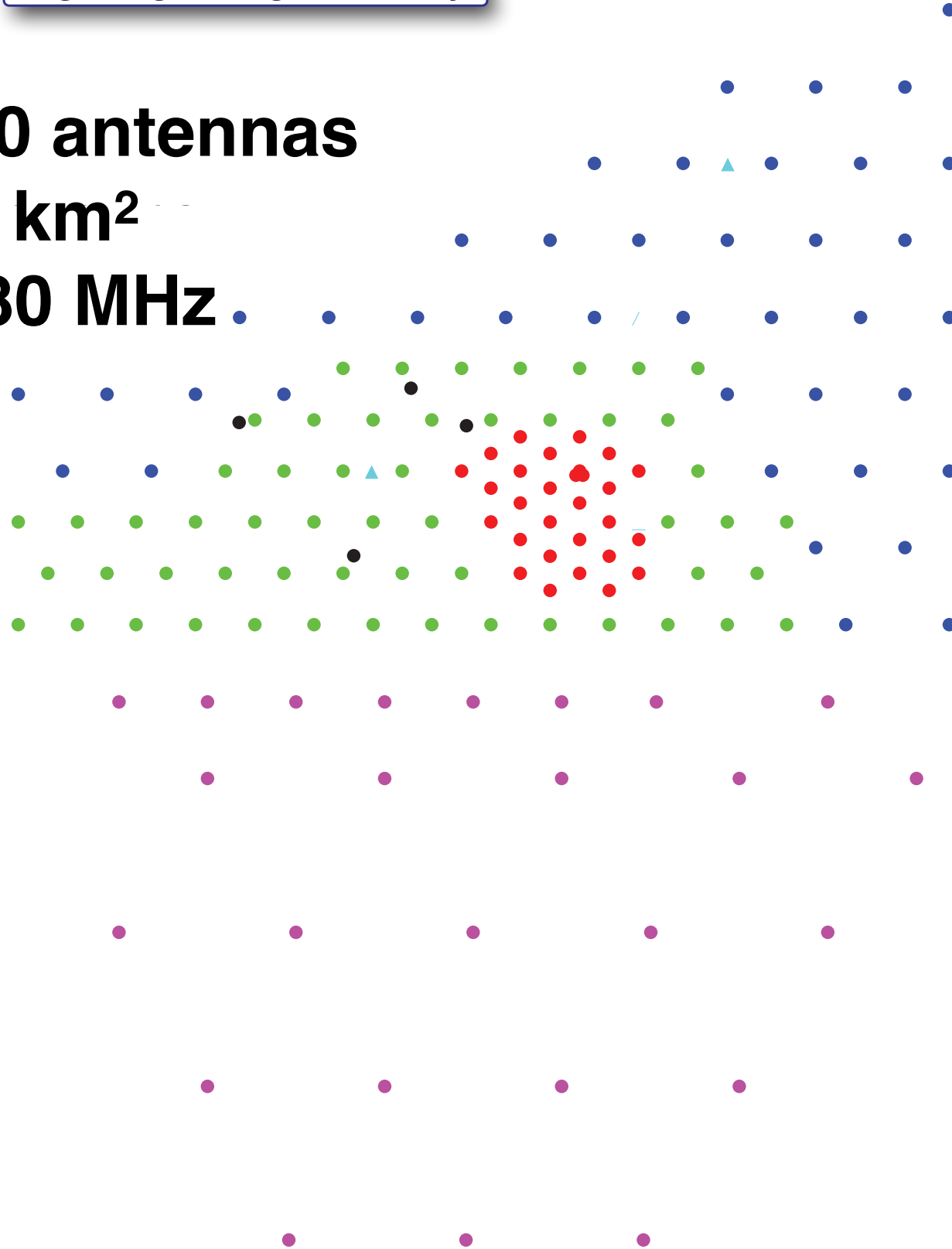


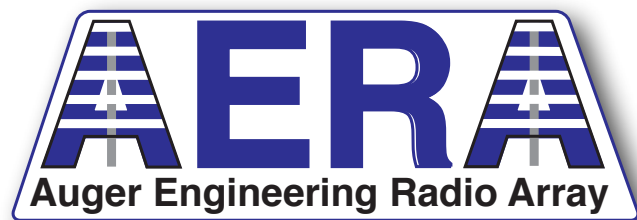


~150 antennas

~17 km<sup>2</sup>

30-80 MHz

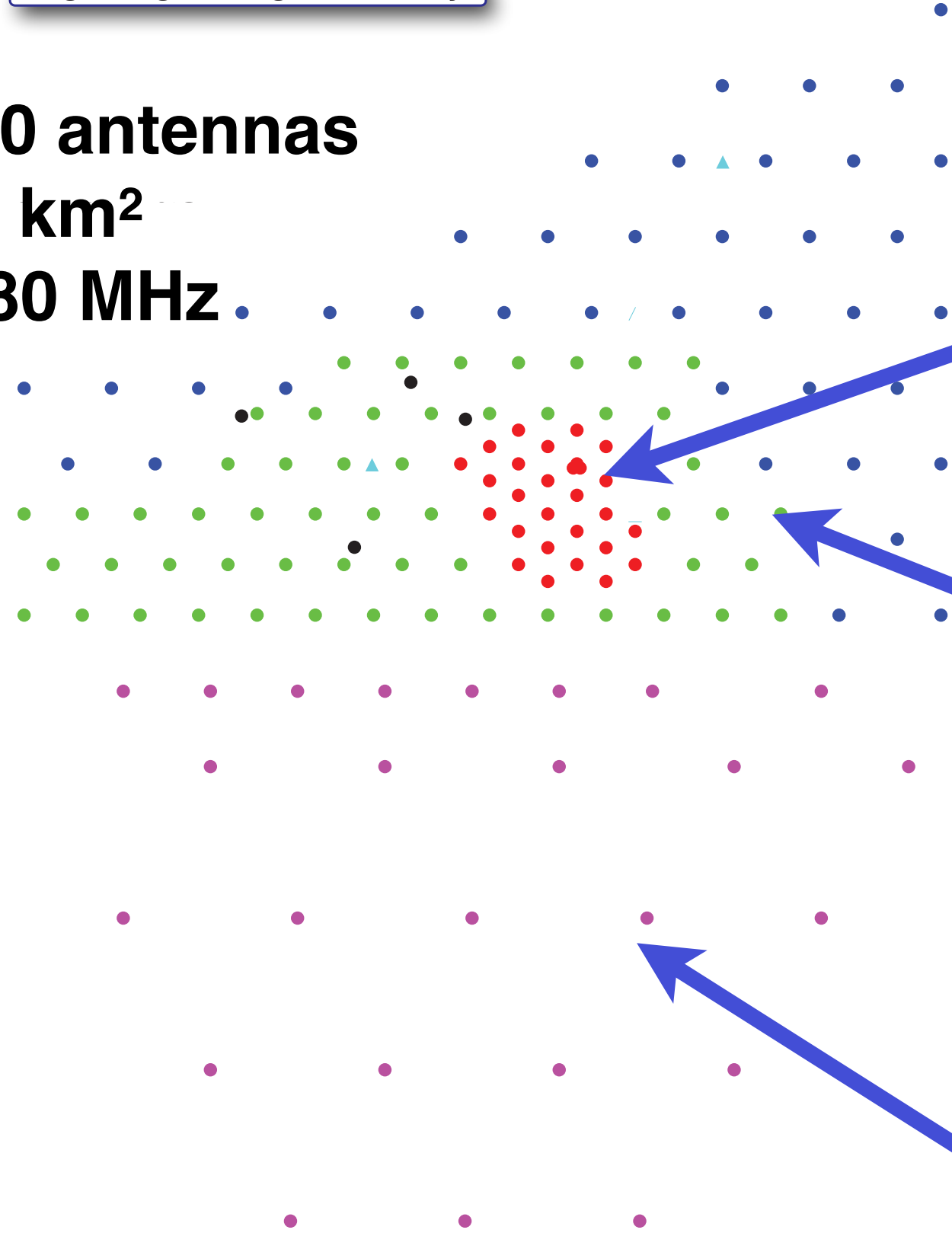




**~150 antennas**

**~17 km<sup>2</sup>**

**30-80 MHz**

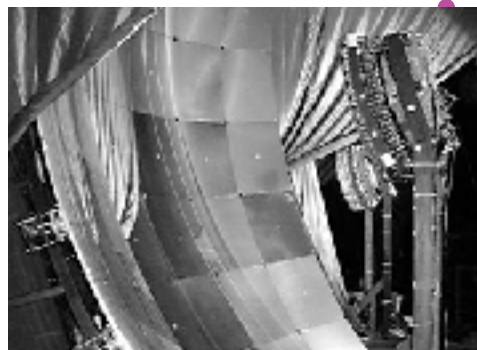




**~150 antennas**

**~17 km<sup>2</sup>**

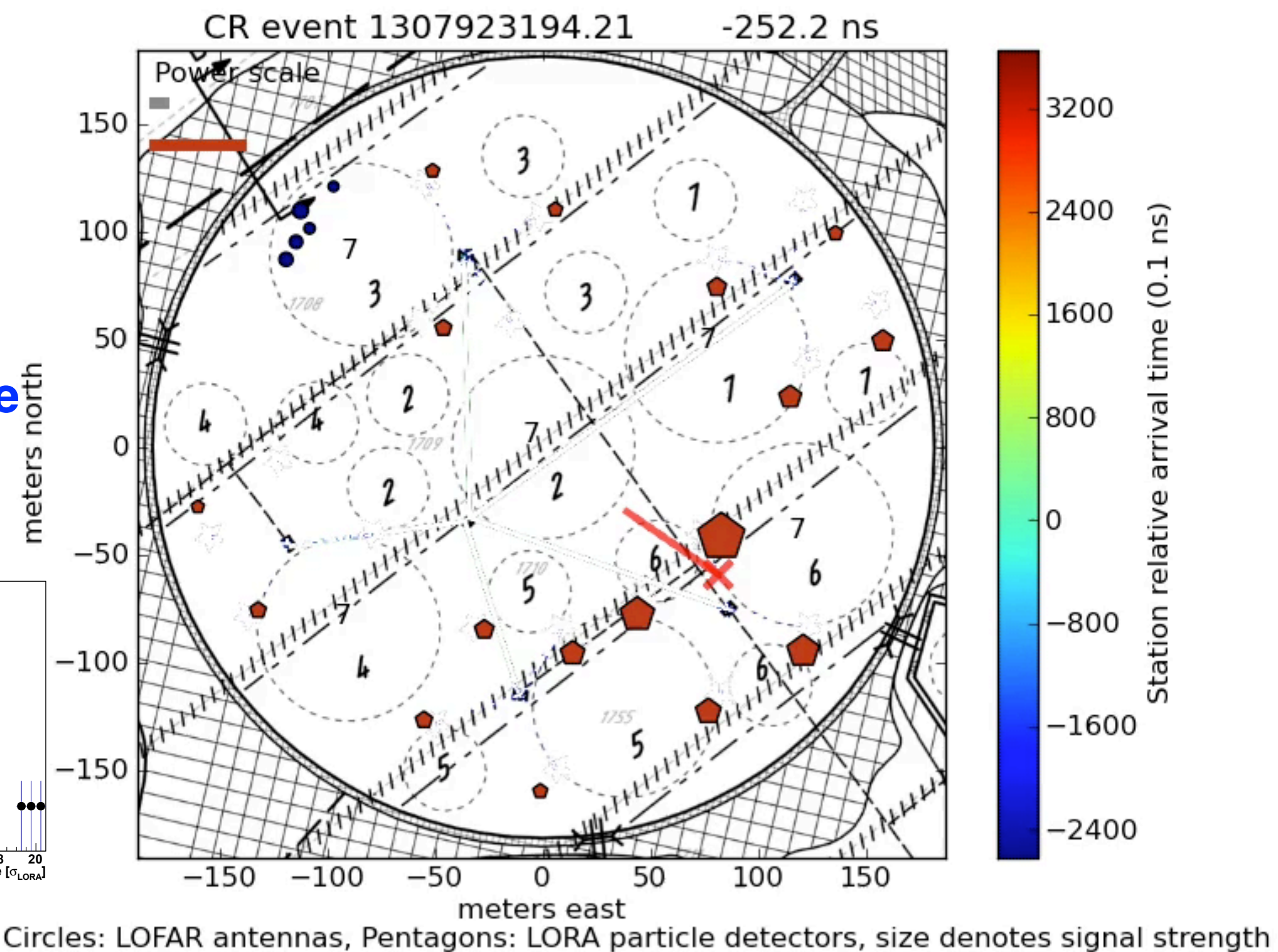
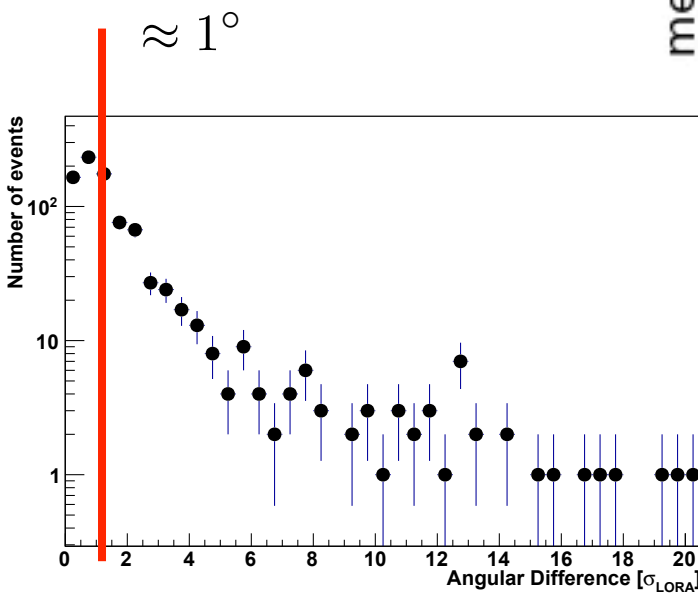
**30-80 MHz**





# A measured air shower

angular difference  
particles - radio

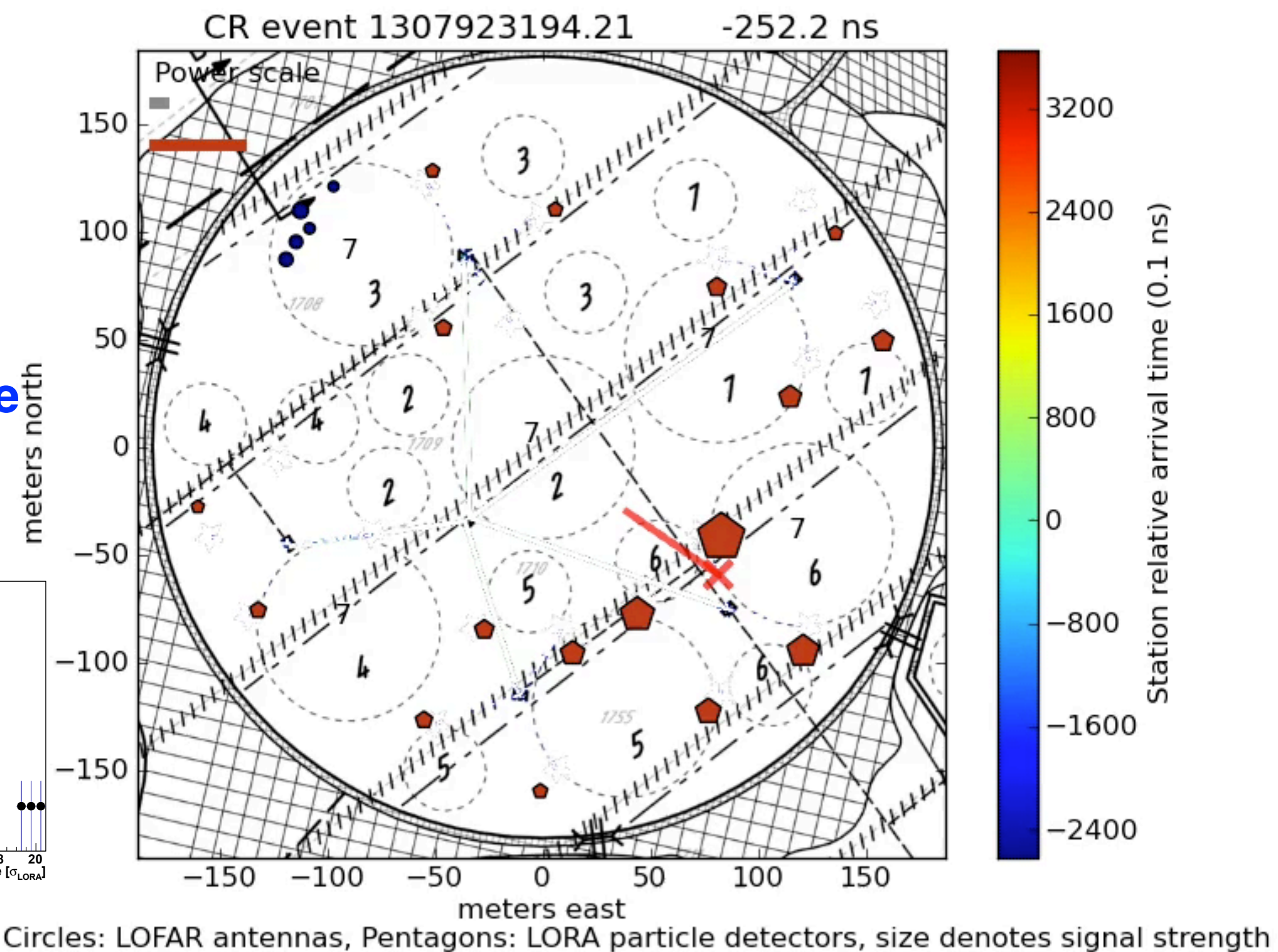
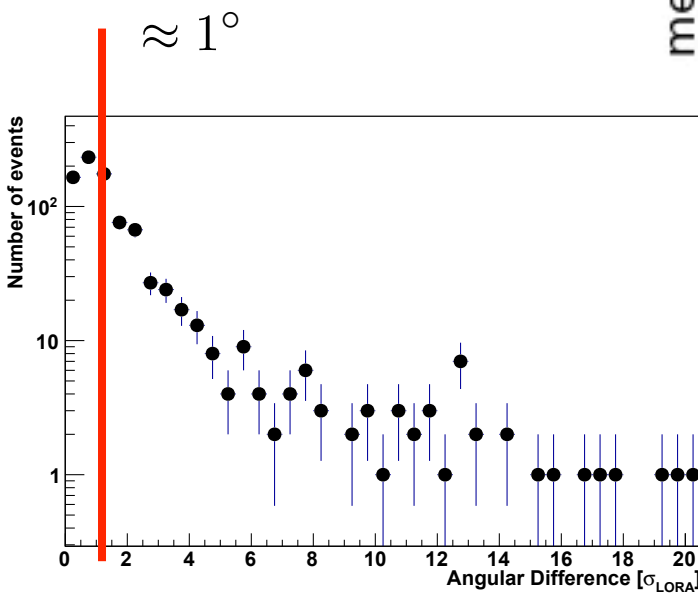


Circles: LOFAR antennas, Pentagons: LORA particle detectors, size denotes signal strength



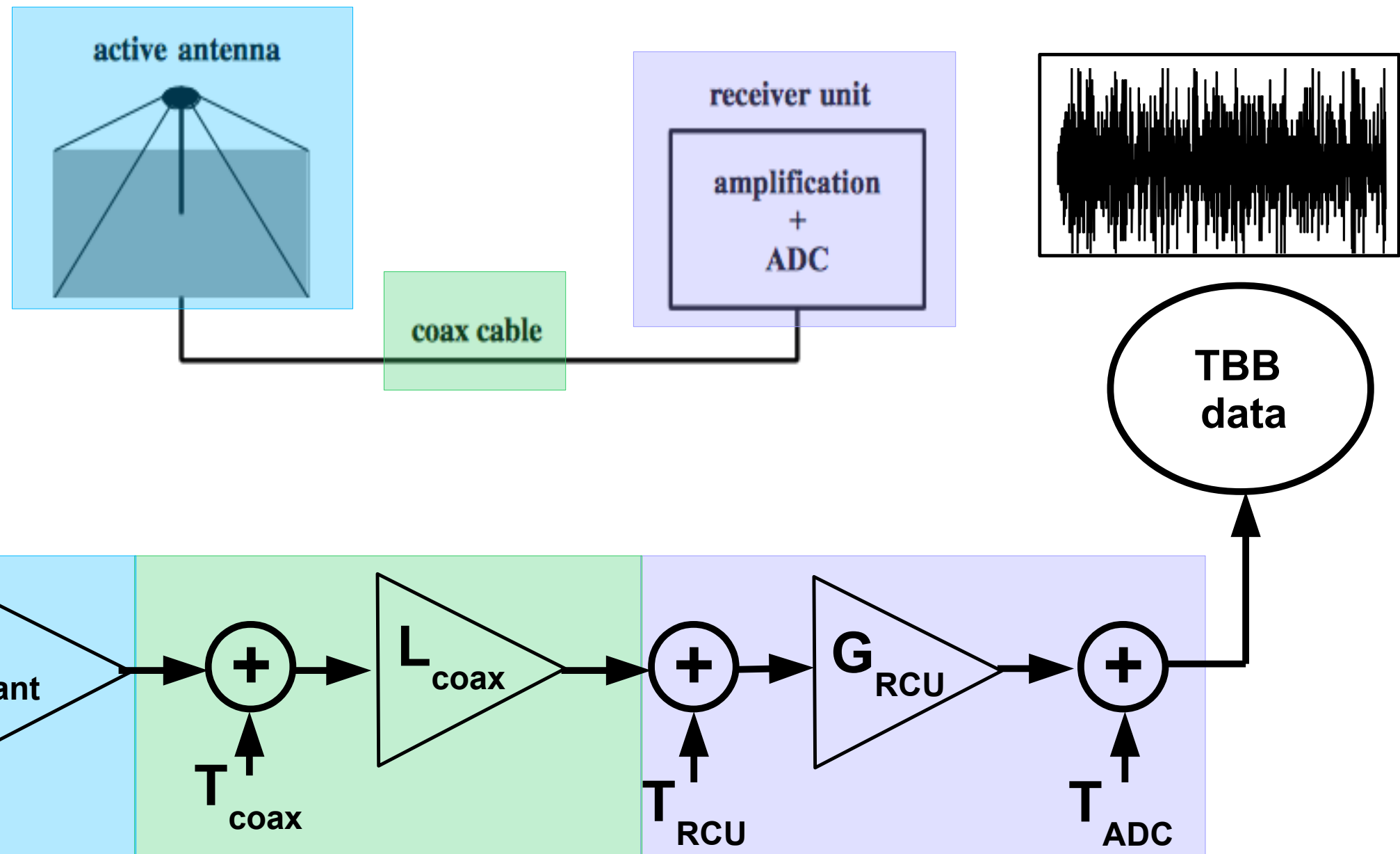
# A measured air shower

angular difference  
particles - radio





# LOFAR Signal Chain

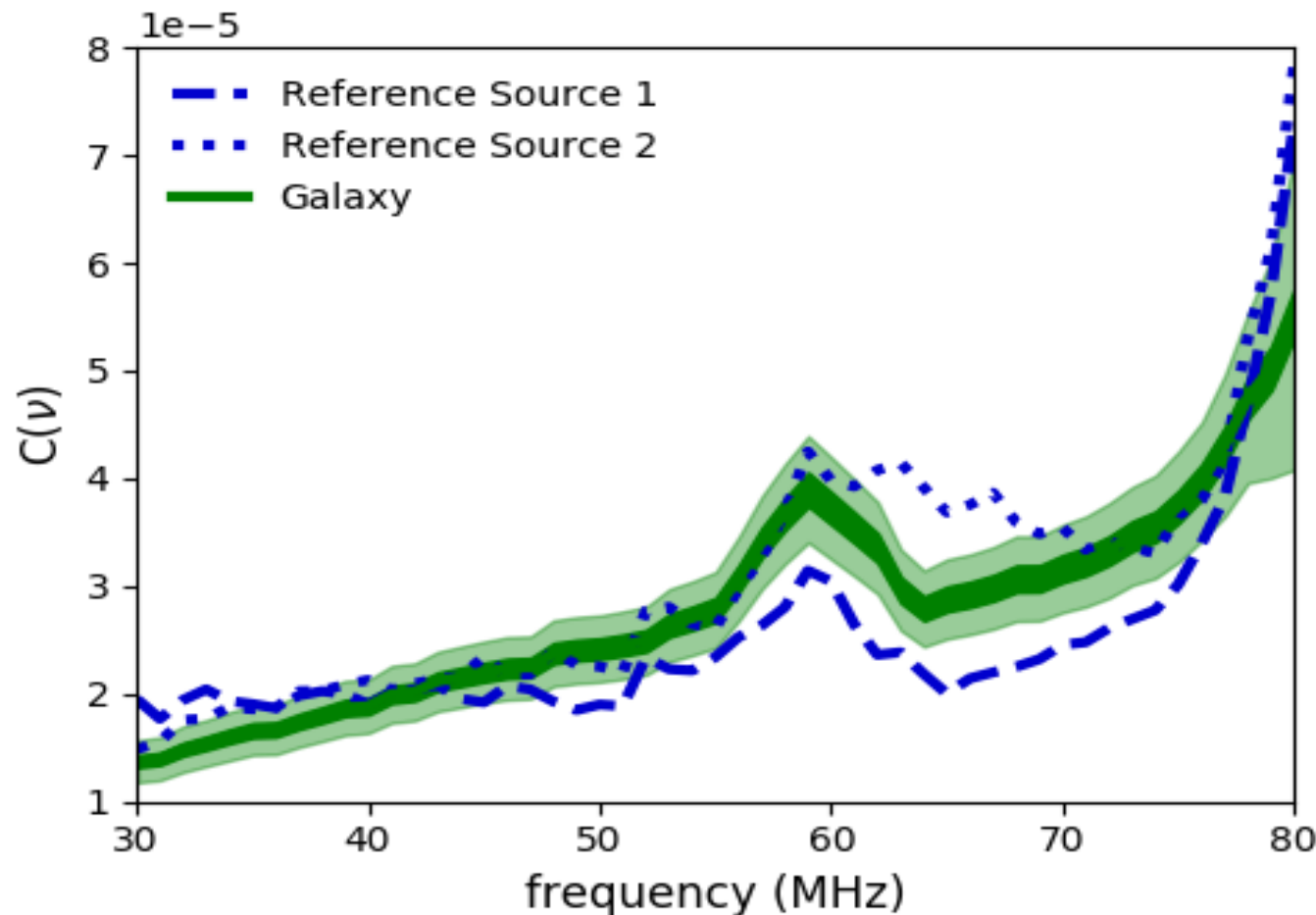


$G_{\text{ant}}, L_{\text{coax}}, G_{\text{RCU}}$  → Freq. Dependent losses and gains  
 $T_{\text{LNA}}, T_{\text{coax}}, T_{\text{RCU}}, T_{\text{ADC}}$  → Constant noise values



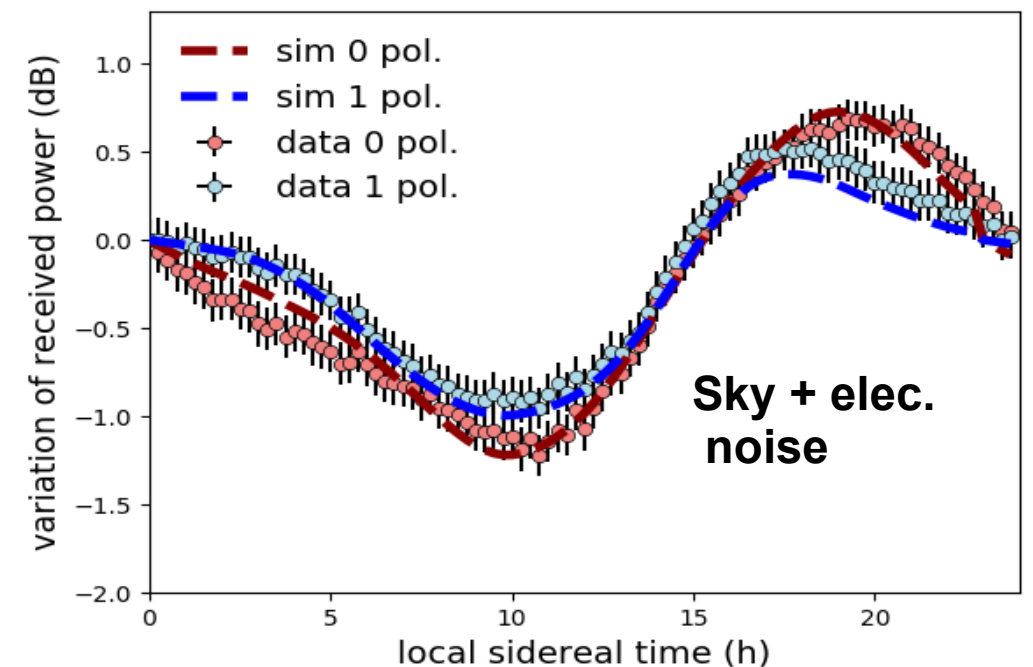
# Calibration Results

$$C^2(\nu) = A(\nu)L_{\text{coax}}(\nu)G_{\text{RCU}}(\nu)S$$



- Galaxy model now limits systematic uncertainties
- Uncertainties from electronic noise are found by comparing resulting calibration constants for different antennas

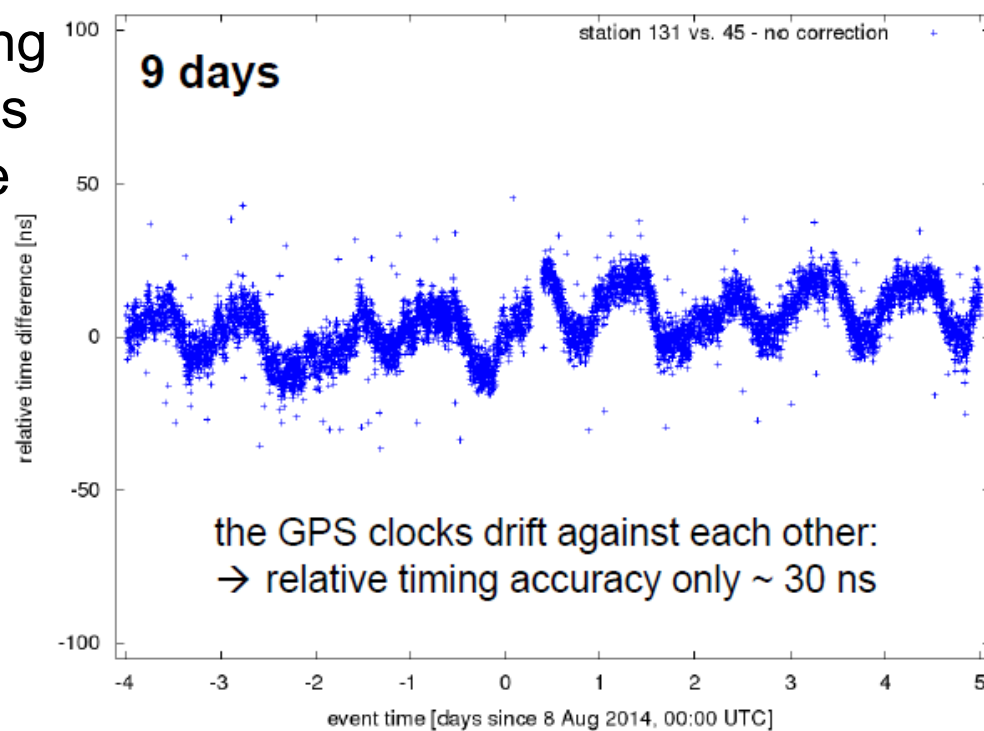
| Uncertainty                | Percentage |
|----------------------------|------------|
| event-to-event fluctuation | 4          |
| galaxy model               | 12         |
| electronic noise < 77 MHz  | 5-6        |
| electronic noise > 77 MHz  | 10-20      |
| <b>total &lt; 77 MHz</b>   | <b>14</b>  |





# Timing calibration

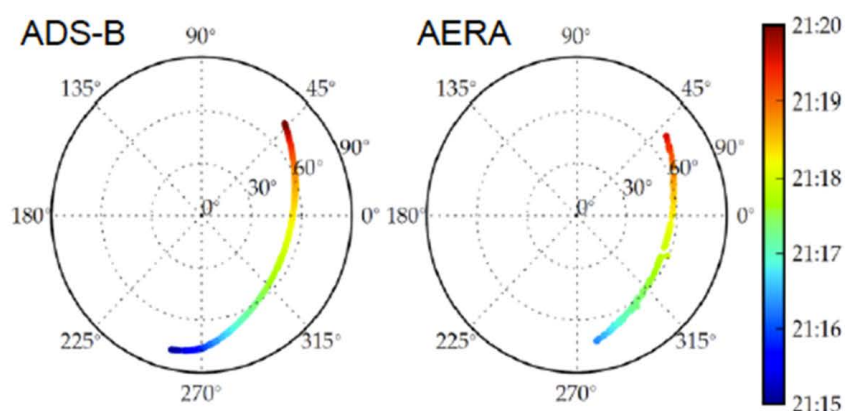
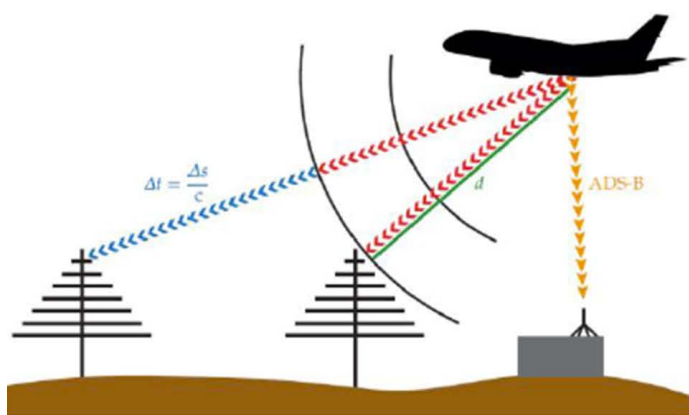
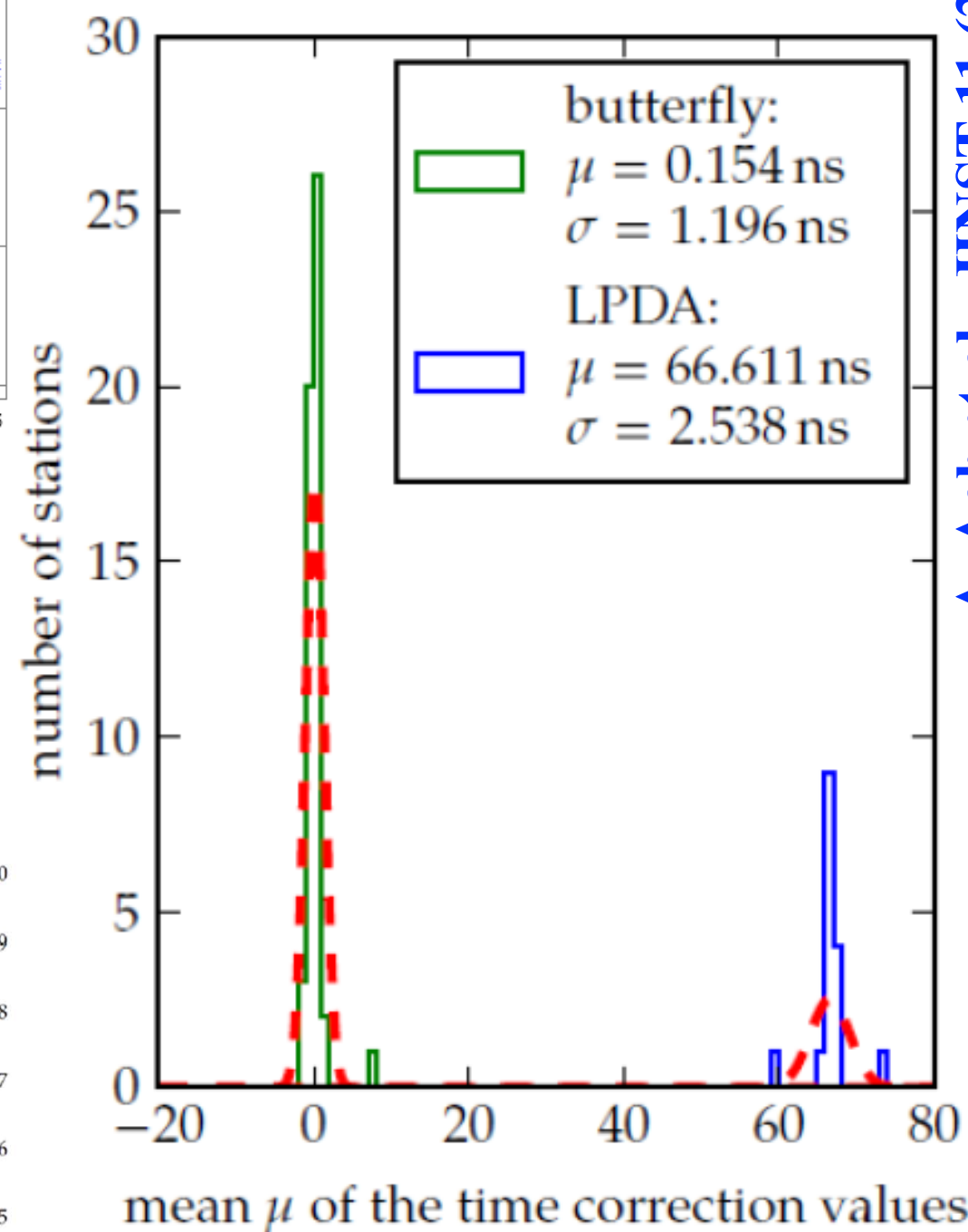
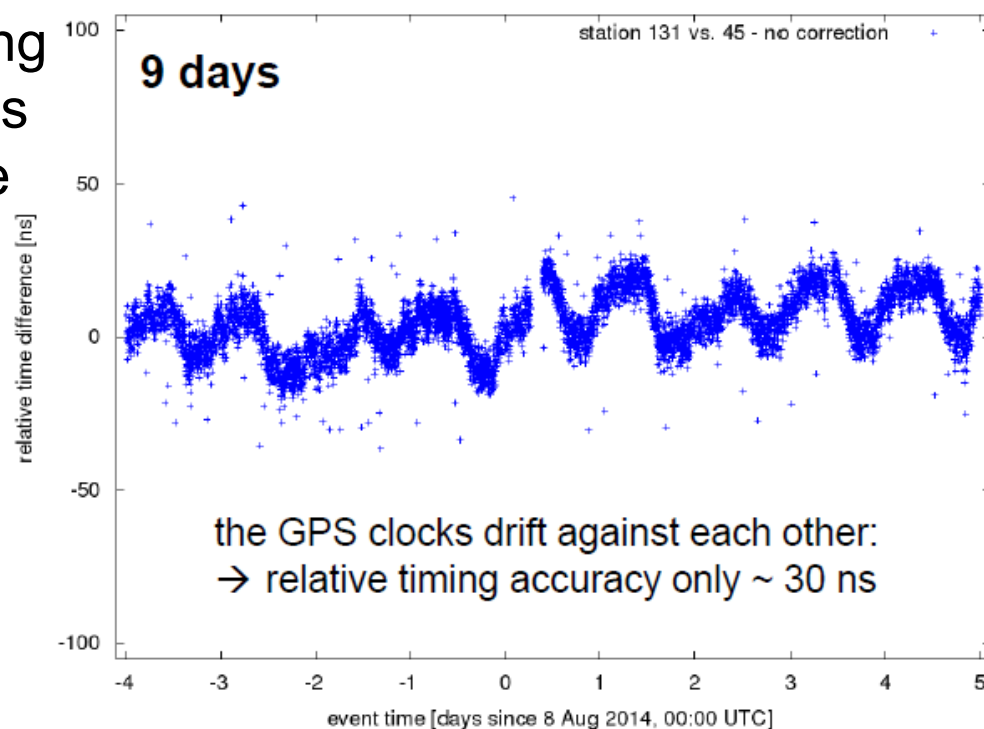
Use beacon broadcasting at 4 different frequencies to measure relative time shifts



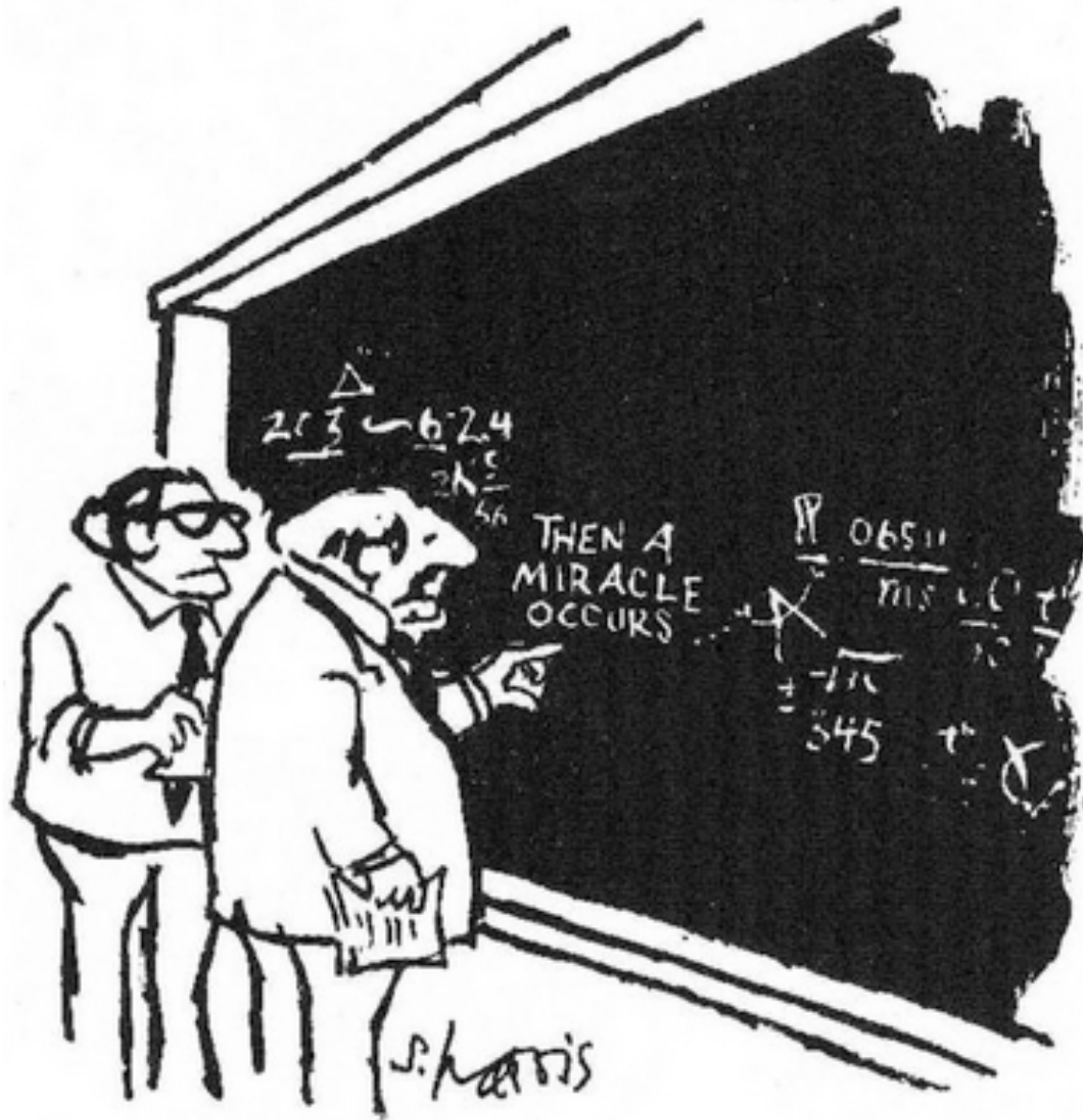


# Timing calibration

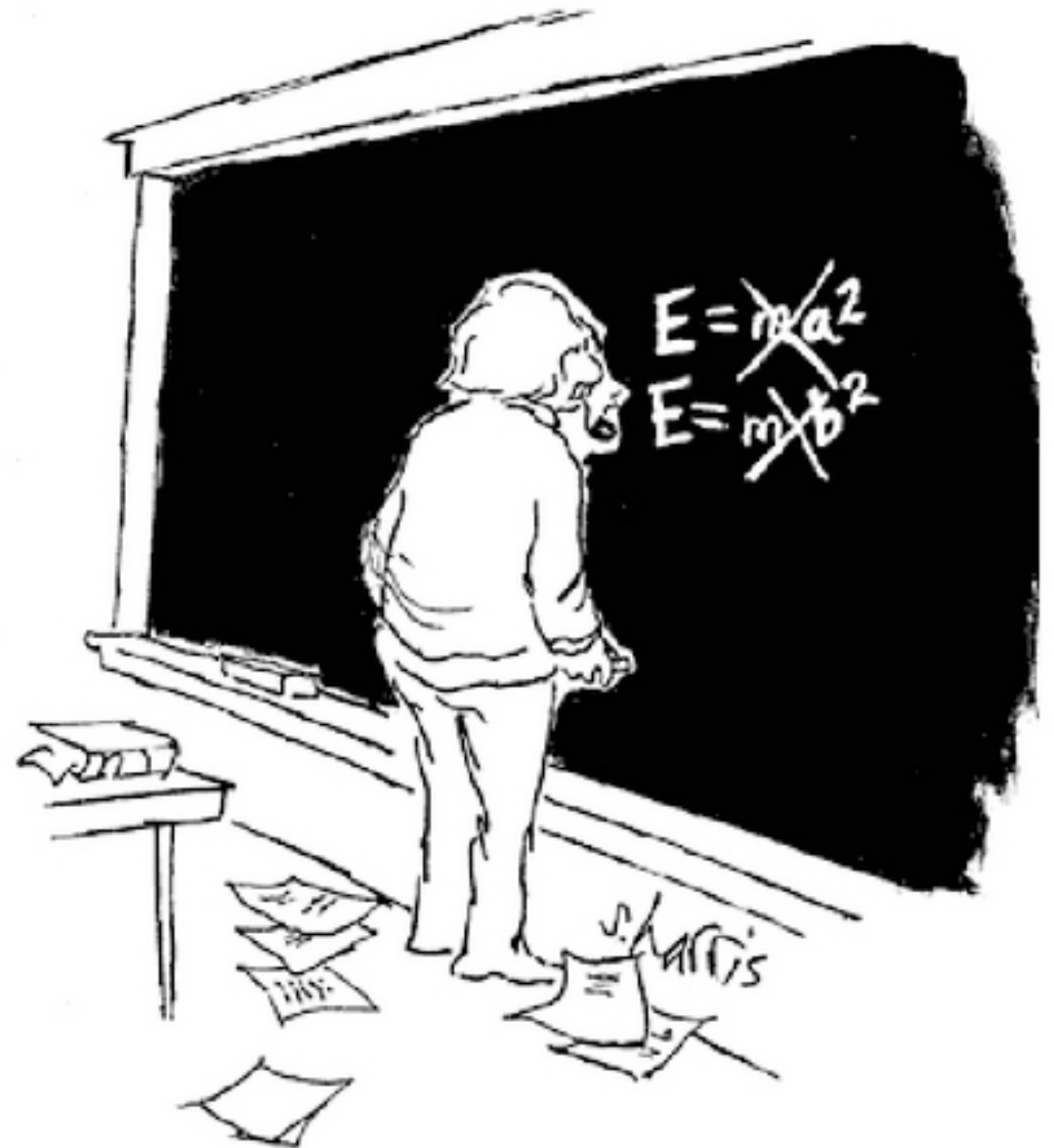
Use beacon broadcasting at 4 different frequencies to measure relative time shifts



# Radiation Processes



"I think you should be more explicit here in step two."



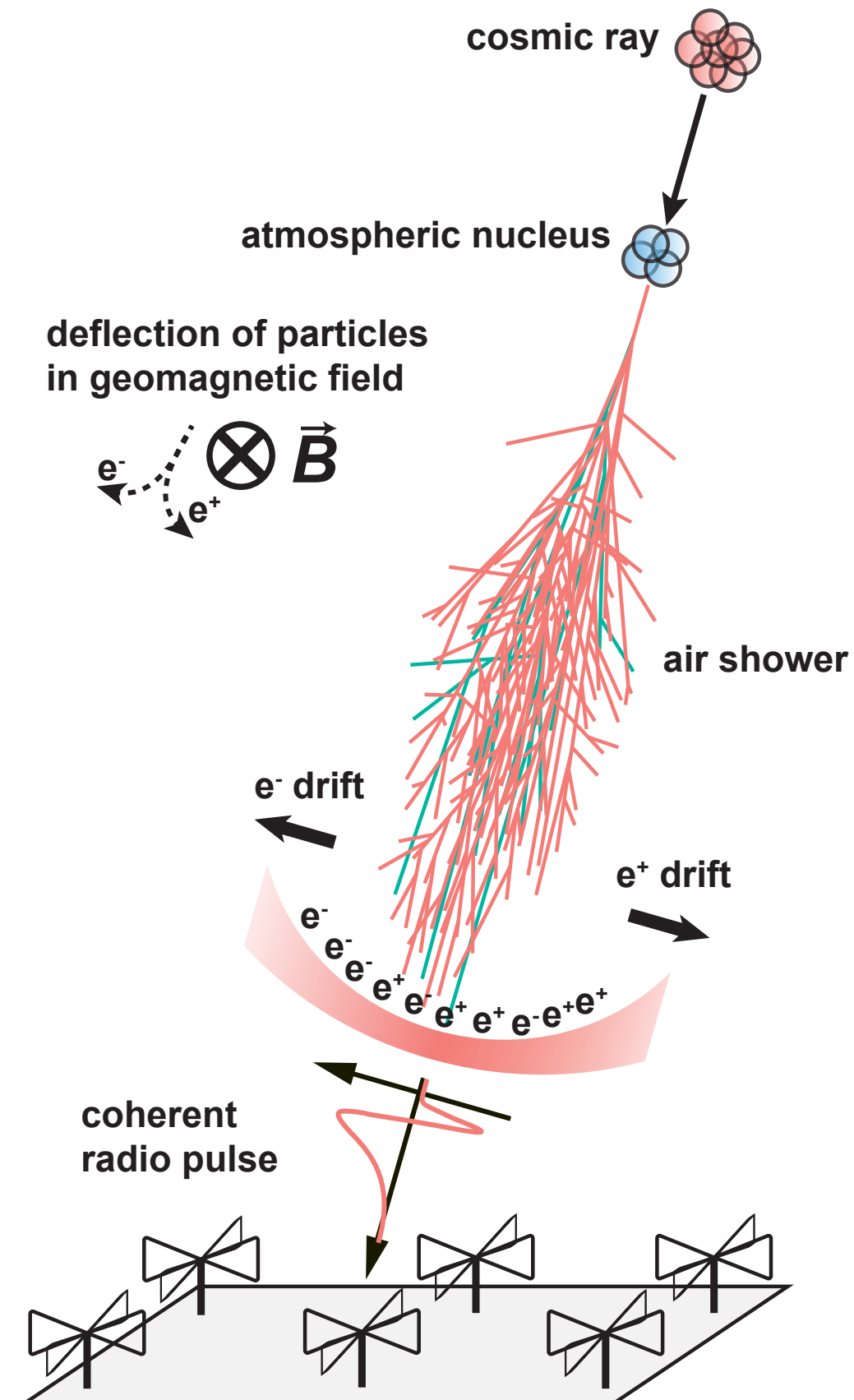


# Radio Emission in Air Showers



Mainly: Charge separation in geomagnetic field

$$\vec{E} \propto \vec{v} \times \vec{B}$$

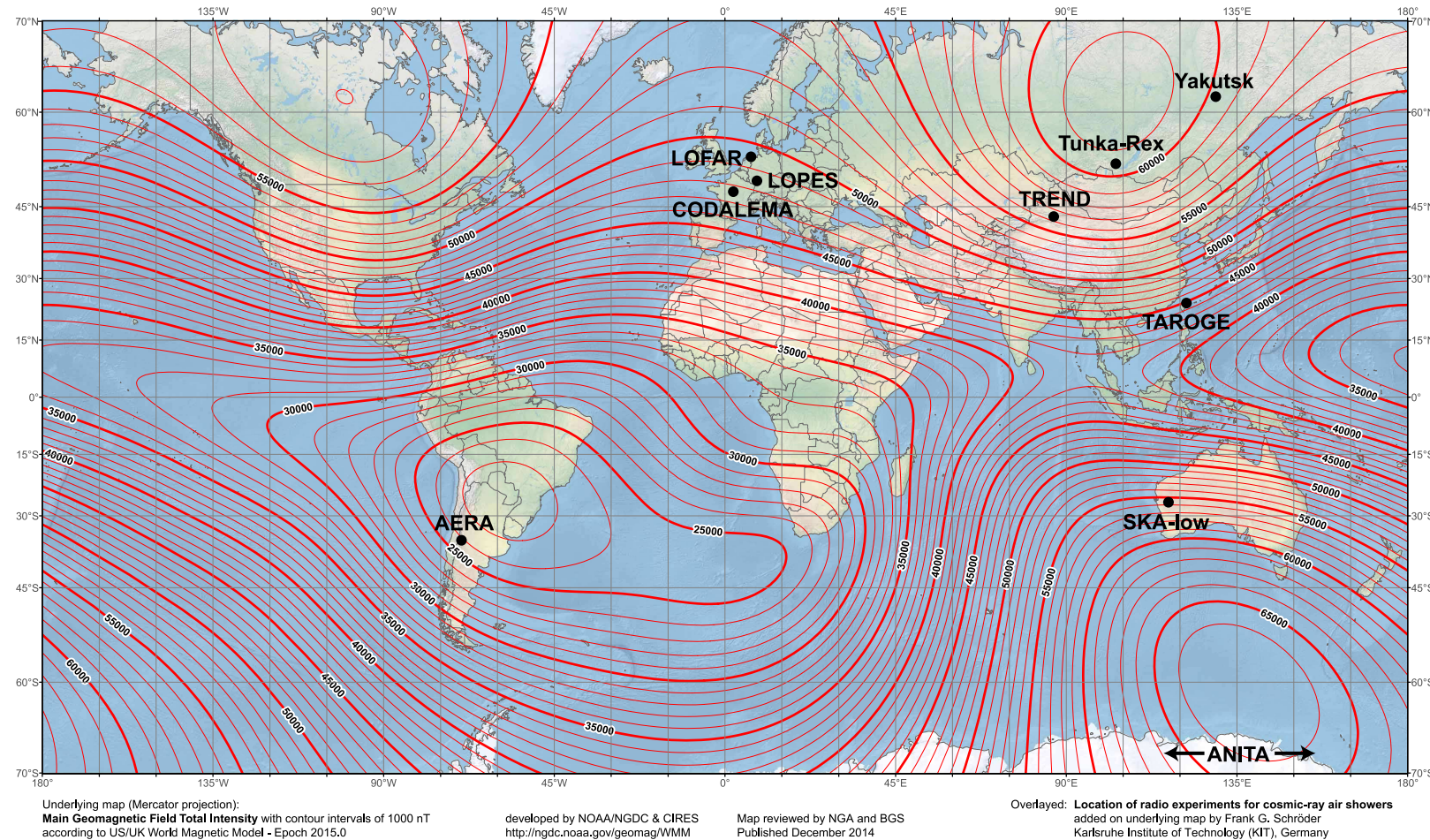


# Radio Emission in Air Showers

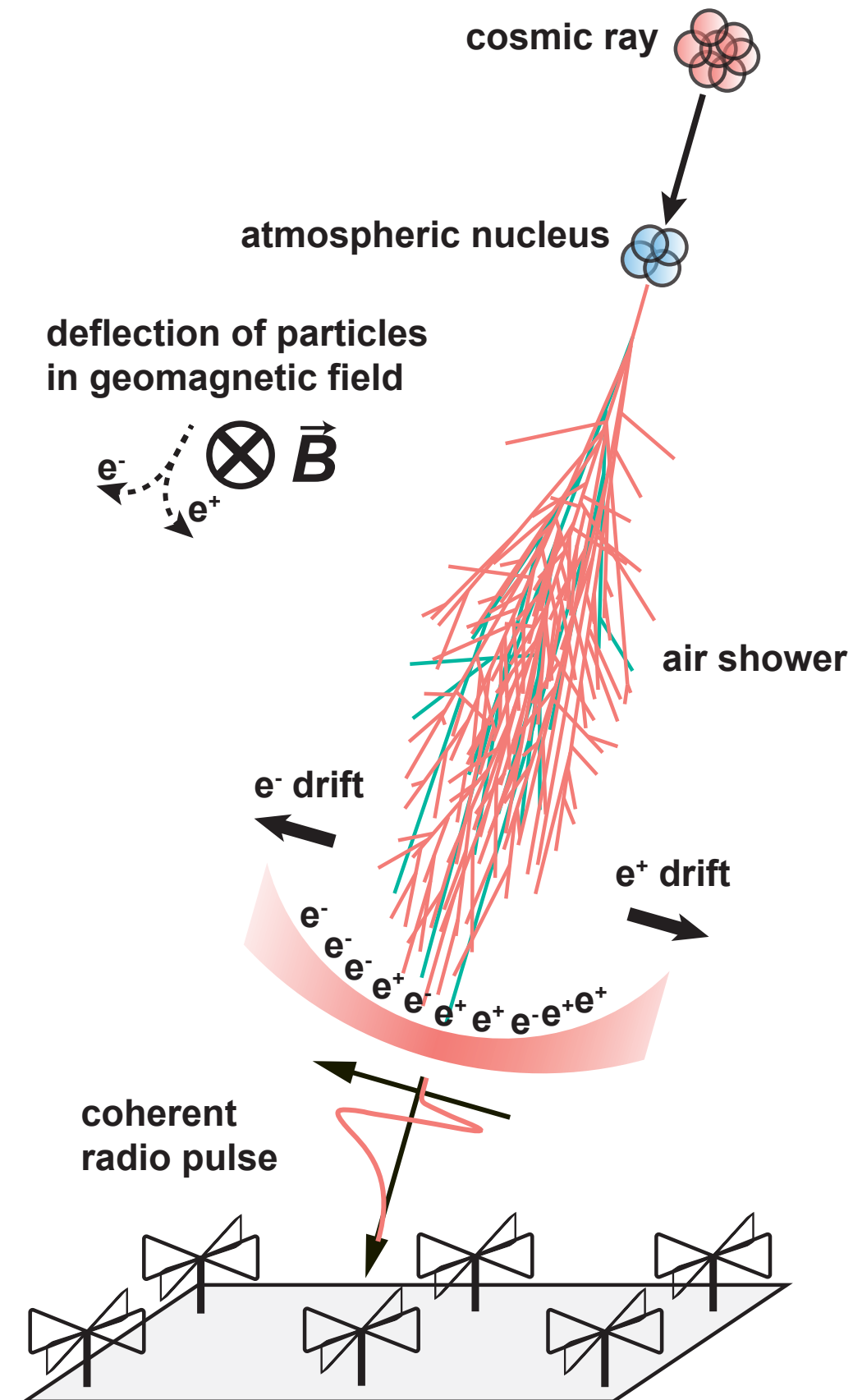


Mainly: Charge separation in geomagnetic field

$$\vec{E} \propto \vec{v} \times \vec{B}$$



F. Schröder, Prog. Part. Nucl. Phys. 93 (2017) 1

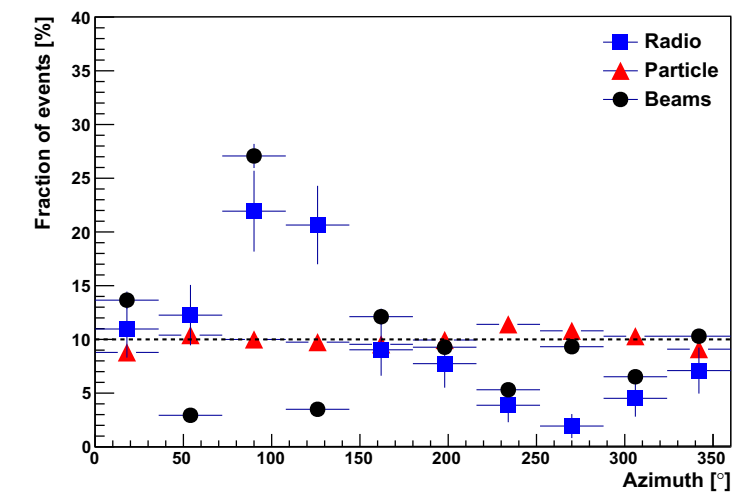
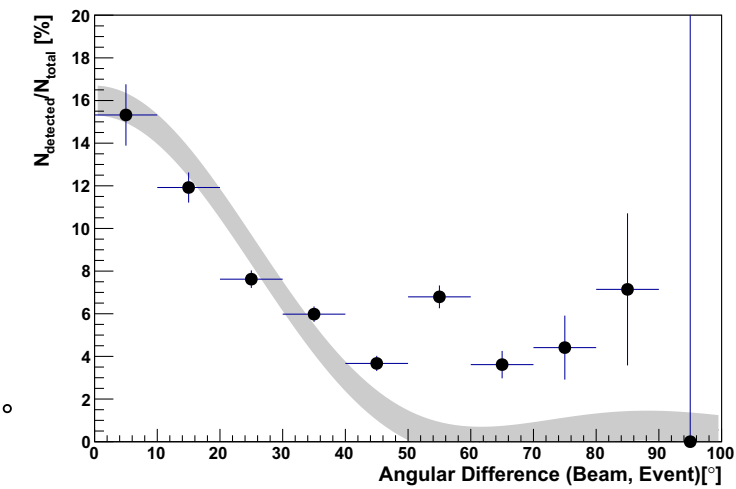
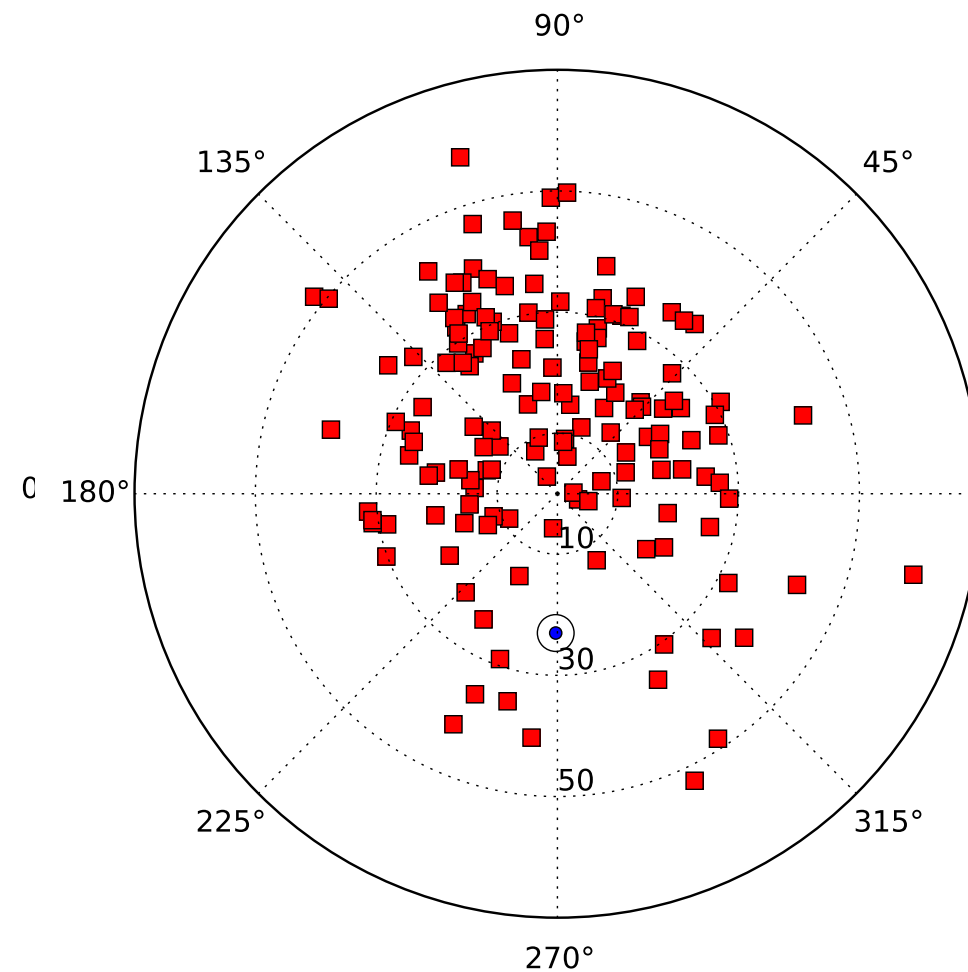
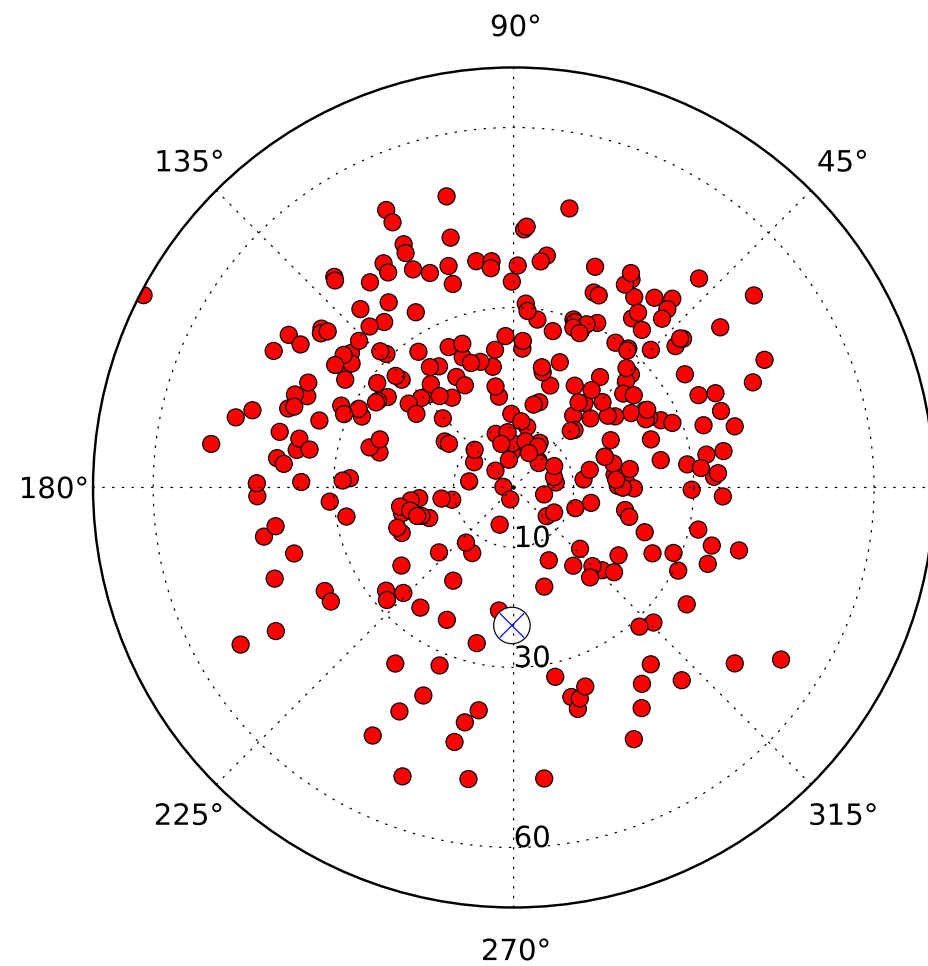




# Arrival direction of showers with strong radio signals

north-south asymmetry

$\mathbf{v} \times \mathbf{B}$  effect



LOFAR

30 - 80 MHz

110 - 190 MHz

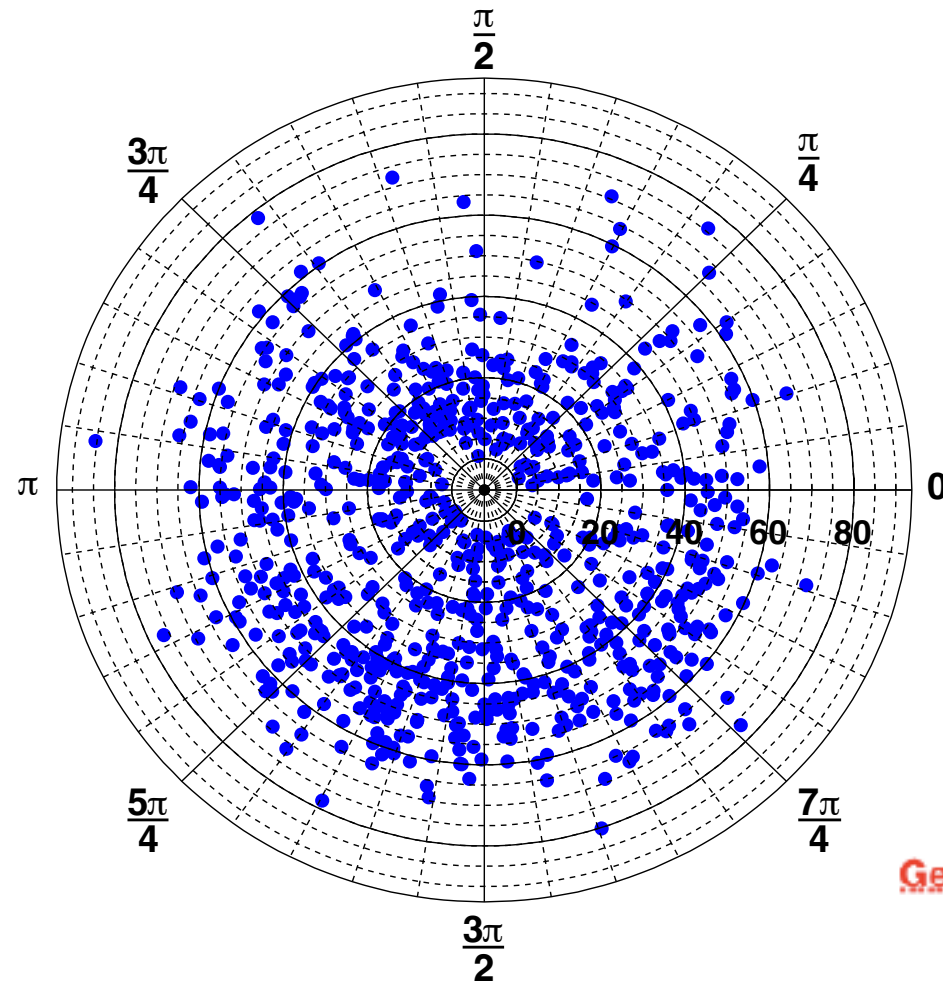
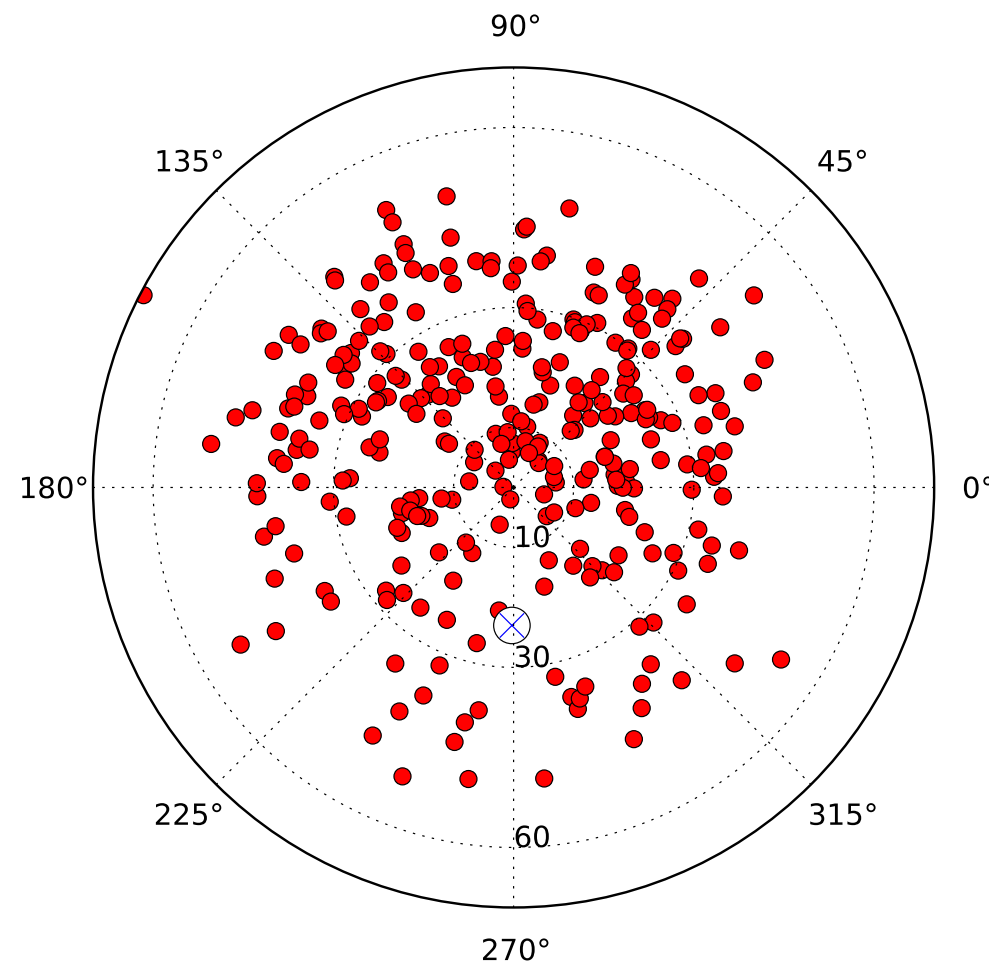
A. Nelles et al., Astroparticle Physics 65 (2015) 11

P. Schellart et al., A&A 560 (2013) A98

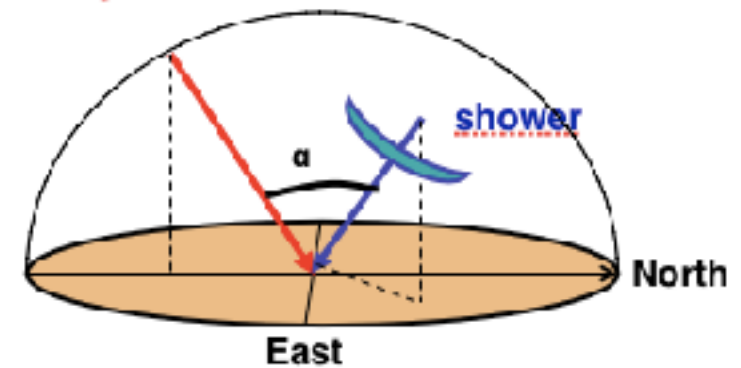
# Arrival direction of showers with strong radio signals

north-south asymmetry

$\mathbf{v} \times \mathbf{B}$  effect



Geomagnetic field



 LOFAR

 AERA  
Auger Engineering Radio Array

30 - 80 MHz



# Geomagnetic effect

T. Huege / Physics Reports 620 (2016) 1–52

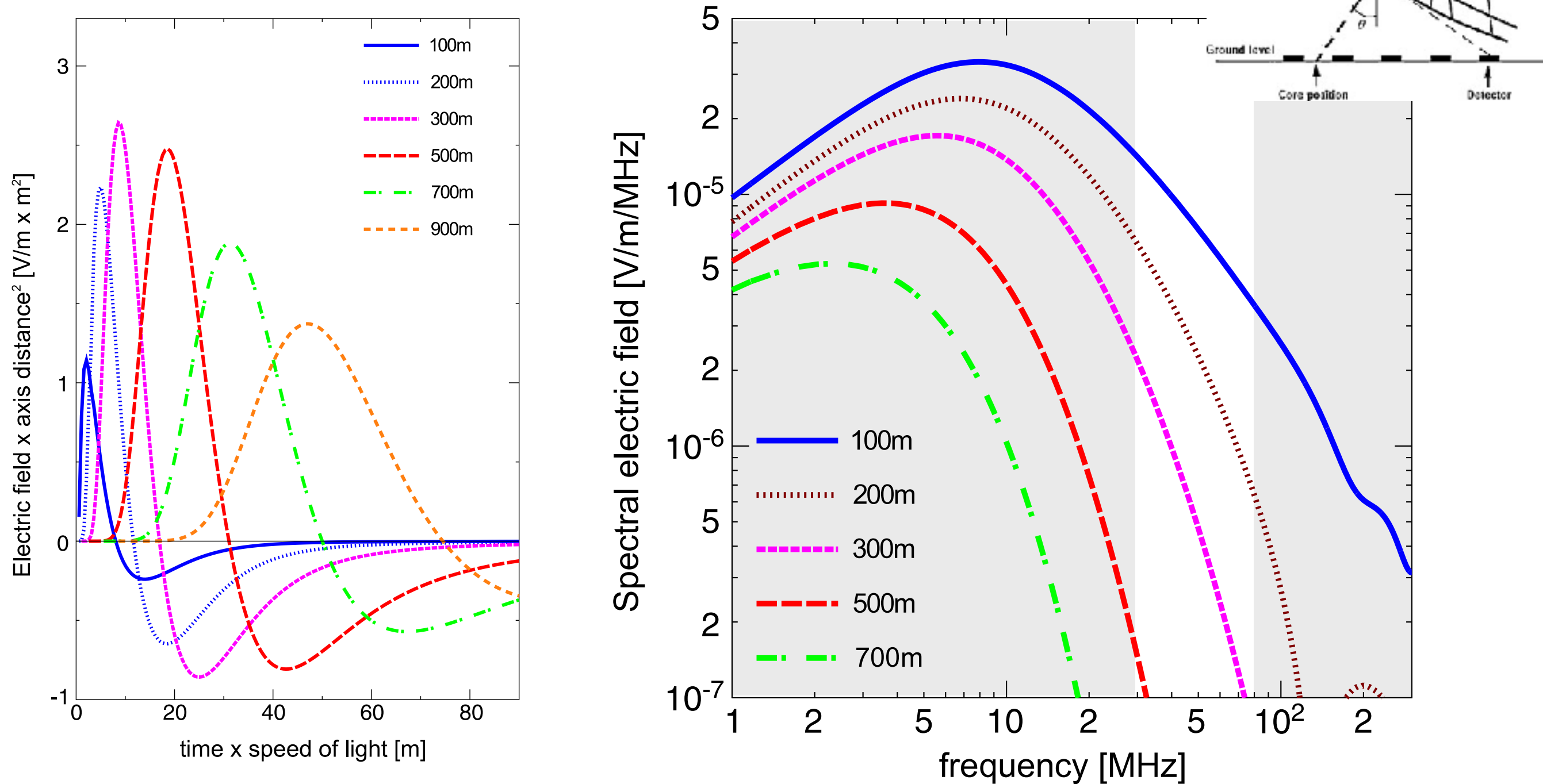


**Fig. 4.** Radio pulses (top) arising from the time-variation of the geomagnetically induced transverse currents in a  $10^{17}$  eV air shower as observed at various observer distances from the shower axis and their corresponding frequency spectra (bottom). Refractive index effects are not included.  
Source: Adapted from [18].

# Radio Emission in Air Showers



Mainly: Charge separation in geomagnetic field

$$\vec{E} \propto \vec{v} \times \vec{B}$$

Theory predicts additional mechanisms:



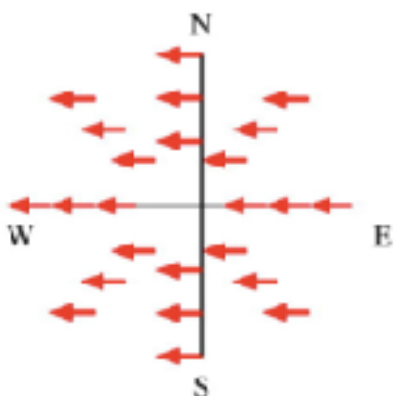
excess of electrons in shower: charge excess



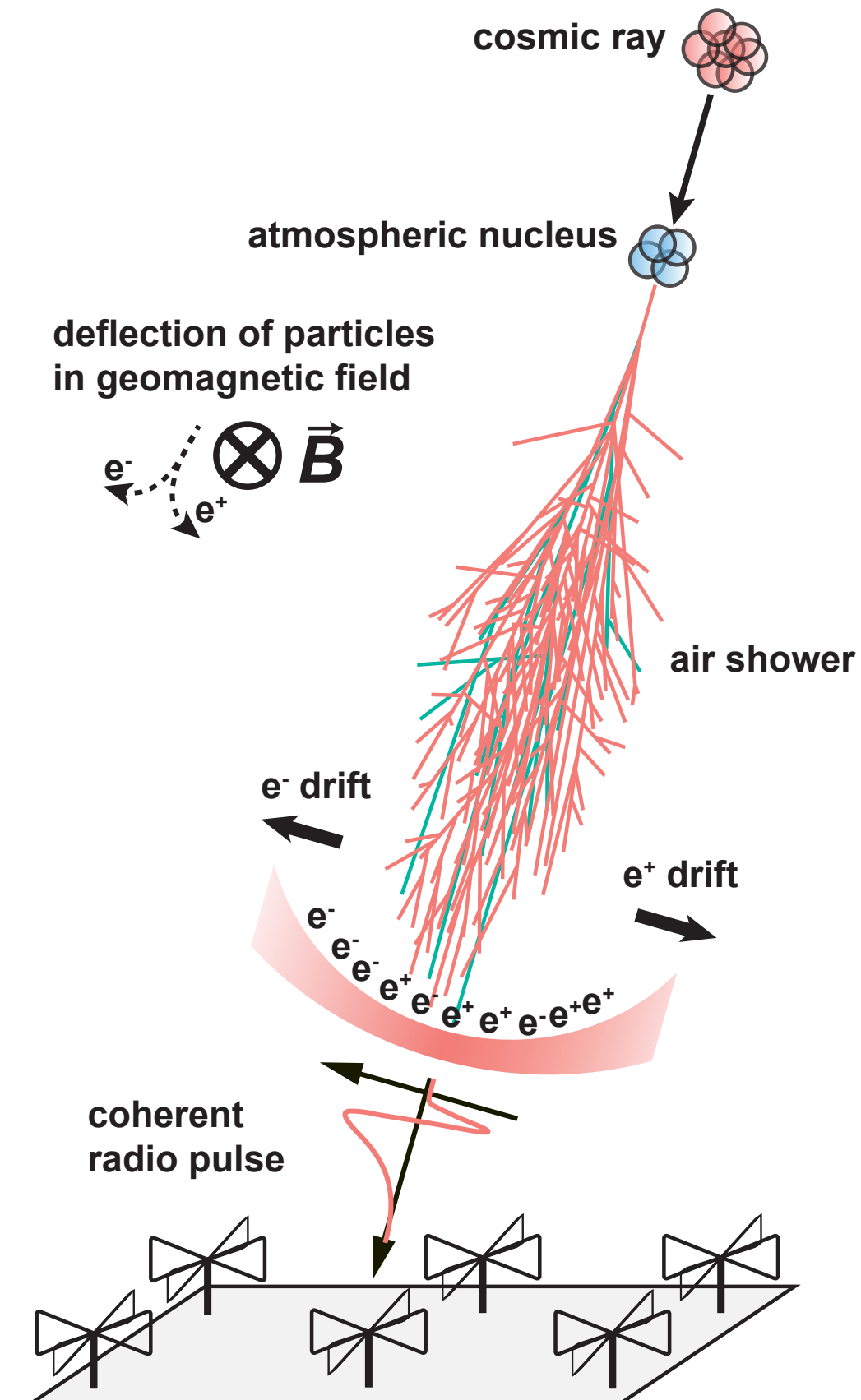
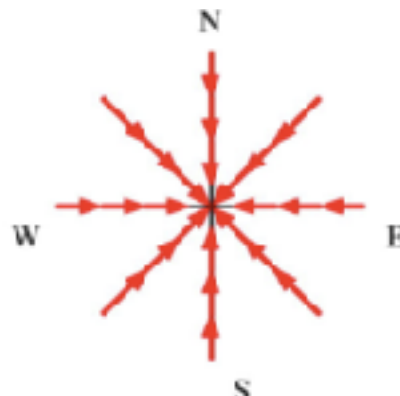
superposition of emission due to Cherenkov effects in atmosphere

## polarization of radio signal

geomagnetic



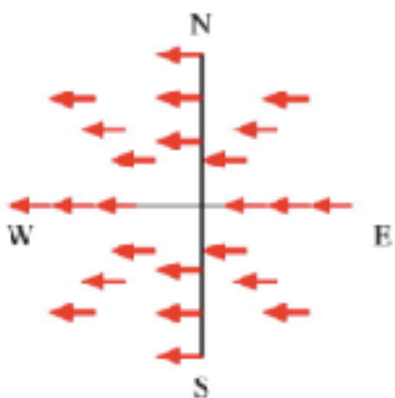
Askaryan



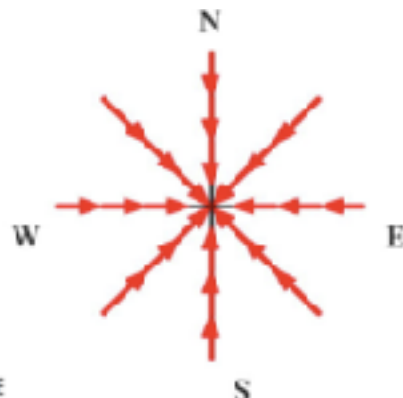


# Polarization footprint of an individual air shower

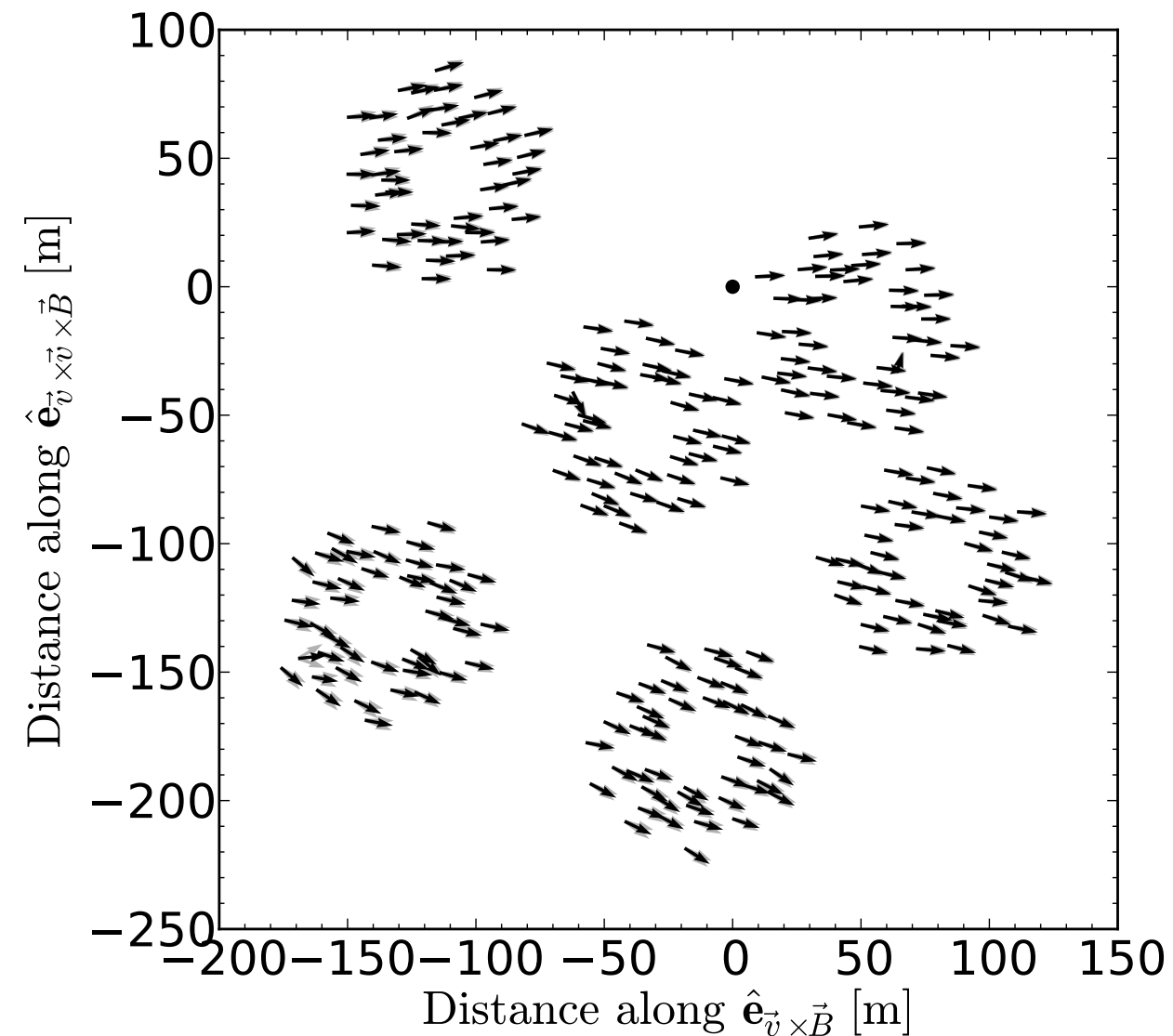
geomagnetic



Askaryan

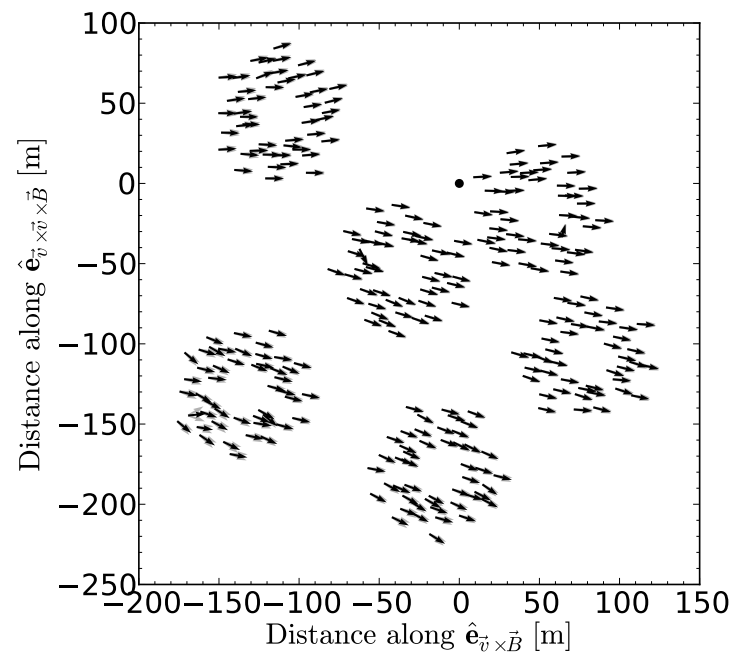


LOFAR



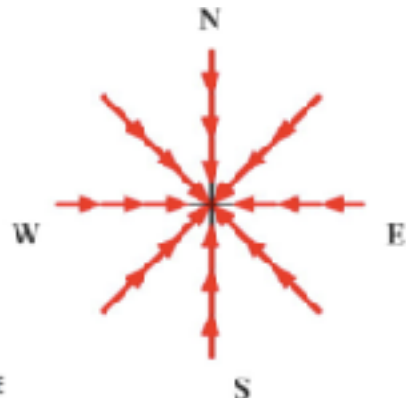
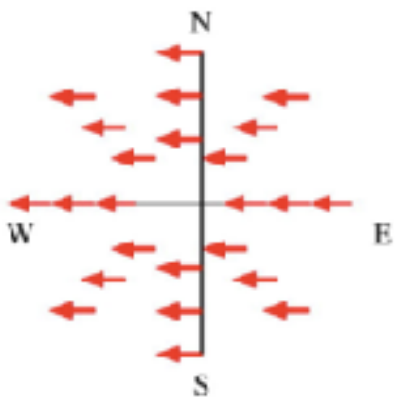
P. Schellart et al., JCAP 10 (2014) 014

# Polarization footprint of an individual air shower



geomagnetic

Askaryan

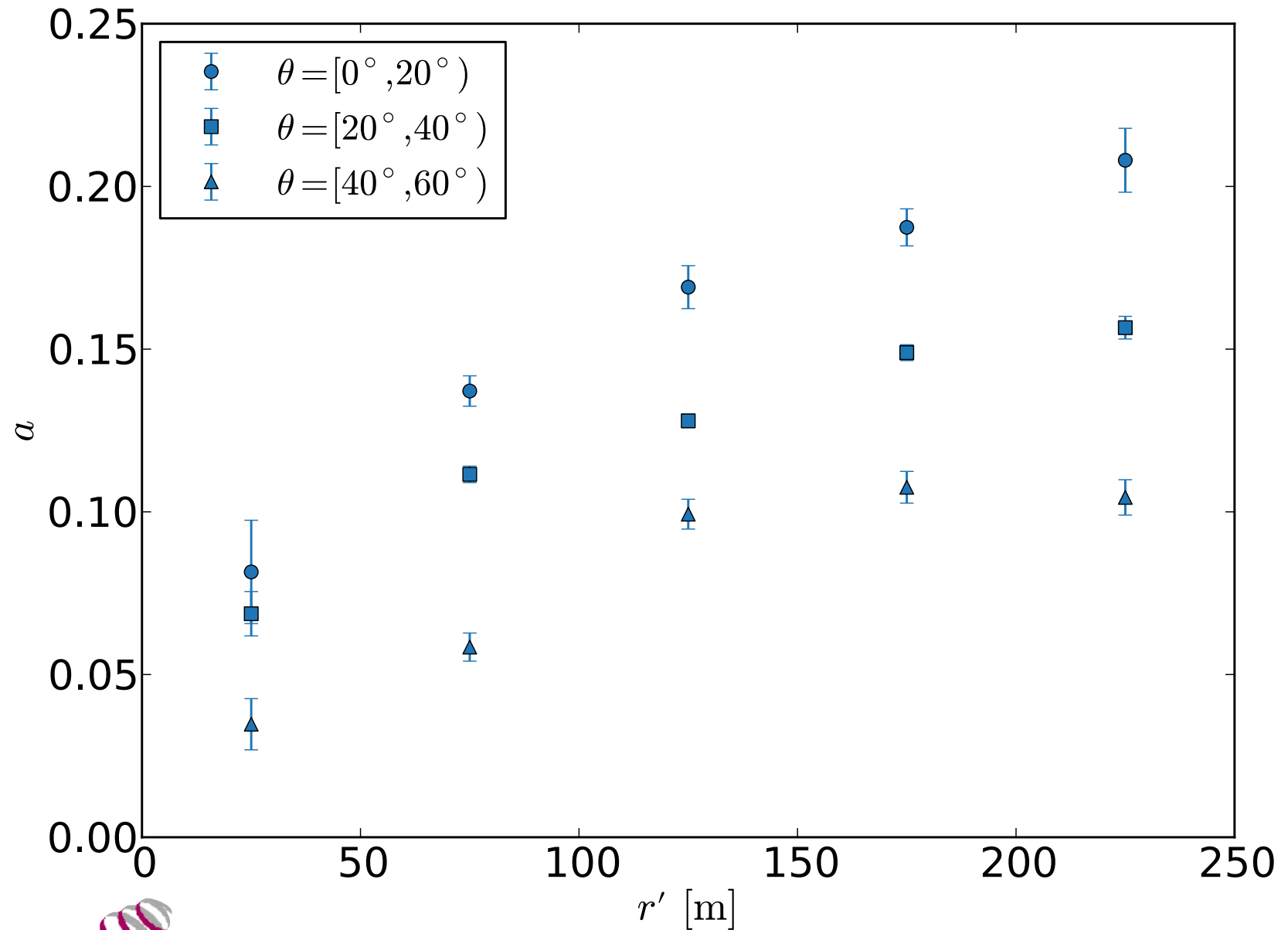
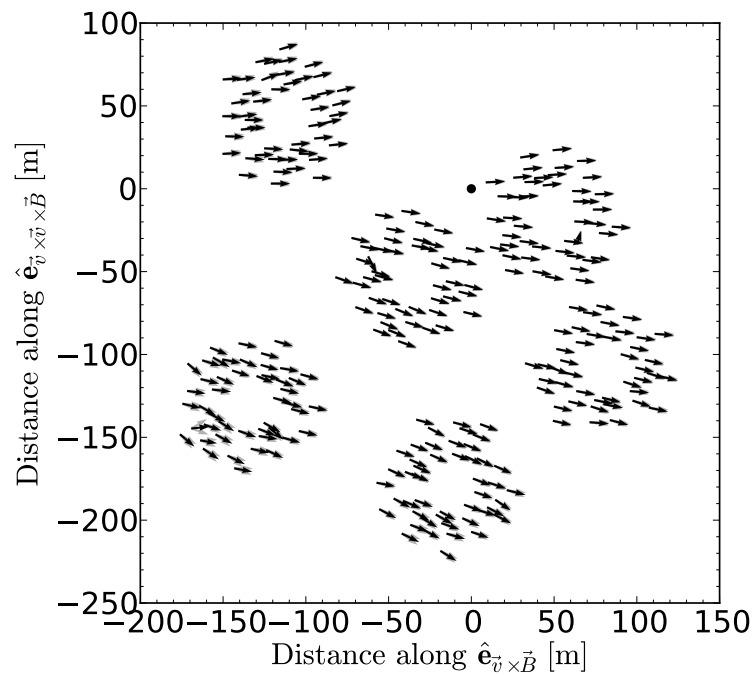


P. Schellart et al., JCAP 10 (2014) 014



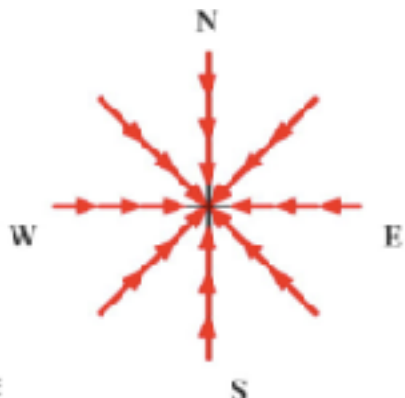
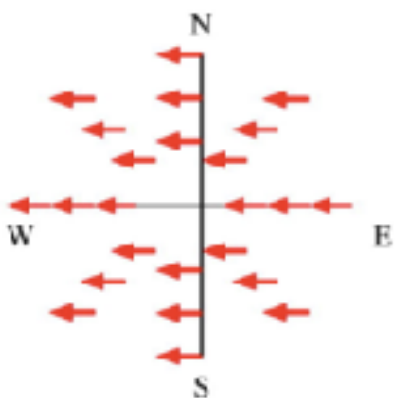
# Charge excess fraction

## Askaryan geomagnetic



geomagnetic

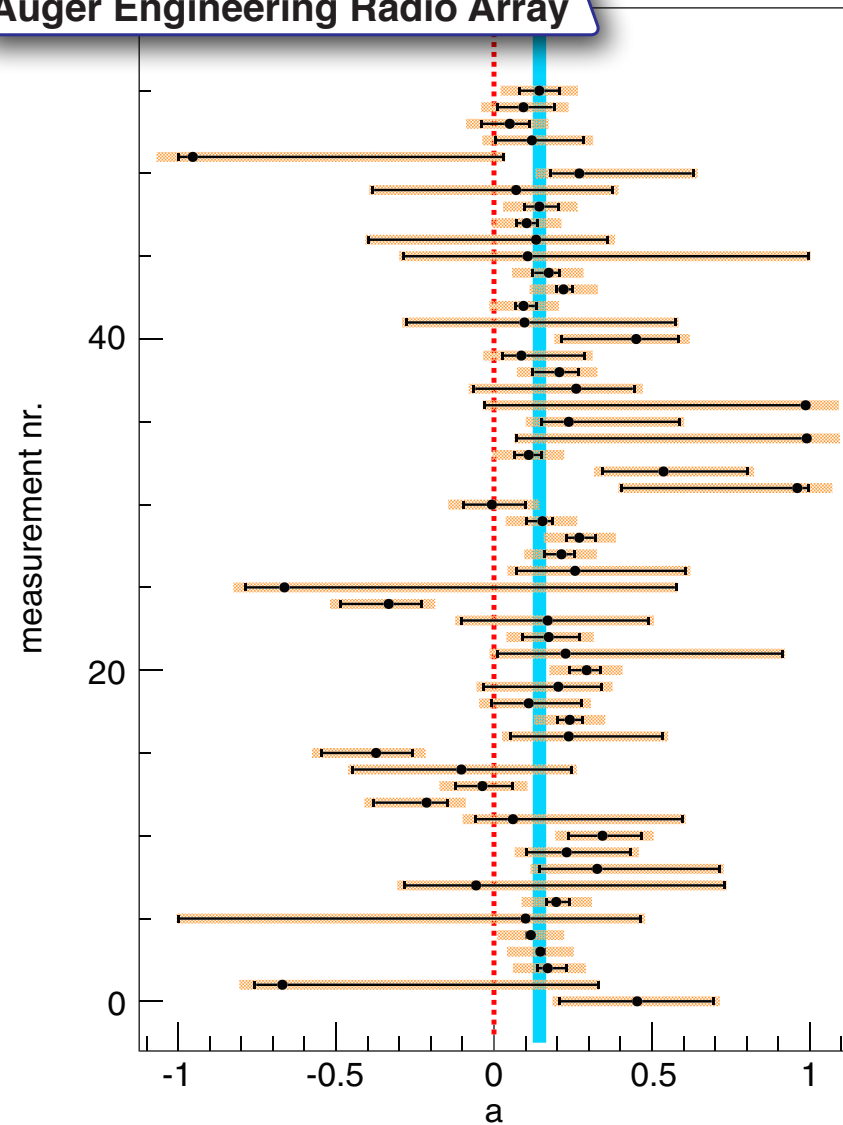
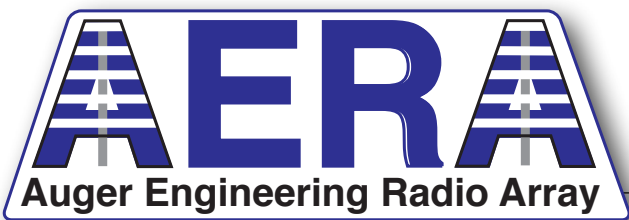
Askaryan



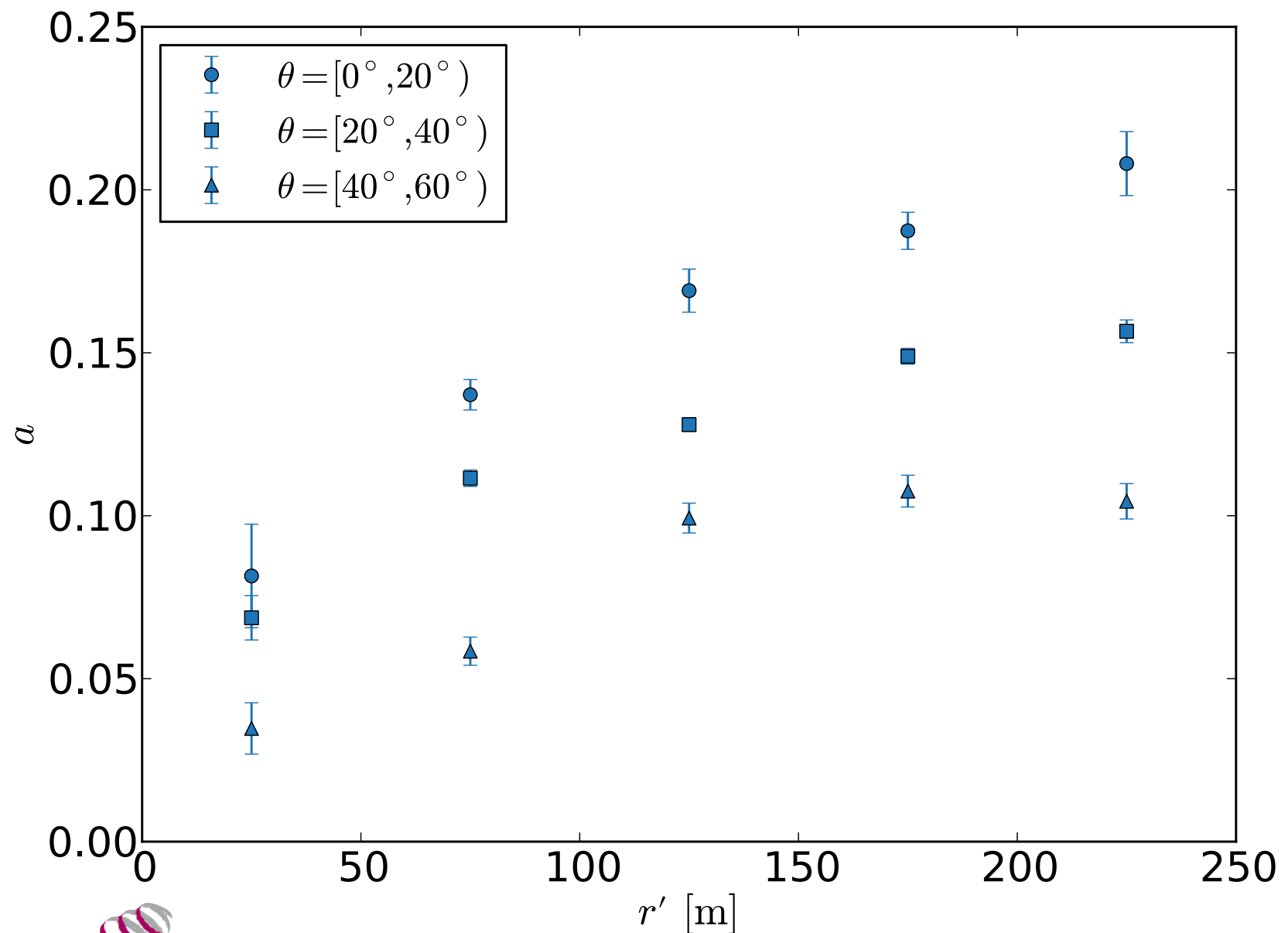
LOFAR

P. Schellart et al., JCAP 10 (2014) 014

# Charge excess fraction

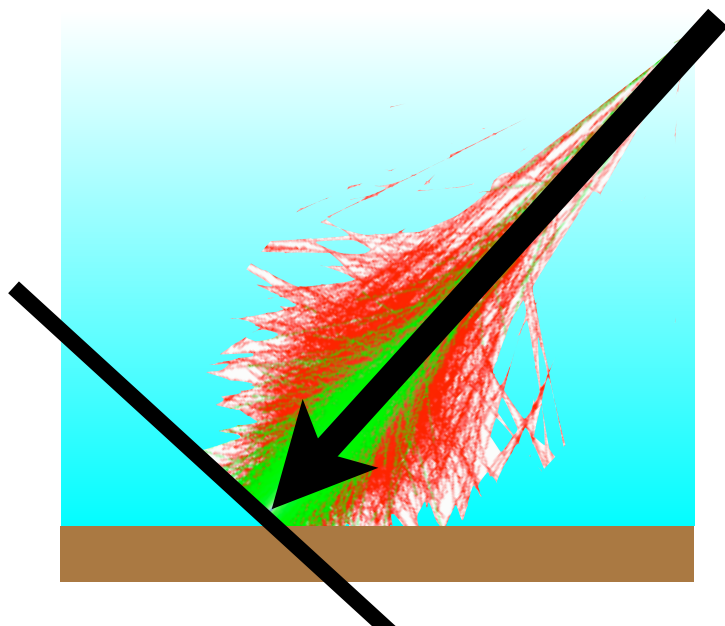
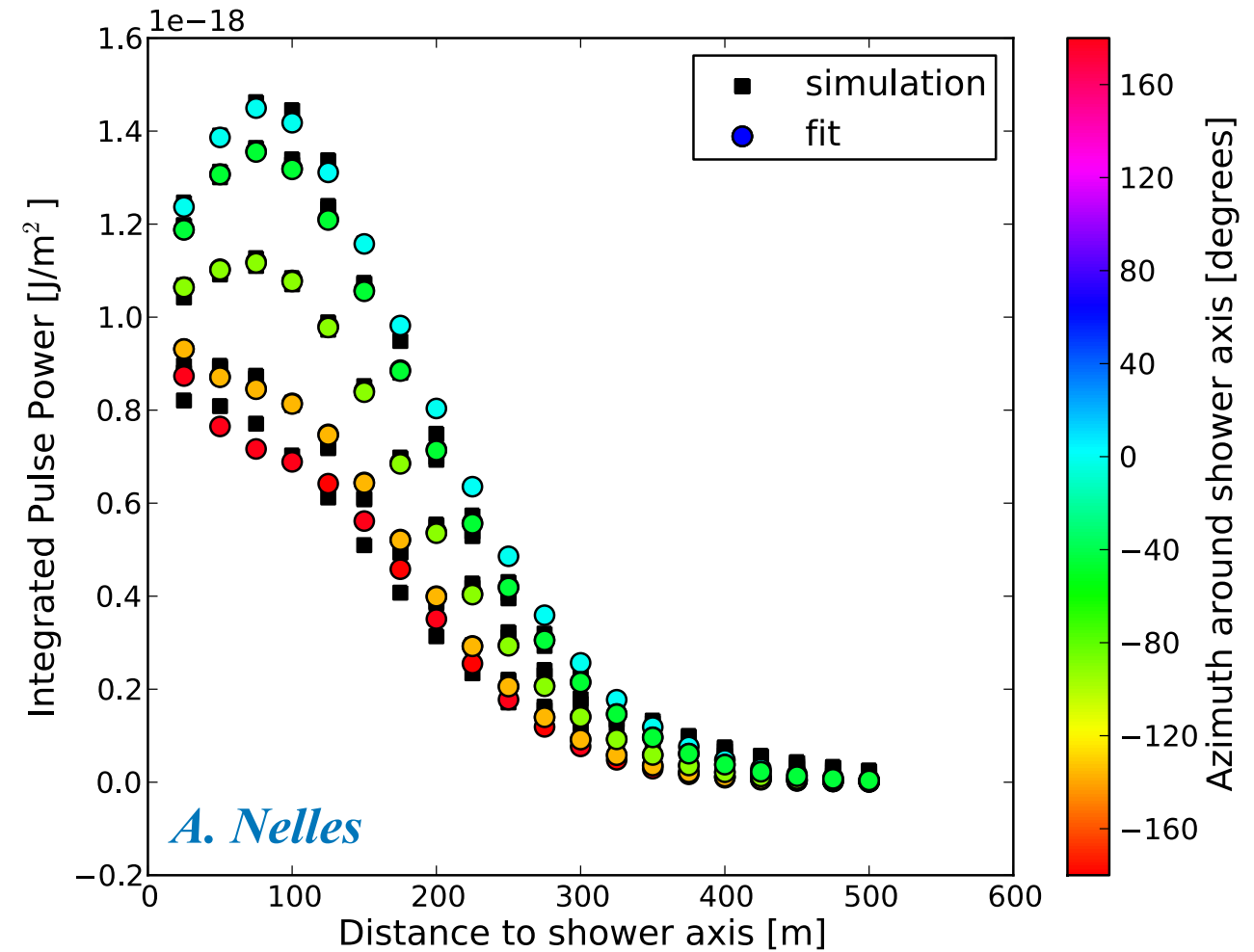
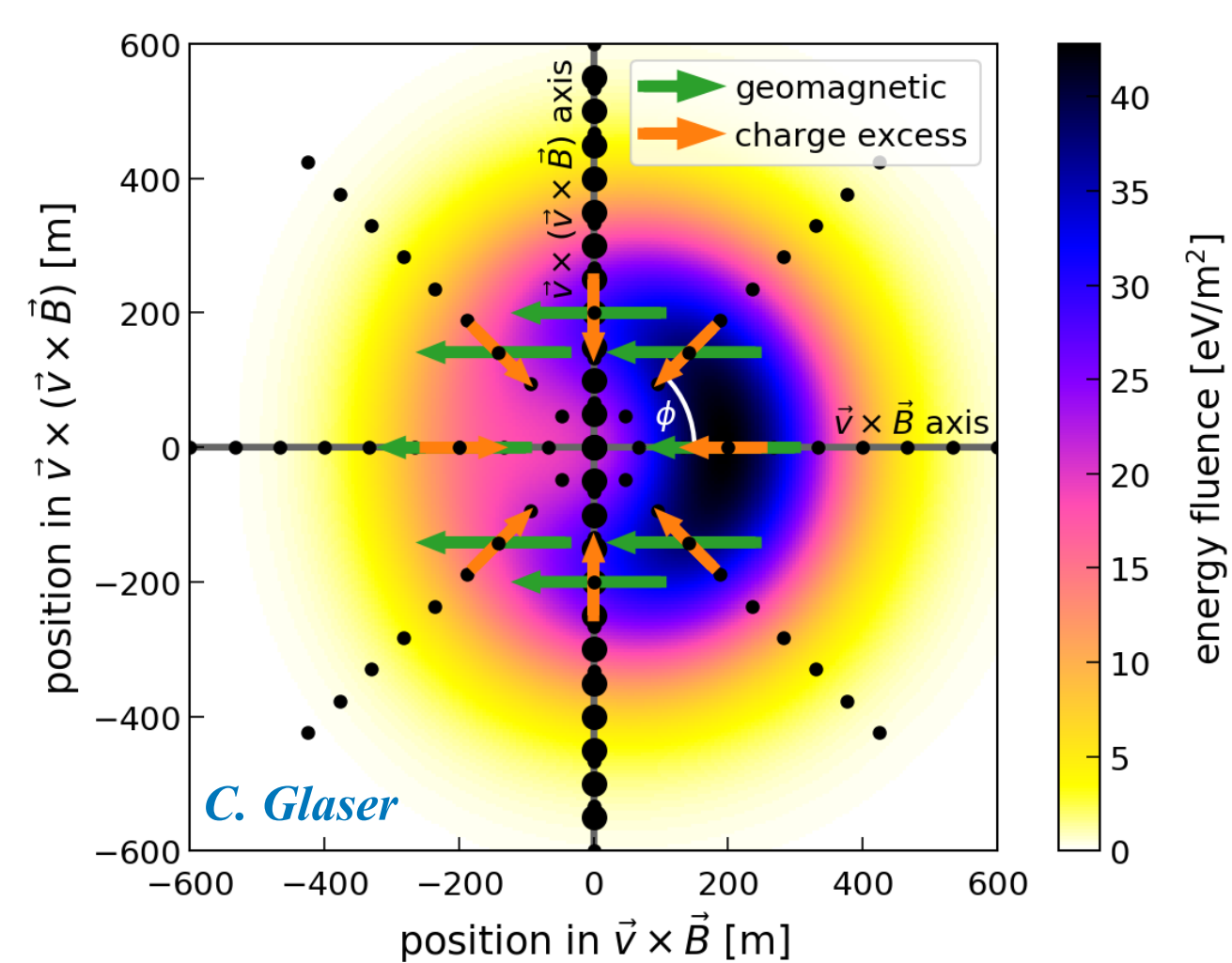


Askaryan  
geomagnetic





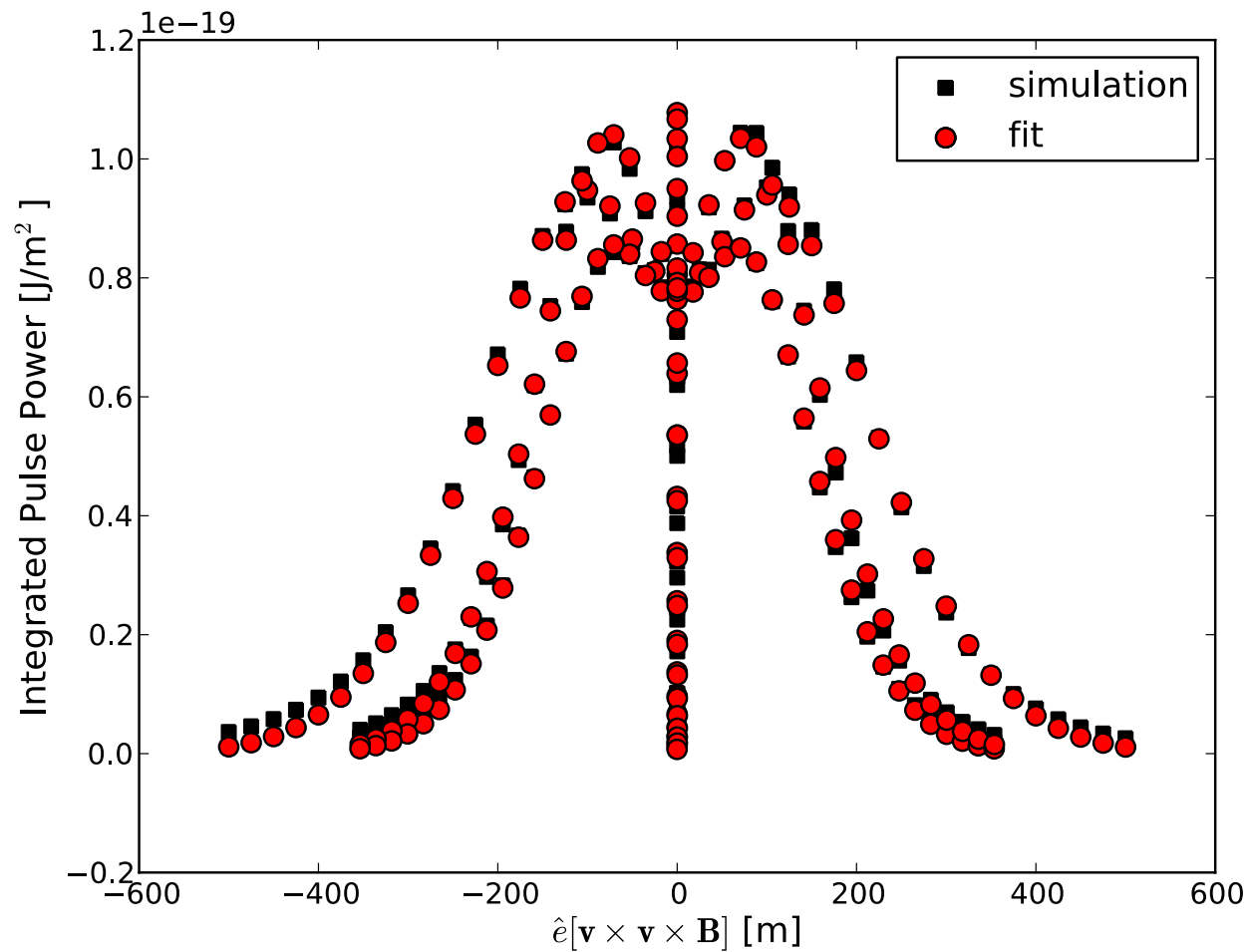
# Footprint of radio emission on the ground



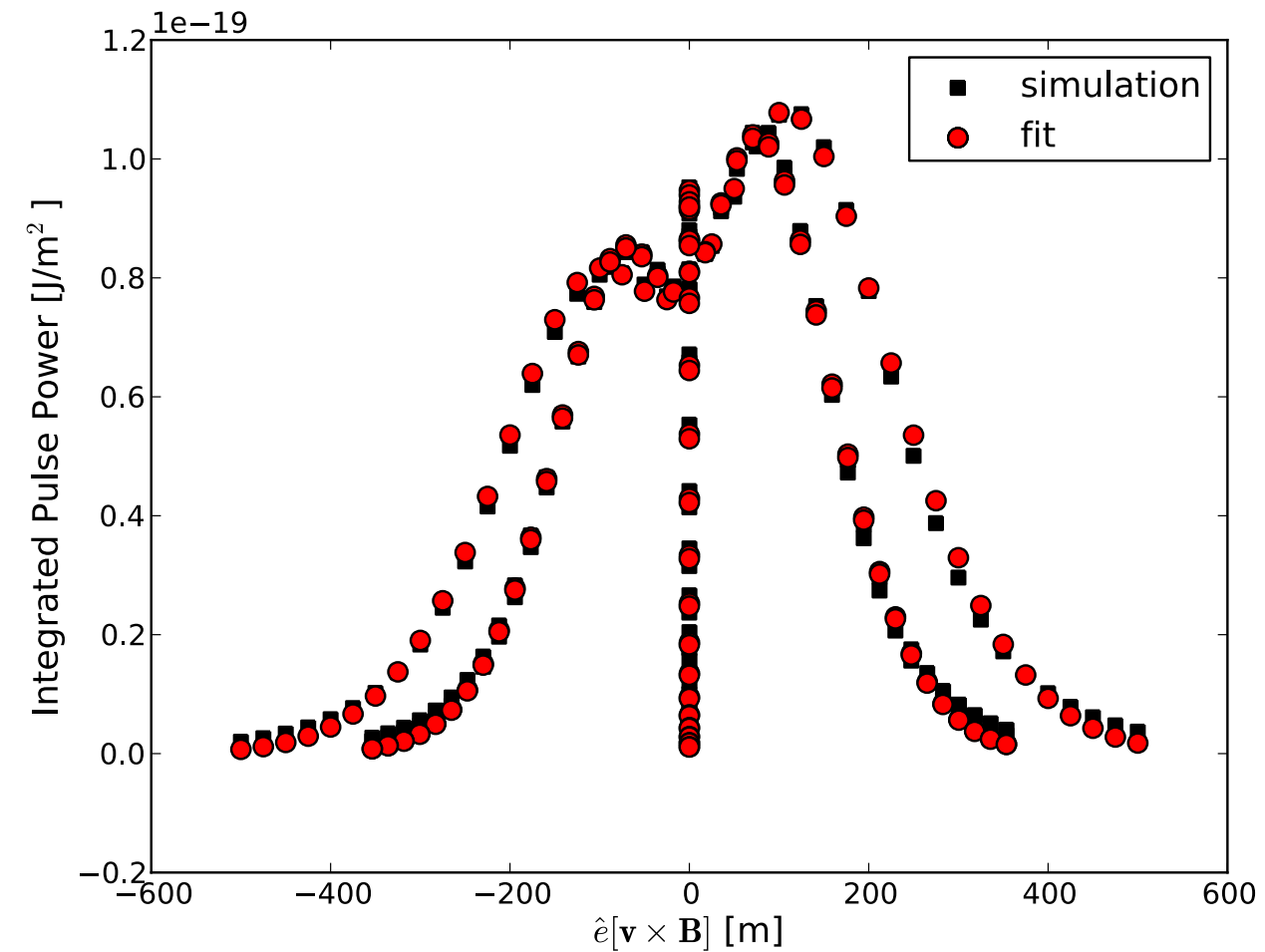
# Lateral distribution of radio signals

not rotationally symmetric → fit two Gaussian functions

$\mathbf{v} \times (\mathbf{v} \times \mathbf{B})$



$\mathbf{v} \times \mathbf{B}$



$$P(x', y') = A_+ \cdot \exp\left(\frac{-[(x' - X_+)^2 + (y' - Y_+)^2]}{\sigma_+^2}\right) - A_- \cdot \exp\left(\frac{-[(x' - X_-)^2 + (y' - Y_-)^2]}{\sigma_-^2}\right) + O$$



# Properties of incoming cosmic ray

- **direction**
- **energy**
- **type**

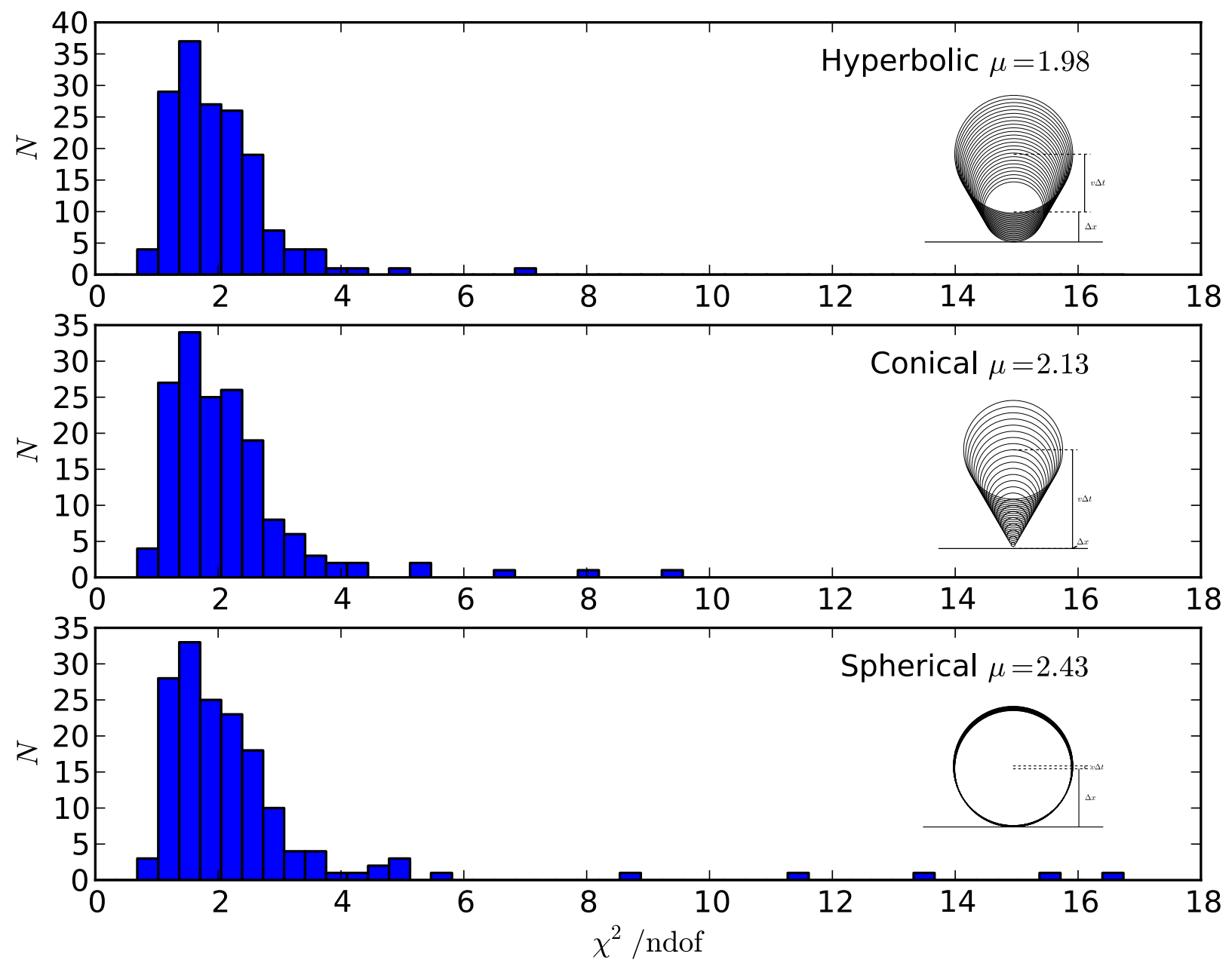
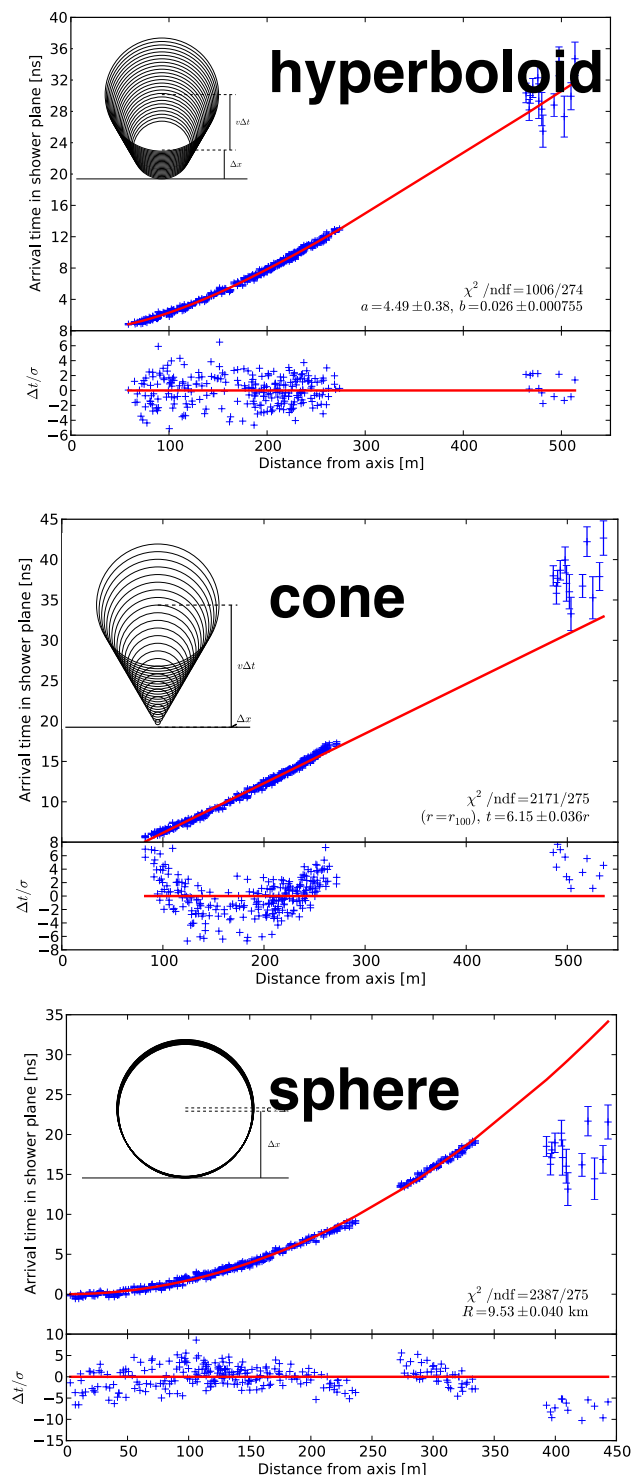
# Direction



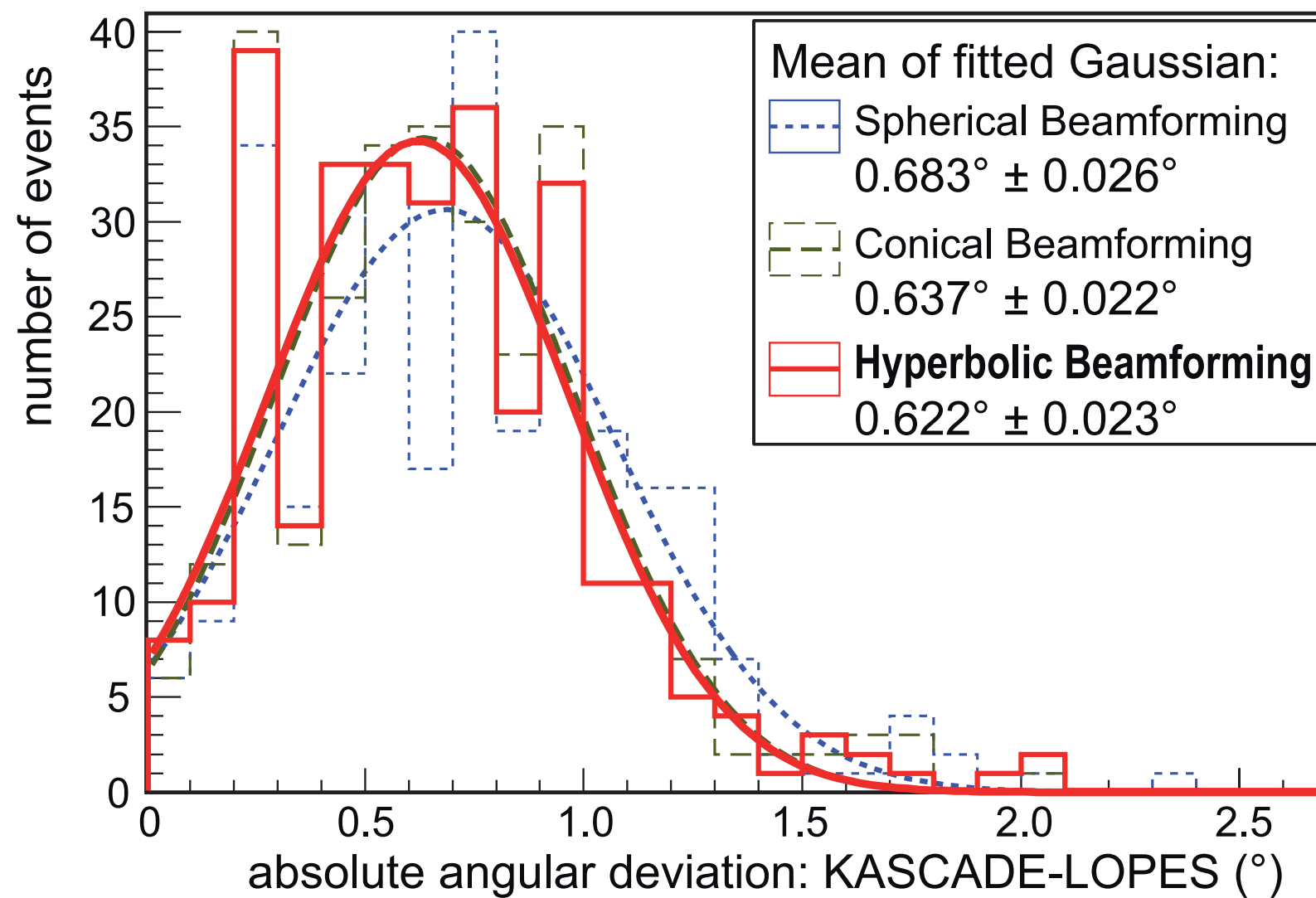
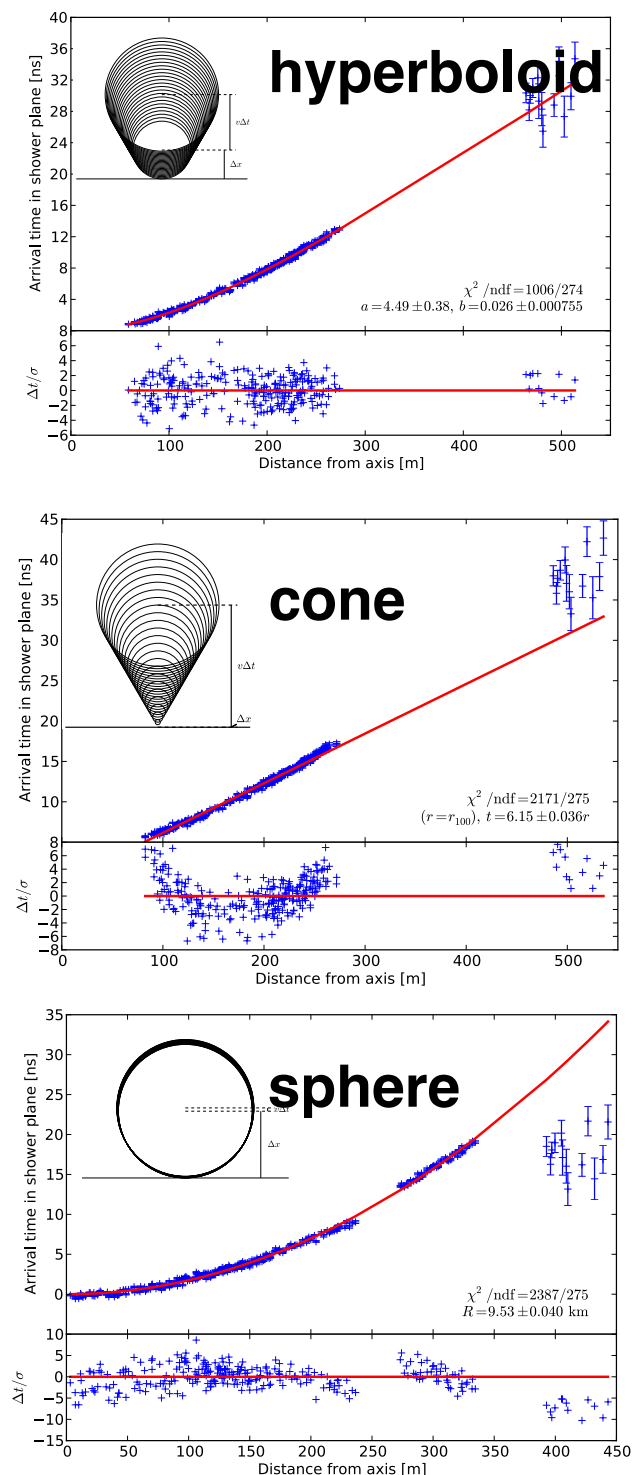


# Shape of Shower Front

## fit quality



# Shape of Shower Front

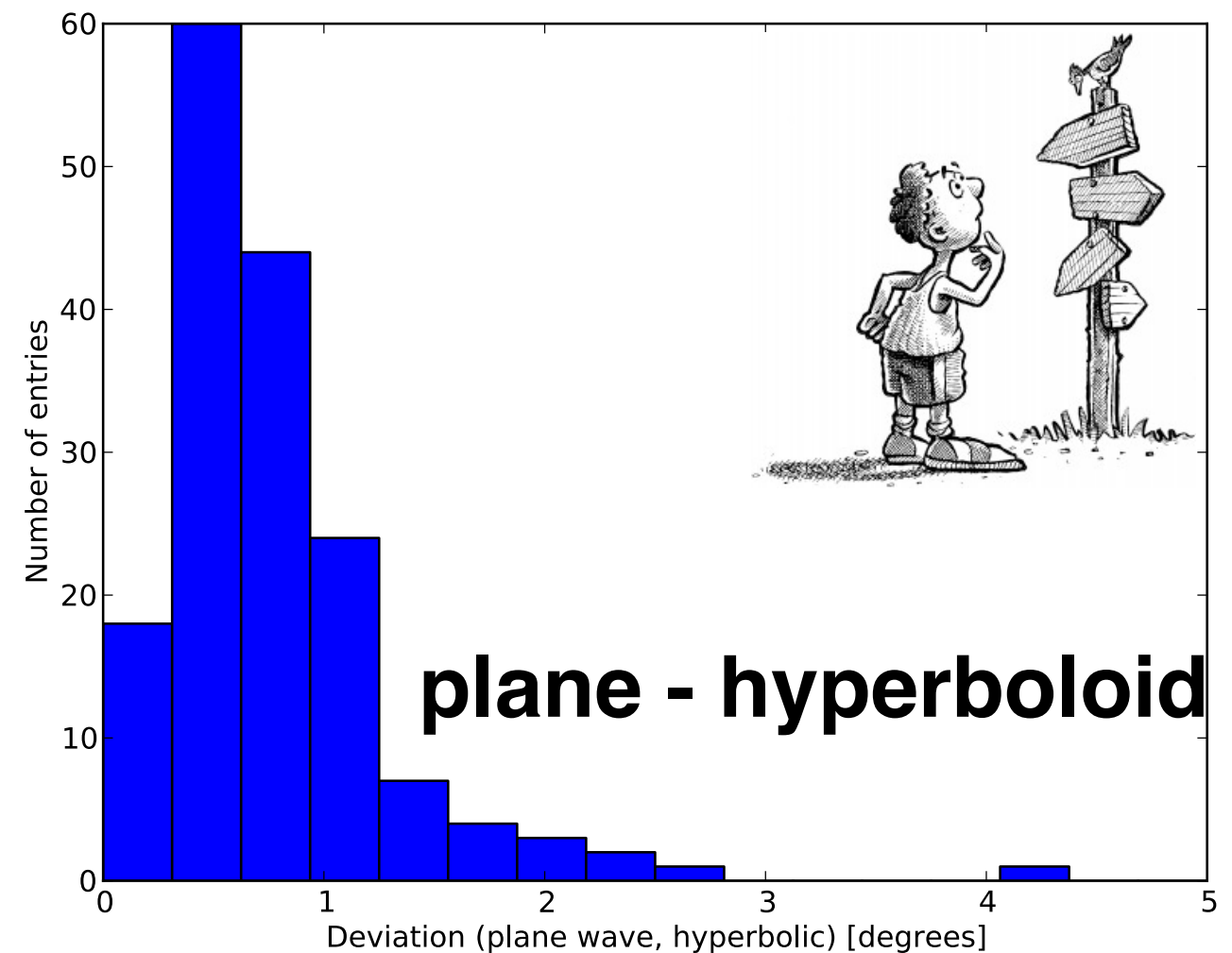
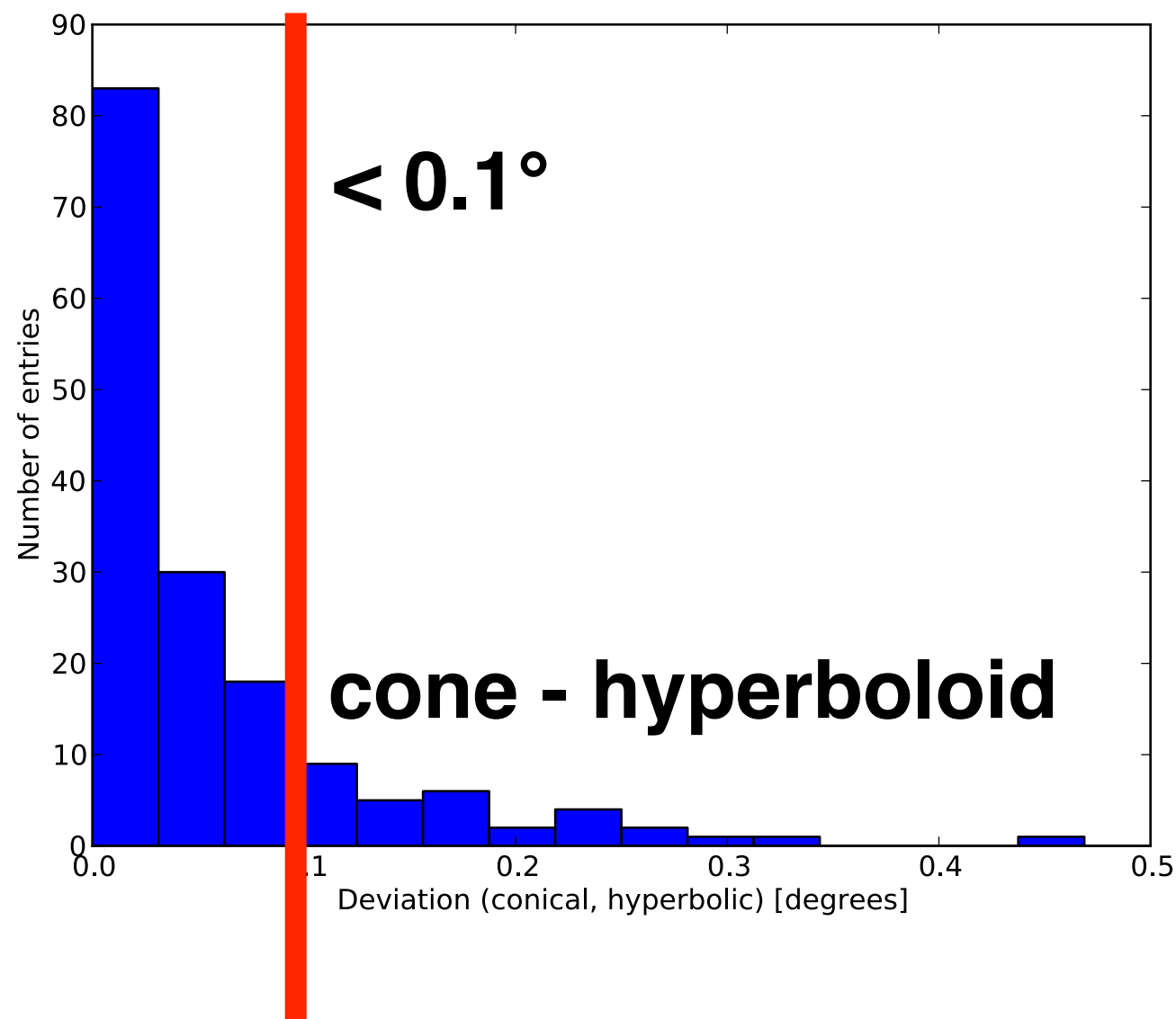


W.D. Apel et al., JCAP 1409 (2014) no.09, 025



# Accuracy of Shower Direction

angular difference  
between..

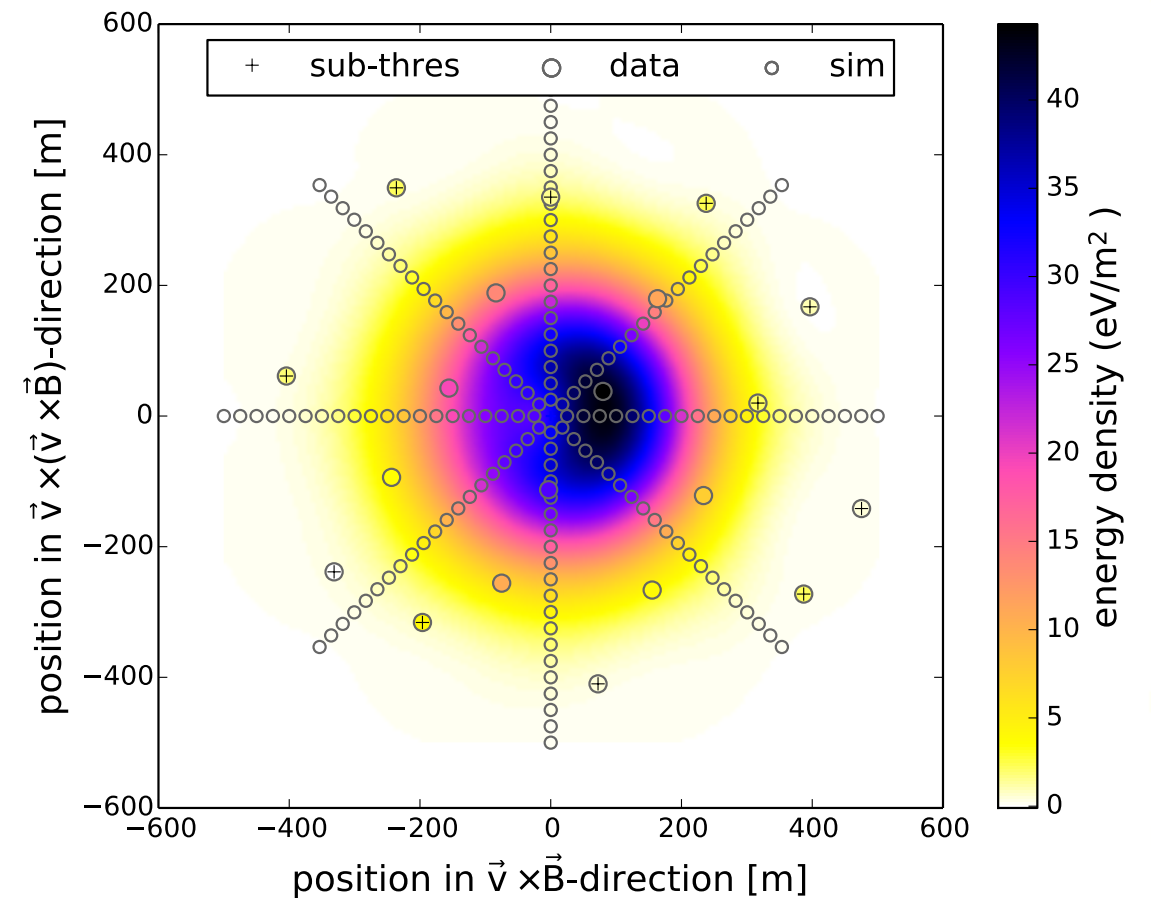
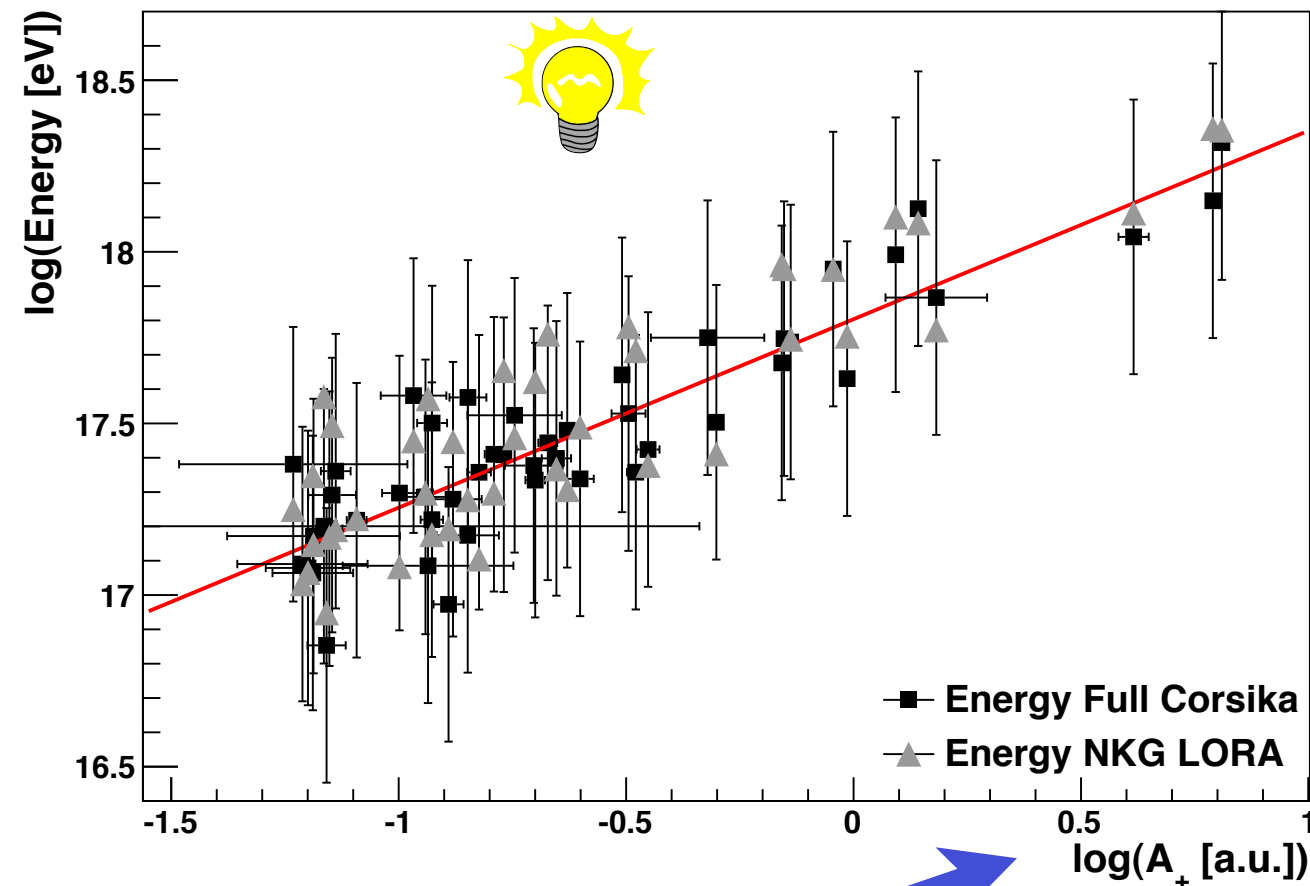


# Energy



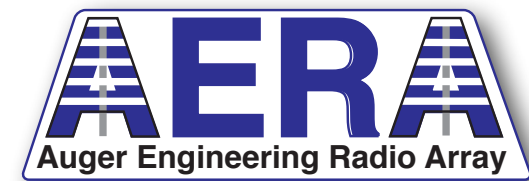
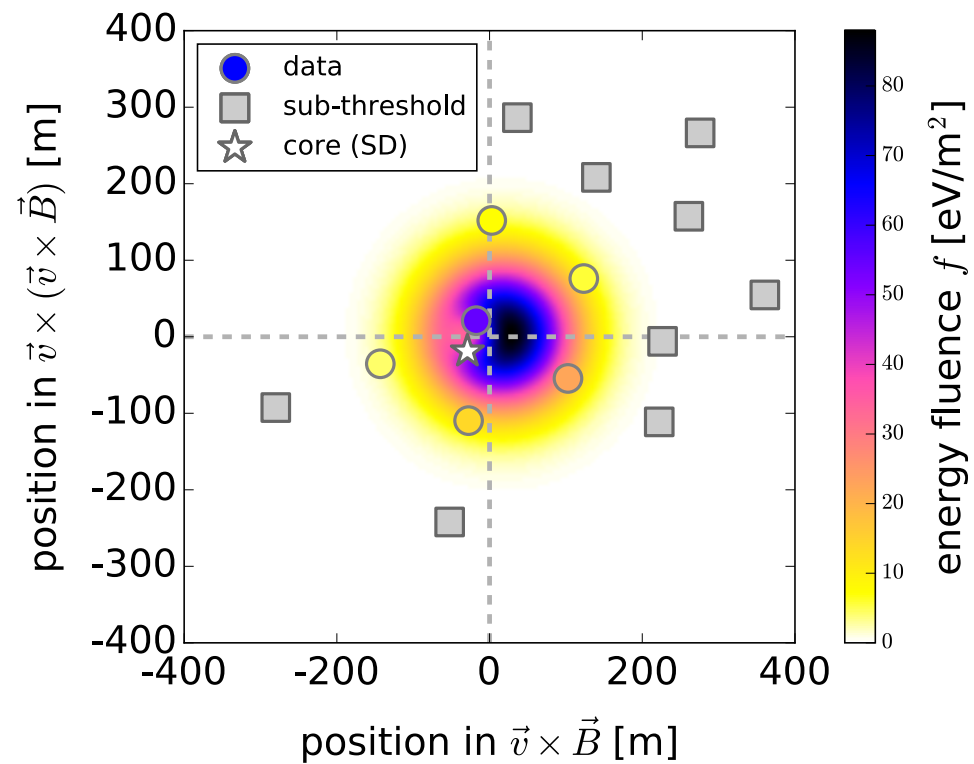


# Energy of primary particle

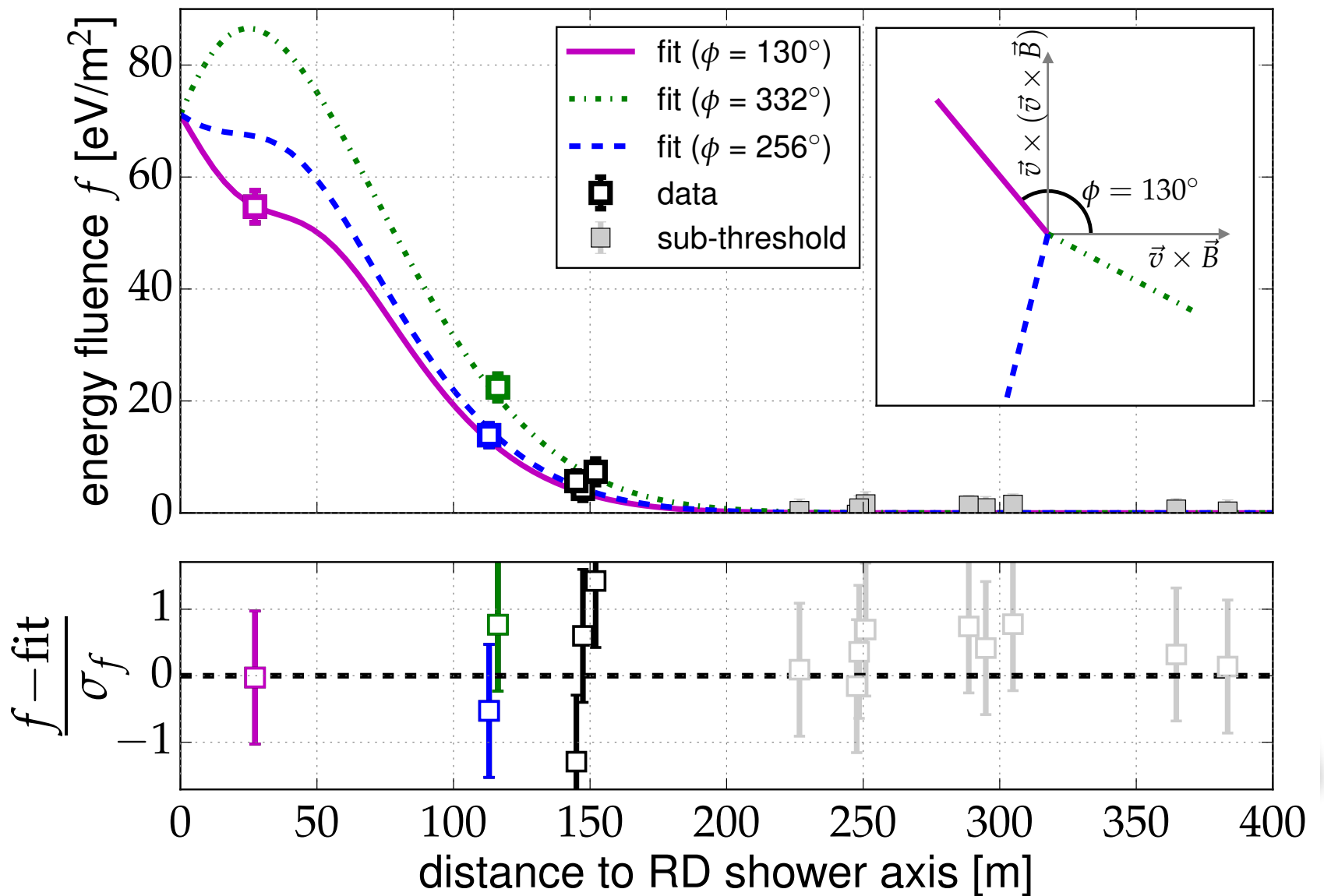
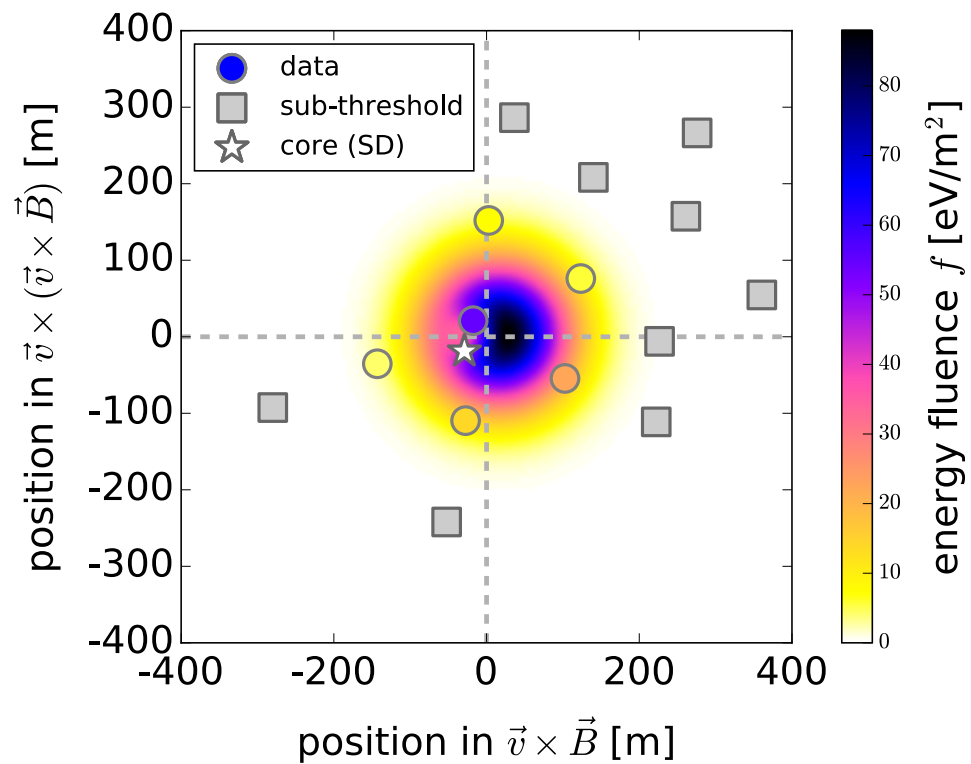


$$P(x', y') = A_+ \cdot \exp\left(\frac{-[(x' - X_+)^2 + (y' - Y_+)^2]}{\sigma_+^2}\right) - A_- \cdot \exp\left(\frac{-[(x' - X_-)^2 + (y' - Y_-)^2]}{\sigma_-^2}\right) + O$$

# Measurement of the Radiation Energy in the Radio Signal of Extensive Air Showers as a Universal Estimator of Cosmic-Ray Energy

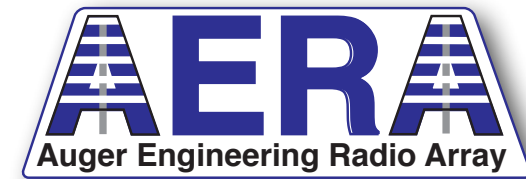
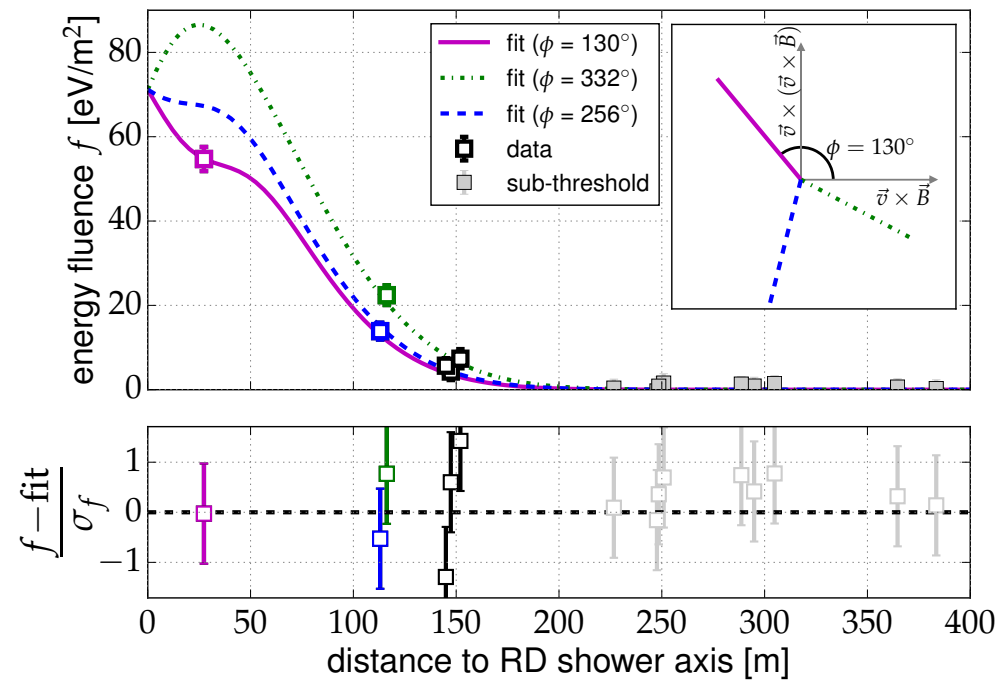
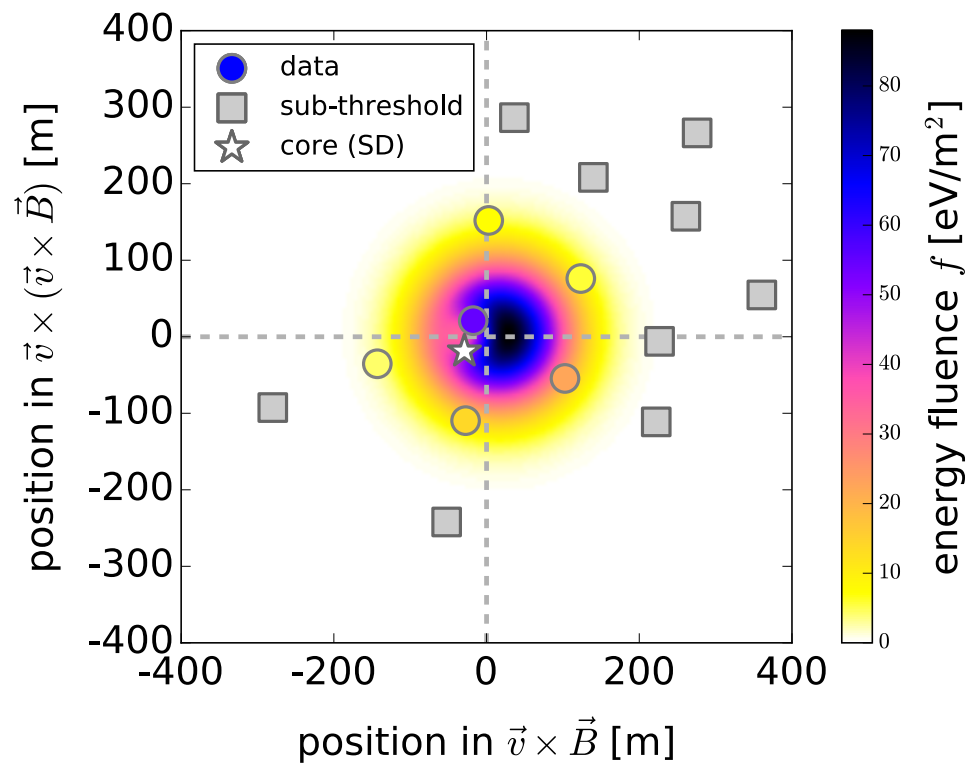


# Measurement of the Radiation Energy in the Radio Signal of Extensive Air Showers as a Universal Estimator of Cosmic-Ray Energy

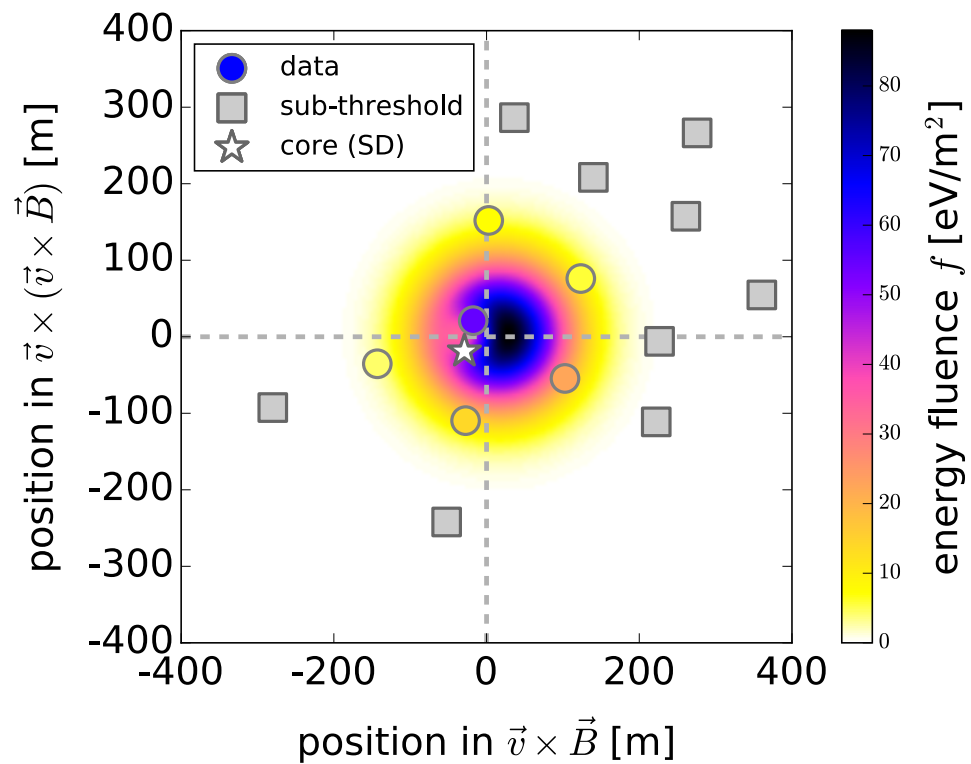




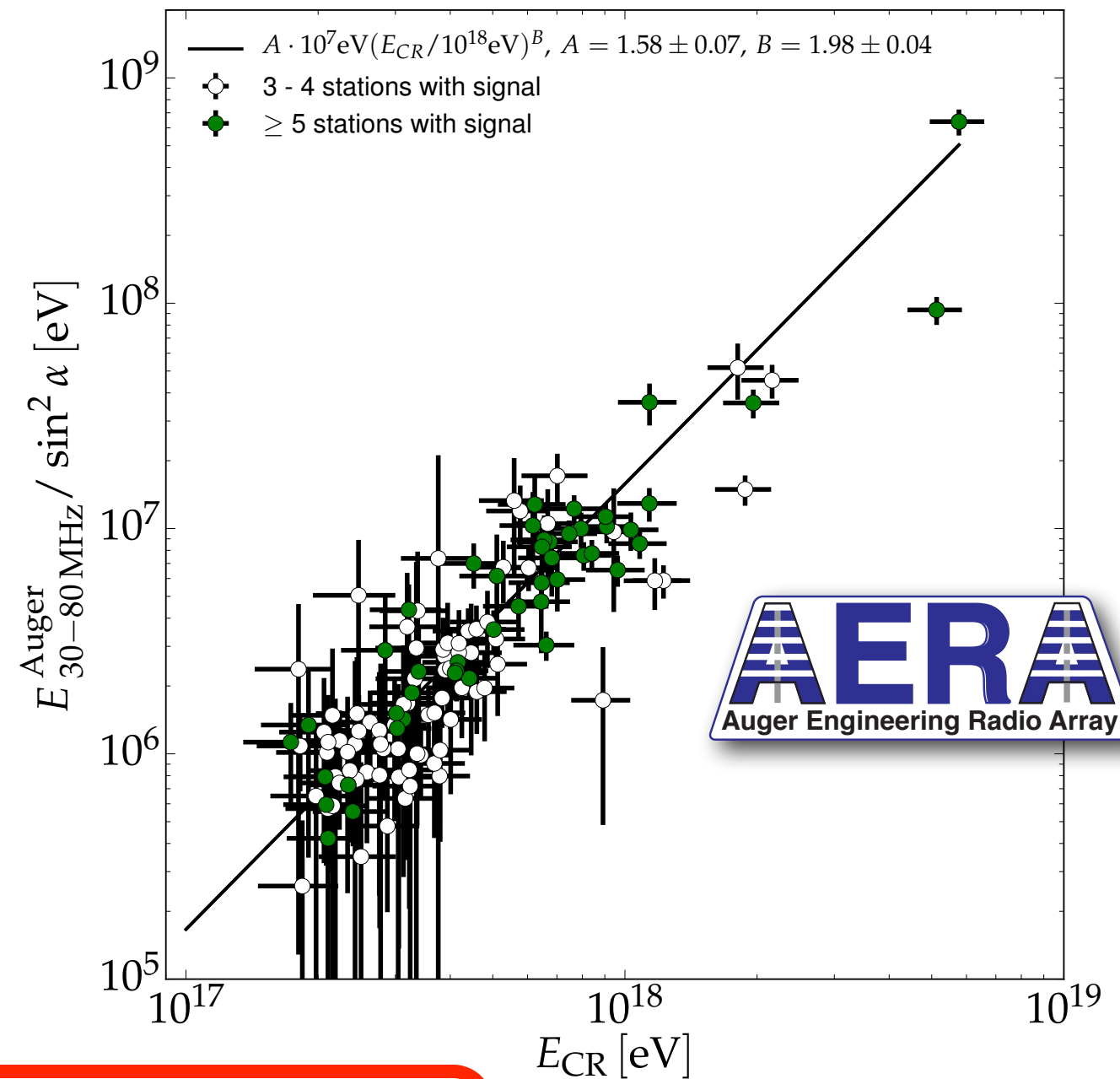
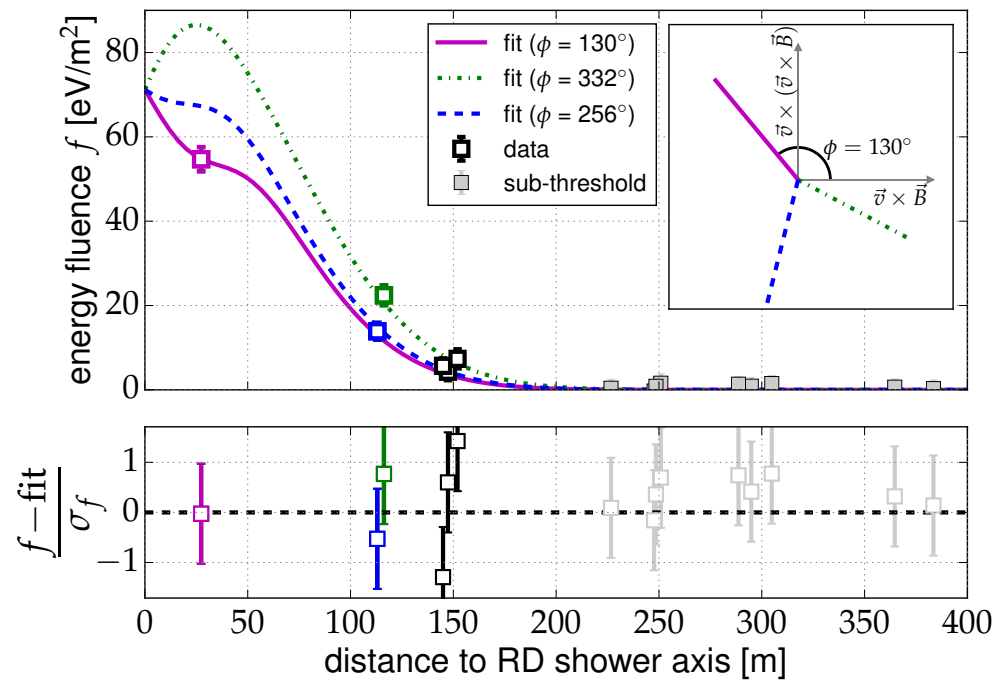
# Measurement of the Radiation Energy in the Radio Signal of Extensive Air Showers as a Universal Estimator of Cosmic-Ray Energy



# Measurement of the Radiation Energy in the Radio Signal of Extensive Air Showers as a Universal Estimator of Cosmic-Ray Energy



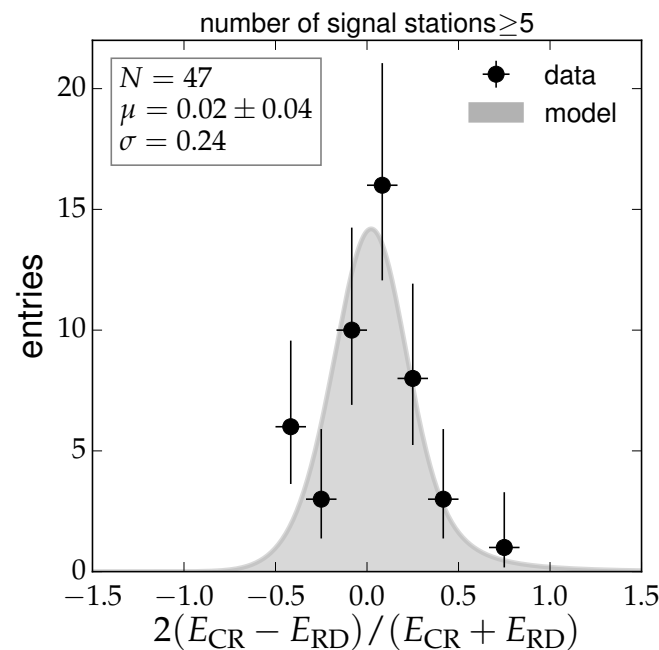
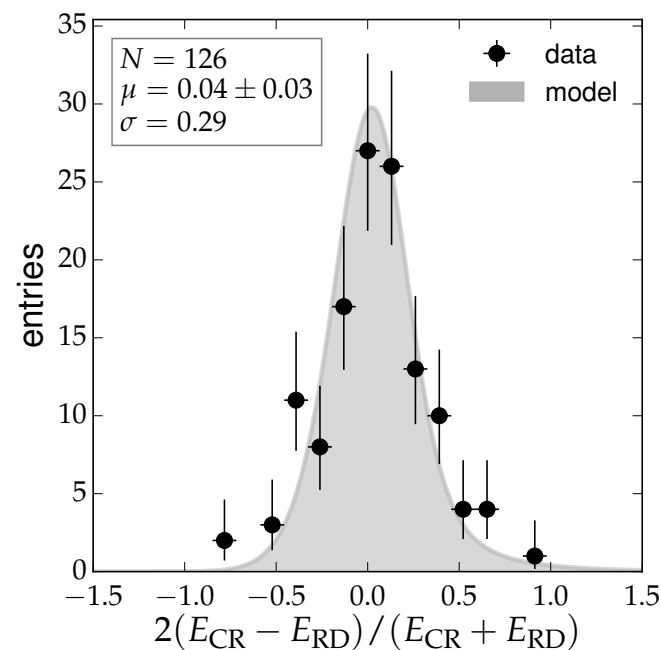
$$E_{30-80 \text{ MHz}} = 15.8 \text{ MeV} @ 10^{18} \text{ eV}$$



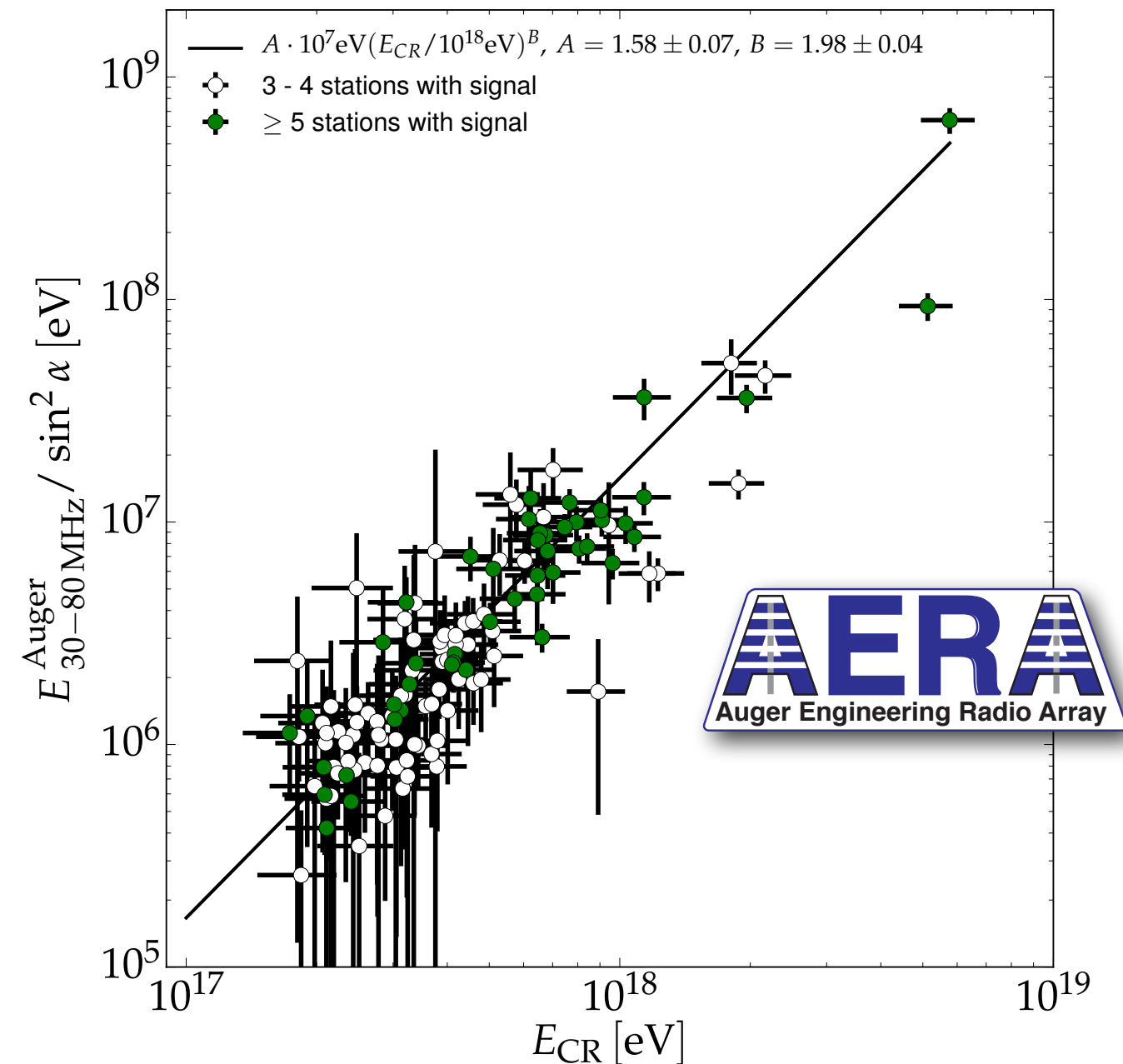
$$E_{30-80 \text{ MHz}} = (15.8 \pm 0.7(\text{stat}) \pm 6.7(\text{syst}) \text{ MeV}) \times \left( \sin \alpha \frac{E_{CR}}{10^{18} \text{ eV}} \frac{B_{Earth}}{0.24 \text{ G}} \right)^2$$

# Energy Estimation of Cosmic Rays with the Engineering Radio Array of the Pierre Auger Observatory

$$E_{30-80} \text{ MHz} = 15.8 \text{ MeV} @ 10^{18} \text{ eV}$$



$$\sigma \approx 24\%$$





# Cosmic-ray energy (Cherenkov) vs radio signal

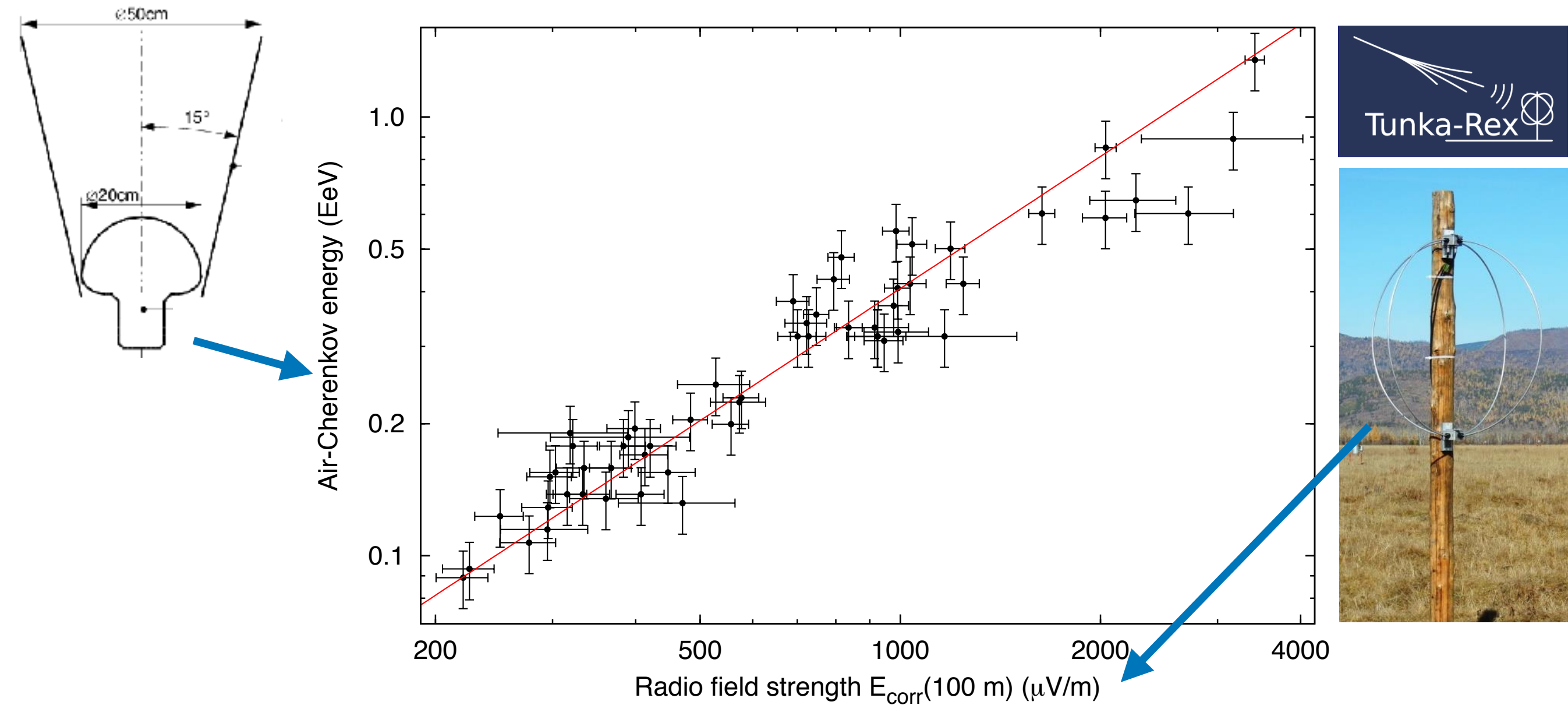


**Fig. 3.** Correlation of the energy measured with the air-Cherenkov array and an energy estimator based on the radio amplitude at 100 m measured with Tunka-Rex. The line indicates a linear correlation.

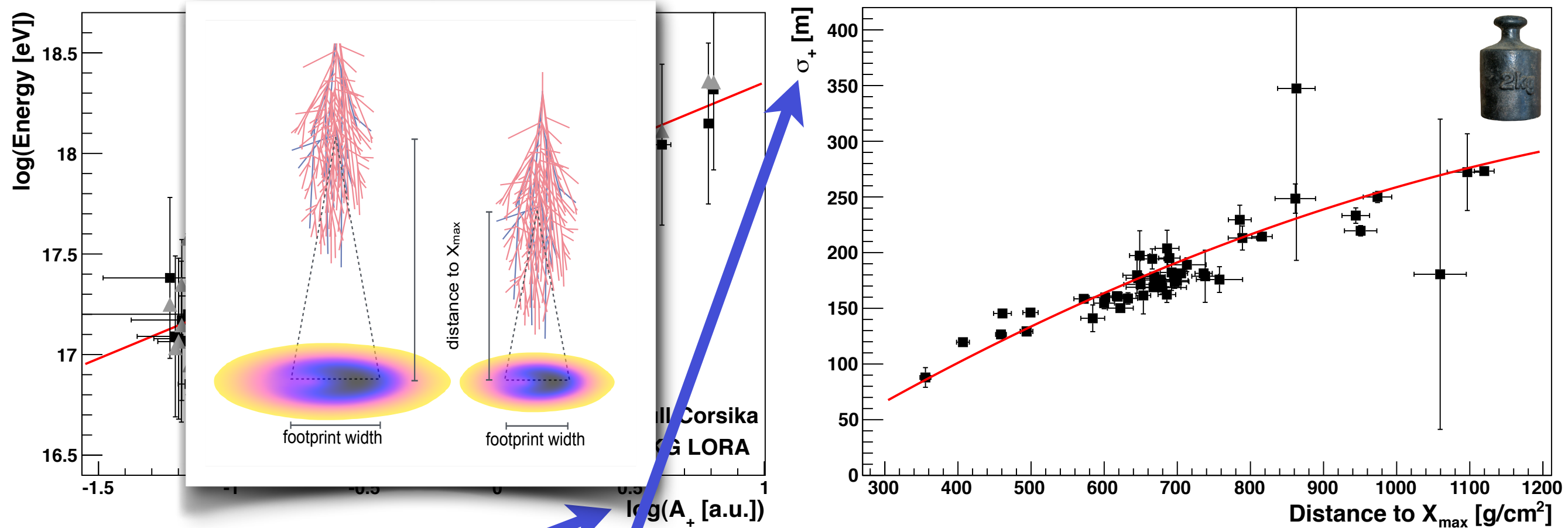
# Mass



# Properties of primary particle

energy

distance to Xmax



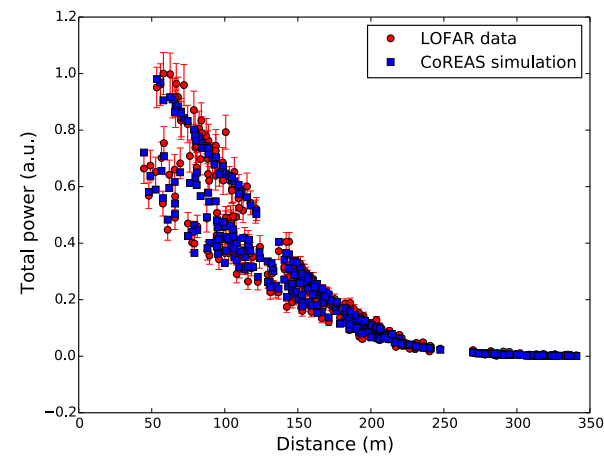
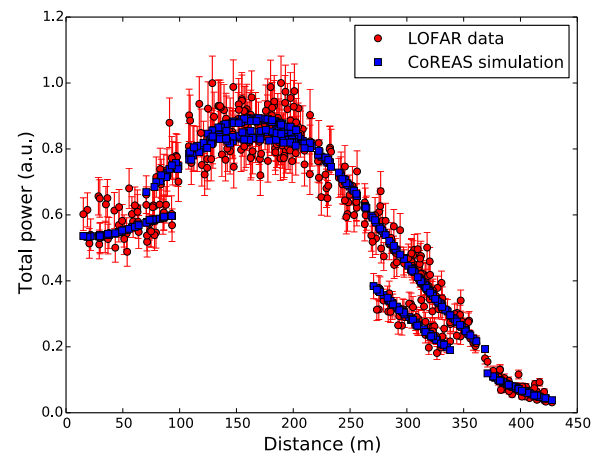
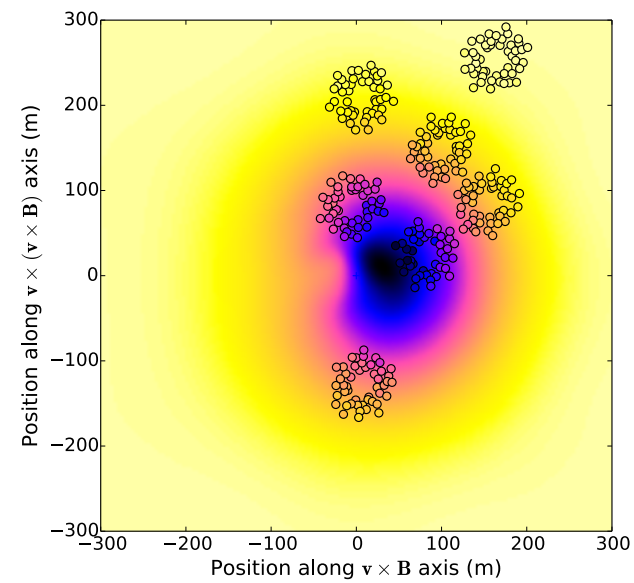
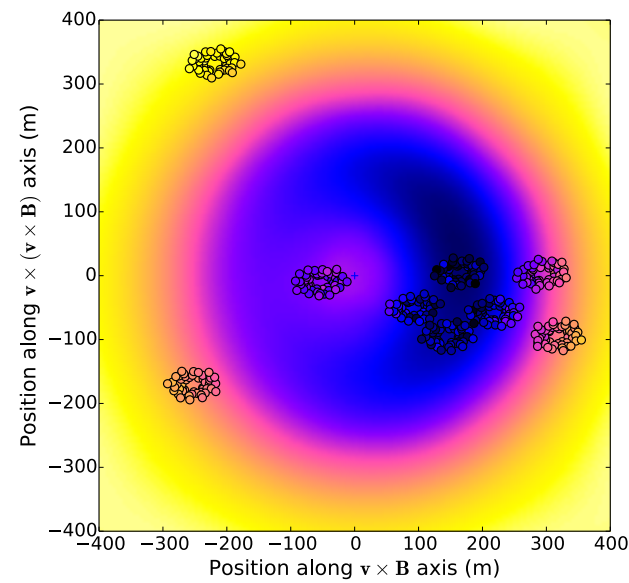
$$P(x', y') = A_+ \cdot \exp\left(\frac{-[(x' - X_+)^2 + (y' - Y_+)^2]}{\sigma_+^2}\right) - A_- \cdot \exp\left(\frac{-[(x' - X_-)^2 + (y' - Y_-)^2]}{\sigma_-^2}\right) + O$$



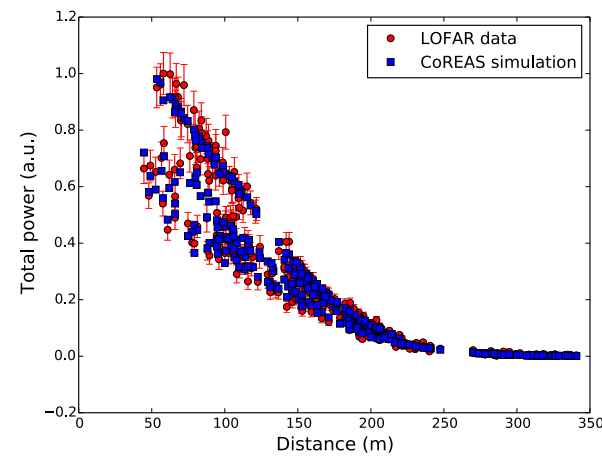
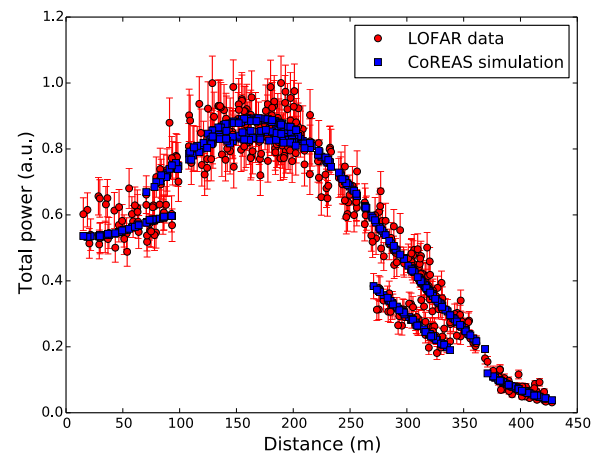
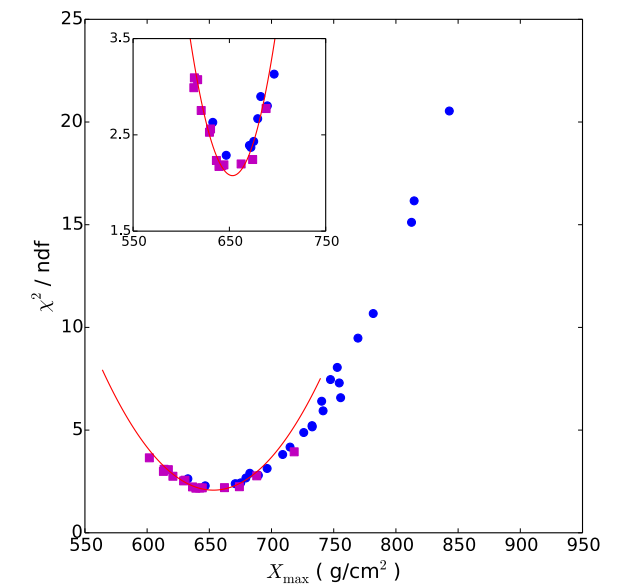
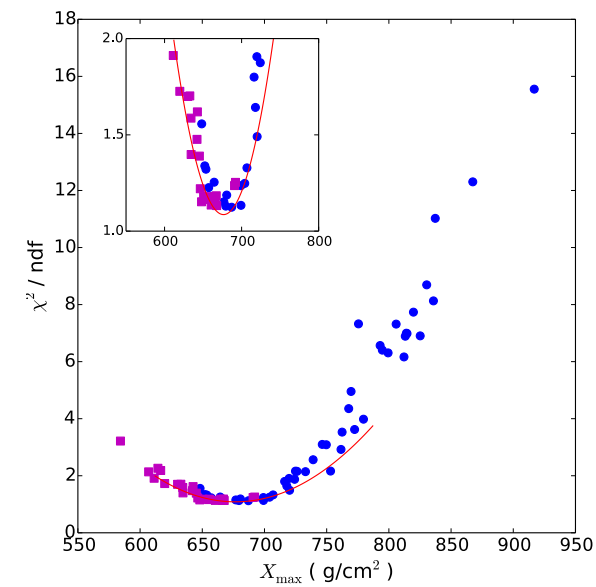
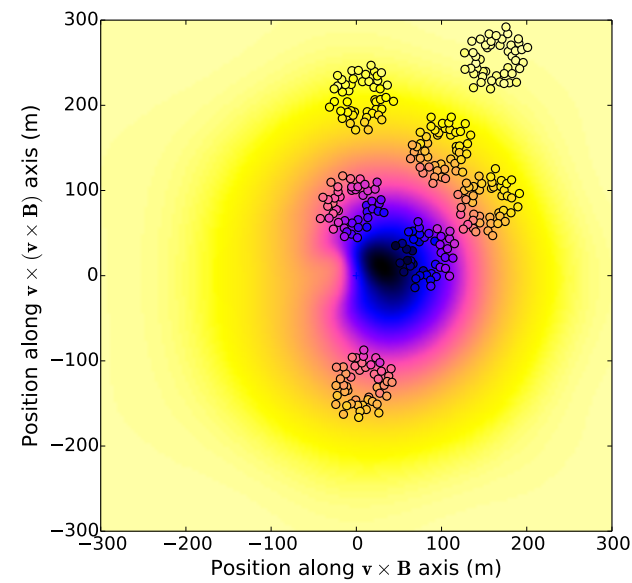
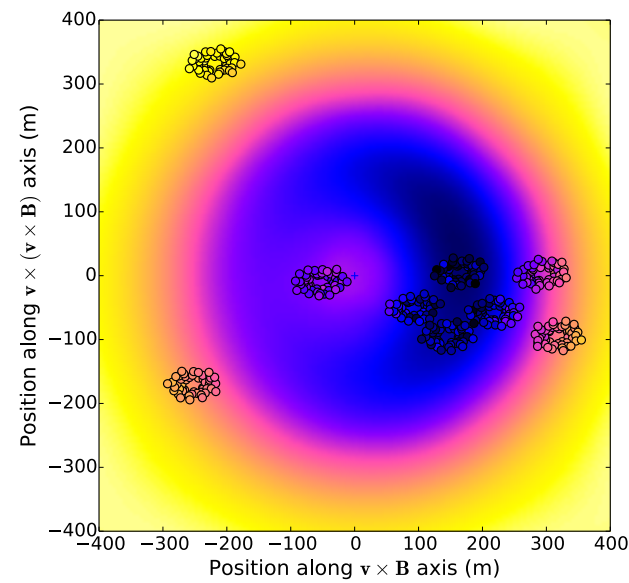
LOFAR



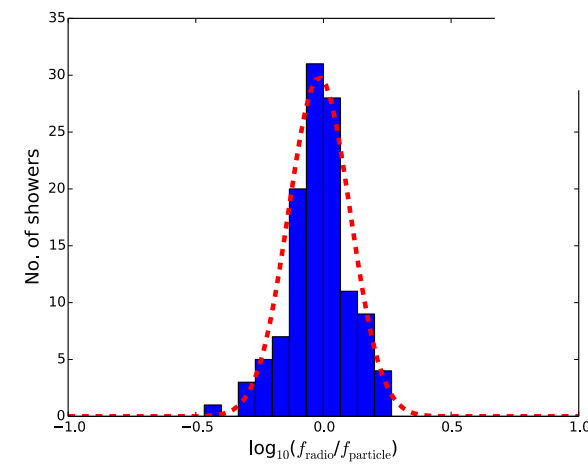
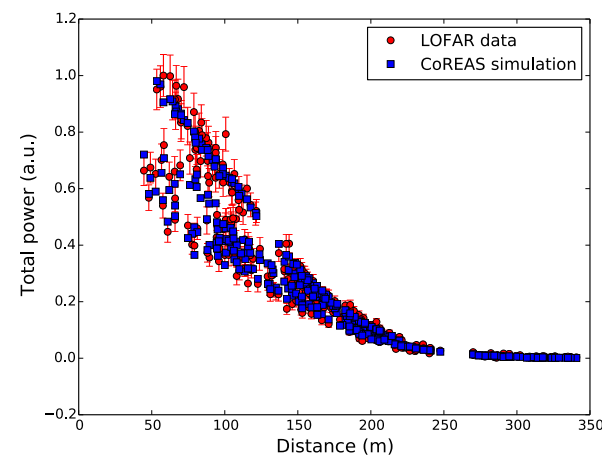
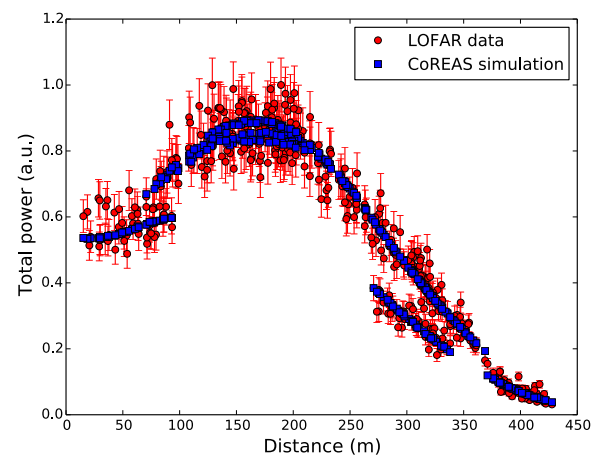
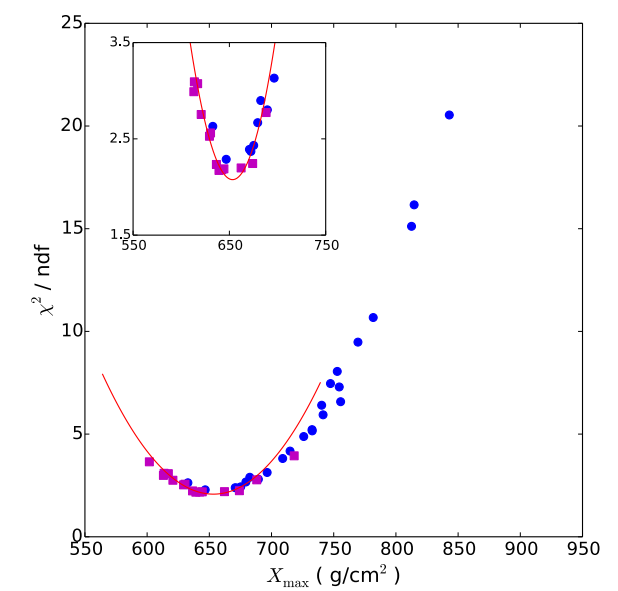
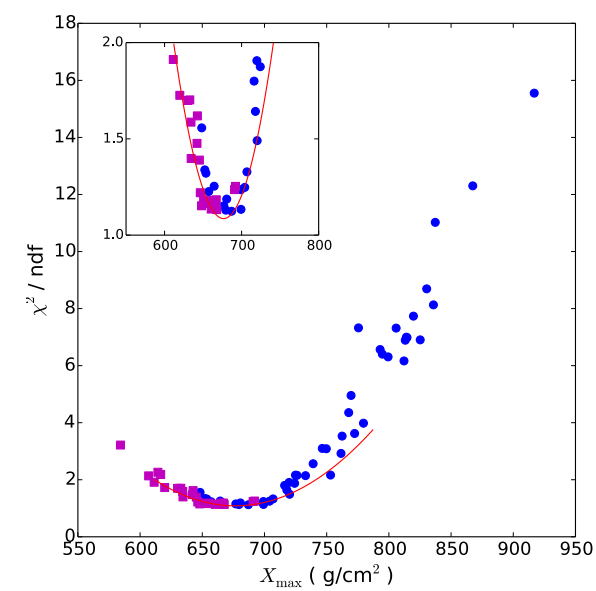
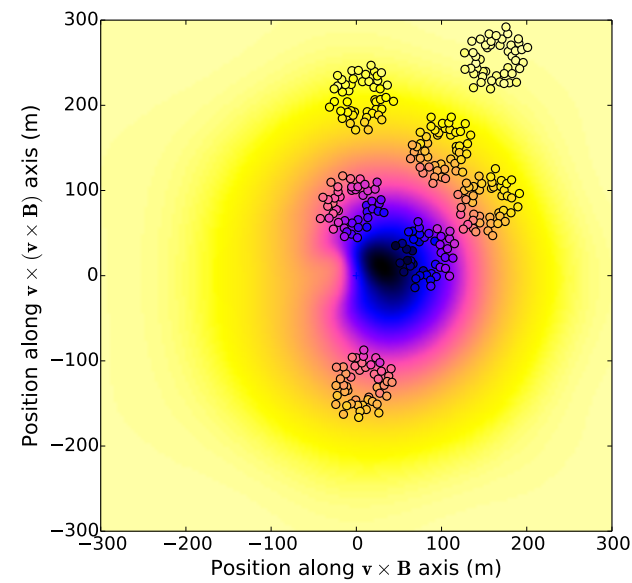
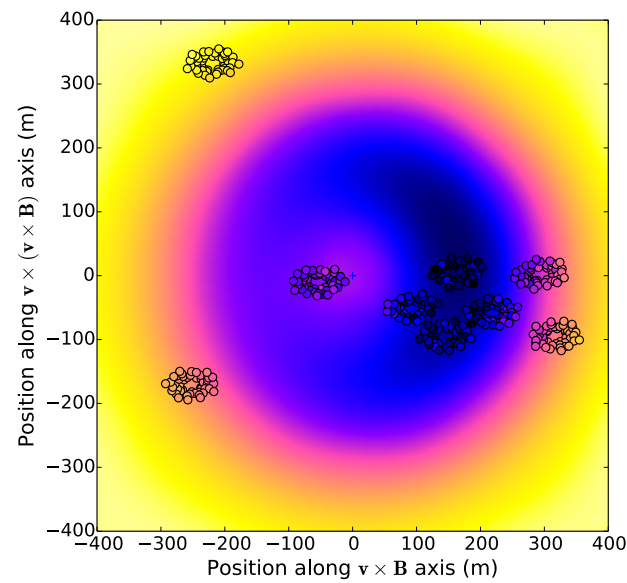
# Measurement of particle mass



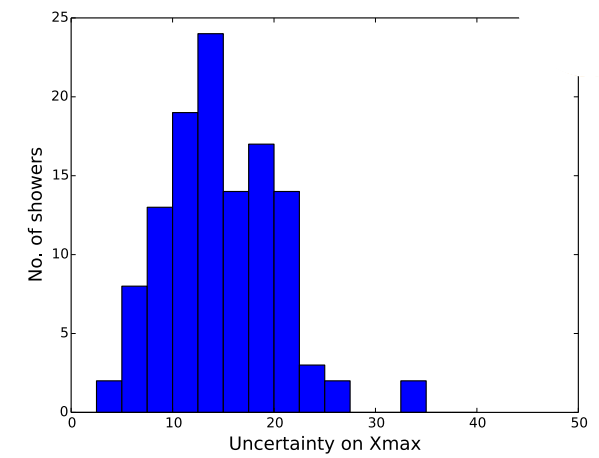
# Measurement of particle mass



# Measurement of particle mass



$$\sigma_E \approx 32\%$$



$$\sigma_{X_{max}} \approx 17 \text{ g/cm}^2$$



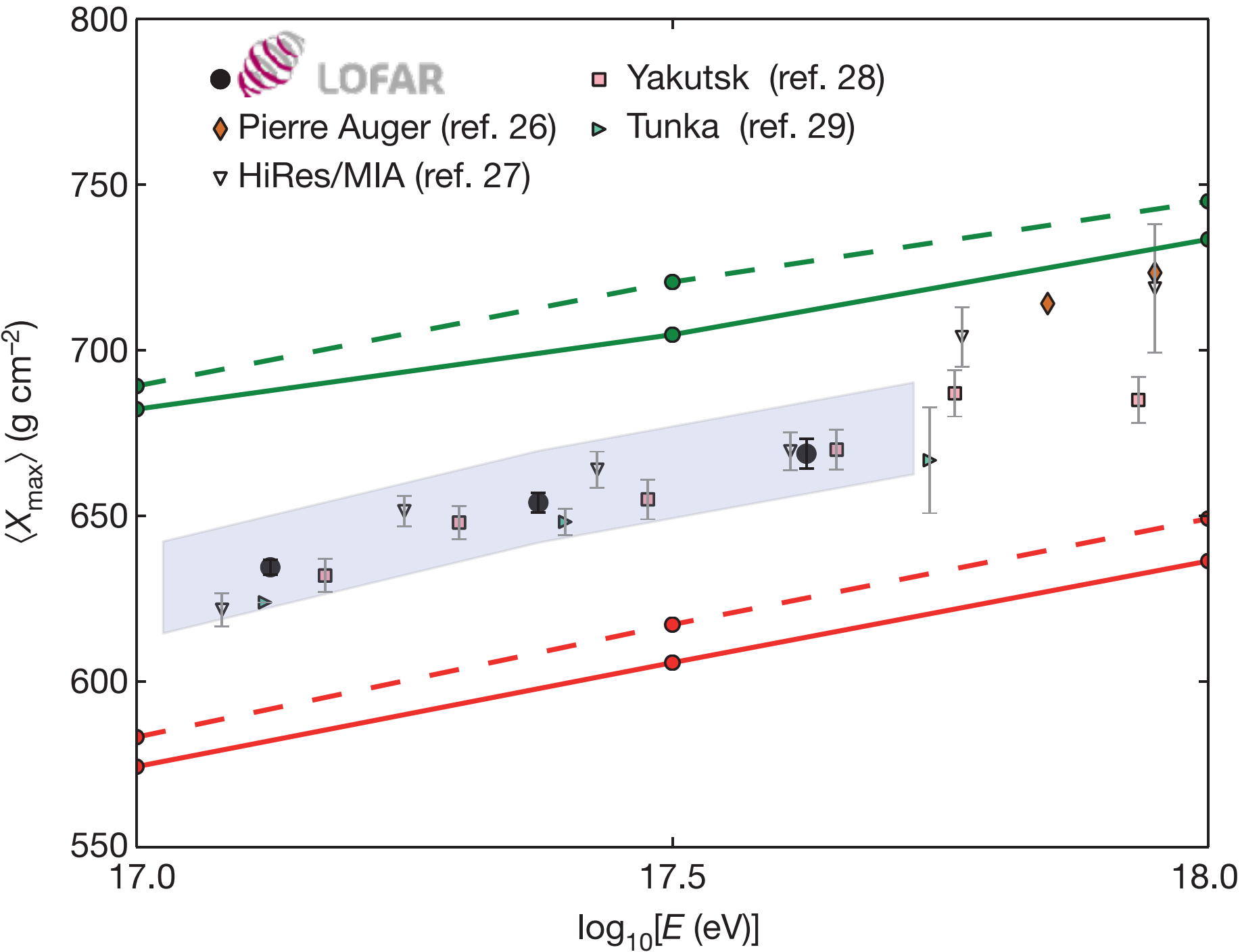
# Depth of the shower maximum

## A large light-mass component of cosmic rays at $10^{17}$ – $10^{17.5}$ electronvolts from radio observations

S. Buitink<sup>1,2</sup>, A. Corstanje<sup>2</sup>, H. Falcke<sup>2,3,4,5</sup>, J. R. Hörandel<sup>2,4</sup>, T. Huege<sup>6</sup>, A. Nelles<sup>2,7</sup>, J. P. Rachen<sup>2</sup>, L. Rossetto<sup>2</sup>, P. Schellart<sup>2</sup>, O. Scholten<sup>8,9</sup>, S. ter Veen<sup>3</sup>, S. Thoudam<sup>2</sup>, T. N. G. Trinh<sup>8</sup>, J. Anderson<sup>10</sup>, A. Asgekar<sup>3,11</sup>, I. M. Avruch<sup>12,13</sup>, M. E. Bell<sup>14</sup>, M. J. Bentum<sup>3,15</sup>, G. Bernardi<sup>16,17</sup>, P. Best<sup>18</sup>, A. Bonafede<sup>19</sup>, F. Breitling<sup>20</sup>, J. W. Broderick<sup>21</sup>, W. N. Brouw<sup>3,15</sup>, M. Brüggen<sup>19</sup>, H. R. Butcher<sup>22</sup>, D. Carbone<sup>23</sup>, B. Ciardi<sup>24</sup>, J. E. Conway<sup>25</sup>, F. de Gasperin<sup>19</sup>, E. de Geus<sup>5,26</sup>, A. Deller<sup>3</sup>, R. J. Dettmar<sup>27</sup>, G. van Diepen<sup>3</sup>, S. Duscha<sup>3</sup>, J. Eislöffel<sup>28</sup>, D. Engels<sup>29</sup>, J. E. Enriquez<sup>3</sup>, R. A. Fallows<sup>3</sup>, R. Fender<sup>30</sup>, C. Ferrari<sup>31</sup>, W. Frieswijk<sup>3</sup>, M. A. Garrett<sup>3,32</sup>, J. M. Grießmeier<sup>33,34</sup>, A. W. Gunst<sup>3</sup>, M. P. van Haarlem<sup>3</sup>, T. E. Hassall<sup>21</sup>, G. Heald<sup>3,13</sup>, J. W. T. Hessels<sup>3,23</sup>, M. Hoeft<sup>28</sup>, A. Horneffer<sup>3</sup>, M. Iacobelli<sup>3</sup>, H. Intema<sup>32,35</sup>, E. Jette<sup>27</sup>, A. Karastergiou<sup>30</sup>, V. I. Kondratiev<sup>3,36</sup>, M. Kramer<sup>5,37</sup>, M. Kuniyoshi<sup>38</sup>, G. Kuper<sup>3</sup>, J. van Leeuwen<sup>3,23</sup>, G. M. Loose<sup>3</sup>, P. Maat<sup>3</sup>, G. Mann<sup>20</sup>, S. Markoff<sup>23</sup>, R. McFadden<sup>3</sup>, D. McKay-Bukowski<sup>39,40</sup>, J. P. McKean<sup>3,13</sup>, M. Mevius<sup>3,13</sup>, D. D. Mulcahy<sup>21</sup>, H. Munk<sup>3</sup>, M. J. Norden<sup>3</sup>, E. Orru<sup>3</sup>, H. Paas<sup>41</sup>, M. Pandey-Pommier<sup>42</sup>, V. N. Pandey<sup>3</sup>, M. Pietka<sup>30</sup>, R. Pizzo<sup>3</sup>, A. G. Polatidis<sup>3</sup>, W. Reich<sup>5</sup>, H. J. A. Röttgering<sup>32</sup>, A. M. M. Scaife<sup>21</sup>, D. J. Schwarz<sup>43</sup>, M. Serylak<sup>30</sup>, J. Sluman<sup>3</sup>, O. Smirnov<sup>17,44</sup>, B. W. Stappers<sup>37</sup>, M. Steinmetz<sup>20</sup>, A. Stewart<sup>30</sup>, J. Swinbank<sup>23,45</sup>, M. Tagger<sup>33</sup>, Y. Tang<sup>3</sup>, C. Tasse<sup>44,46</sup>, M. C. Toribio<sup>3,32</sup>, R. Vermeulen<sup>3</sup>, C. Vocks<sup>20</sup>, C. Vogt<sup>3</sup>, R. J. van Weeren<sup>16</sup>, R. A. M. J. Wijers<sup>23</sup>, S. J. Wijnholds<sup>3</sup>, M. W. Wise<sup>3,23</sup>, O. Wucknitz<sup>3</sup>, S. Yatawatta<sup>3</sup>, P. Zarka<sup>47</sup> & J. A. Zensus<sup>5</sup>

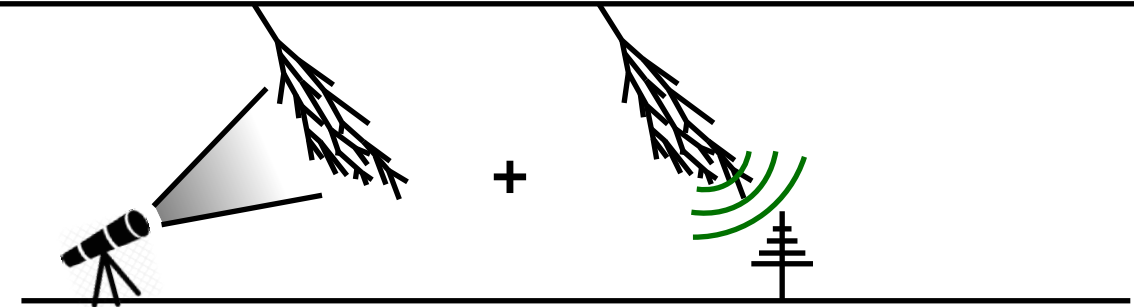
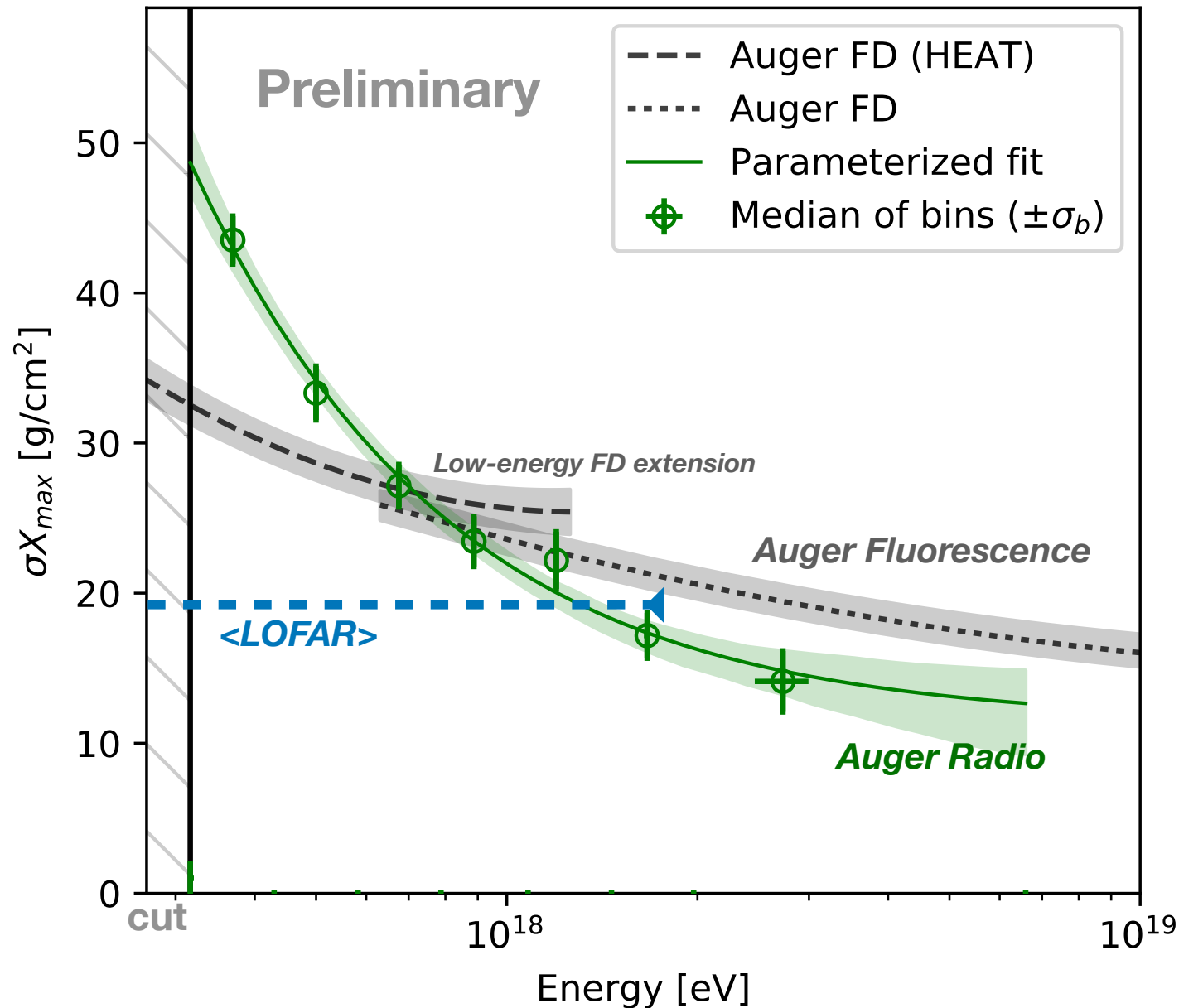
Cosmic rays are the highest-energy particles found in nature. Measurements of the mass composition of cosmic rays with energies of  $10^{17}$ – $10^{18}$  electronvolts are essential to understanding whether they have galactic or extragalactic sources. It has also been proposed that the astrophysical neutrino signal<sup>1</sup> comes from accelerators capable of producing cosmic rays of these energies<sup>2</sup>. Cosmic rays initiate air showers—cascades of secondary particles in the atmosphere—and their masses can be inferred from measurements of the atmospheric depth of the shower maximum<sup>3</sup> ( $X_{\max}$ ; the depth of the air shower when it contains the most particles) or of the composition of shower particles reaching the ground<sup>4</sup>. Current measurements<sup>5</sup> have either high uncertainty, or a low duty cycle and a high energy threshold. Radio detection of cosmic rays<sup>6–8</sup> is a rapidly developing technique<sup>9</sup> for determining  $X_{\max}$  (refs 10, 11) with a duty cycle of, in principle, nearly 100 per cent. The radiation is generated by the separation of relativistic electrons and positrons in the geomagnetic field and a negative charge excess in the shower front<sup>6,12</sup>. Here we report radio measurements of  $X_{\max}$  with a mean uncertainty of 16 grams per square centimetre for air showers

initiated by cosmic rays with energies of  $10^{17}$ – $10^{17.5}$  electronvolts. This high resolution in  $X_{\max}$  enables us to determine the mass spectrum of the cosmic rays: we find a mixed composition, with a light-mass fraction (protons and helium nuclei) of about 80 per cent. Unless, contrary to current expectations, the extragalactic component of cosmic rays contributes substantially to the total flux below  $10^{17.5}$  electronvolts, our measurements indicate the existence of an additional galactic component, to account for the light composition that we measured in the  $10^{17}$ – $10^{17.5}$  electronvolt range. Observations were made with the Low Frequency Array (LOFAR<sup>13</sup>), a radio telescope consisting of thousands of crossed dipoles with built-in air-shower-detection capability<sup>14</sup>. LOFAR continuously records the radio signals from air showers, while simultaneously running astronomical observations. It comprises a scintillator array (LORA) that triggers the read-out of buffers, storing the full waveforms received by all antennas. We selected air showers from the period June 2011 to January 2015 with radio pulses detected in at least 192 antennas. The total uptime was about 150 days, limited by construction and commissioning of the



# Results: Resolution of AERA $X_{\max}$ method

## Radio $X_{\max}$ resolution

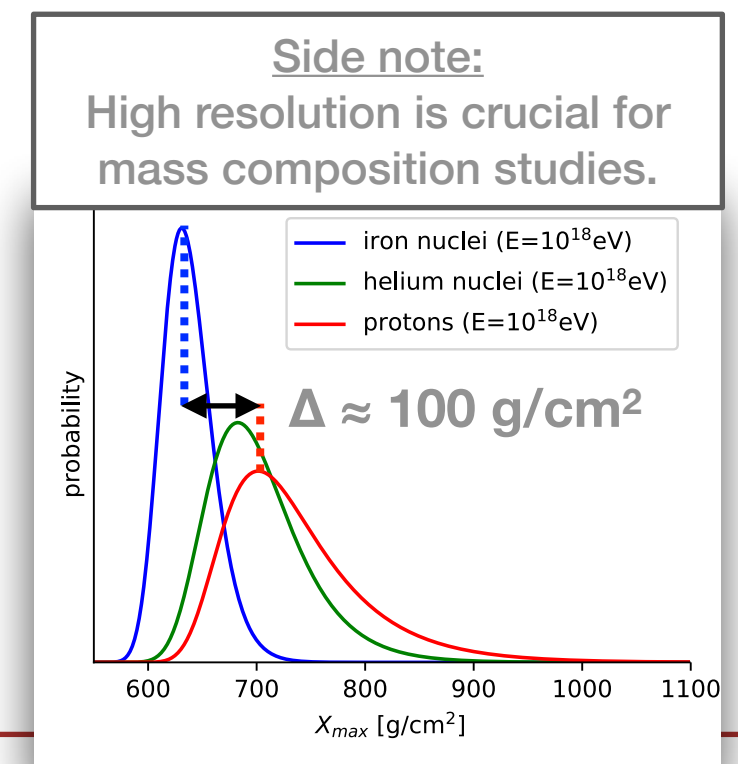


Resolution improves with energy.

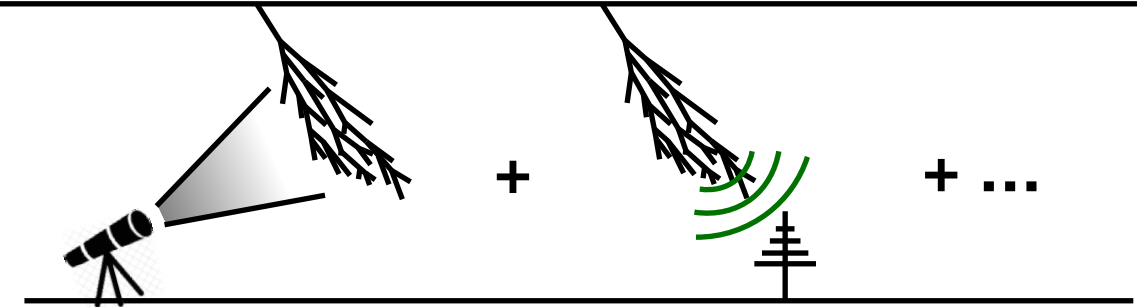
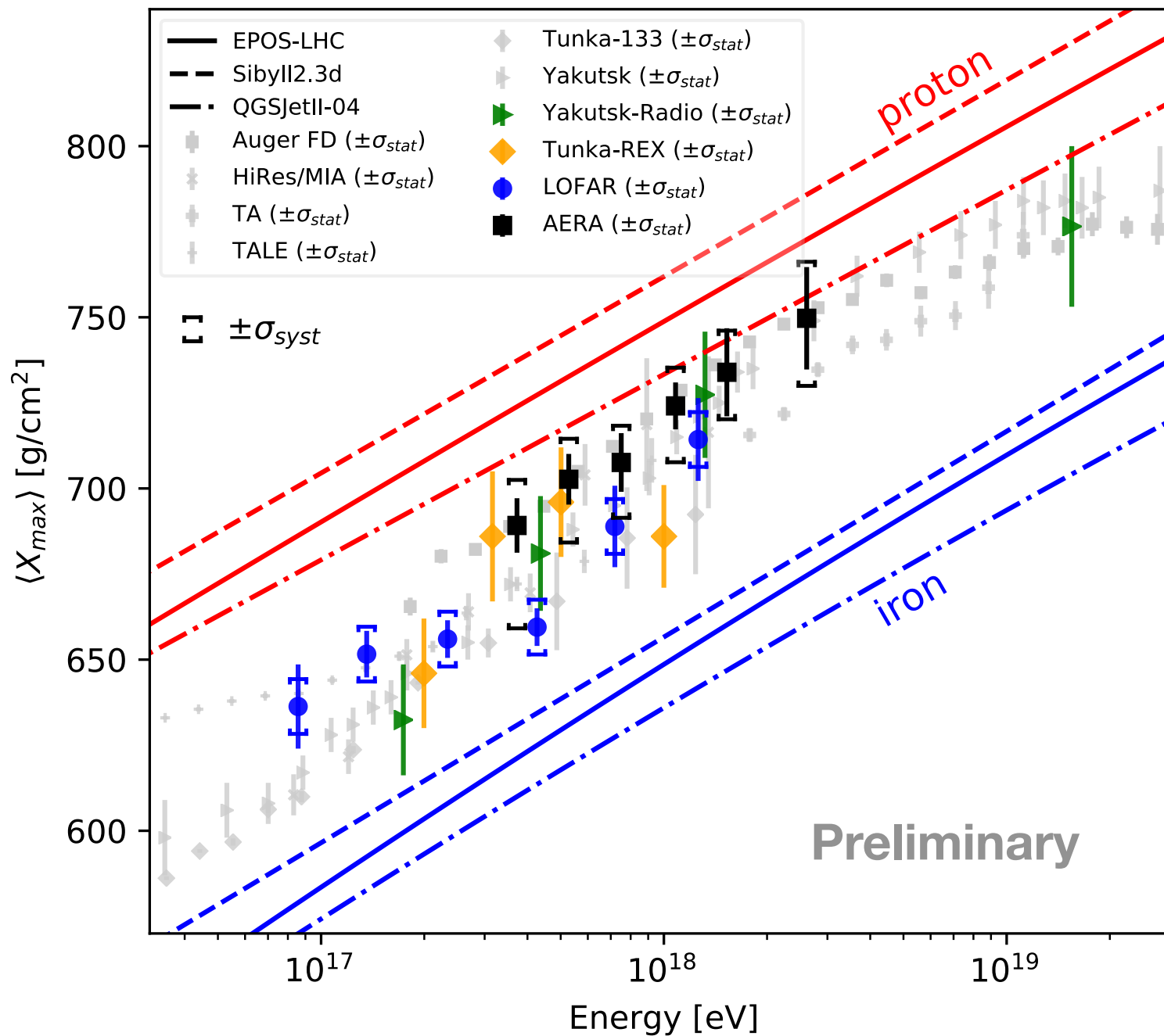
- Up to 'better than 15 g/cm<sup>2</sup>'
- Trend driven by low SNR at low energy.

Resolution competitive with e.g.:

- Auger fluorescence  
[arXiv:1409.4809]
- LOFAR radio ( $E=10^{16.8...18.3}$  eV)  
[arXiv:2103.12549v2]



# Results: AERA vs other (radio) experiments

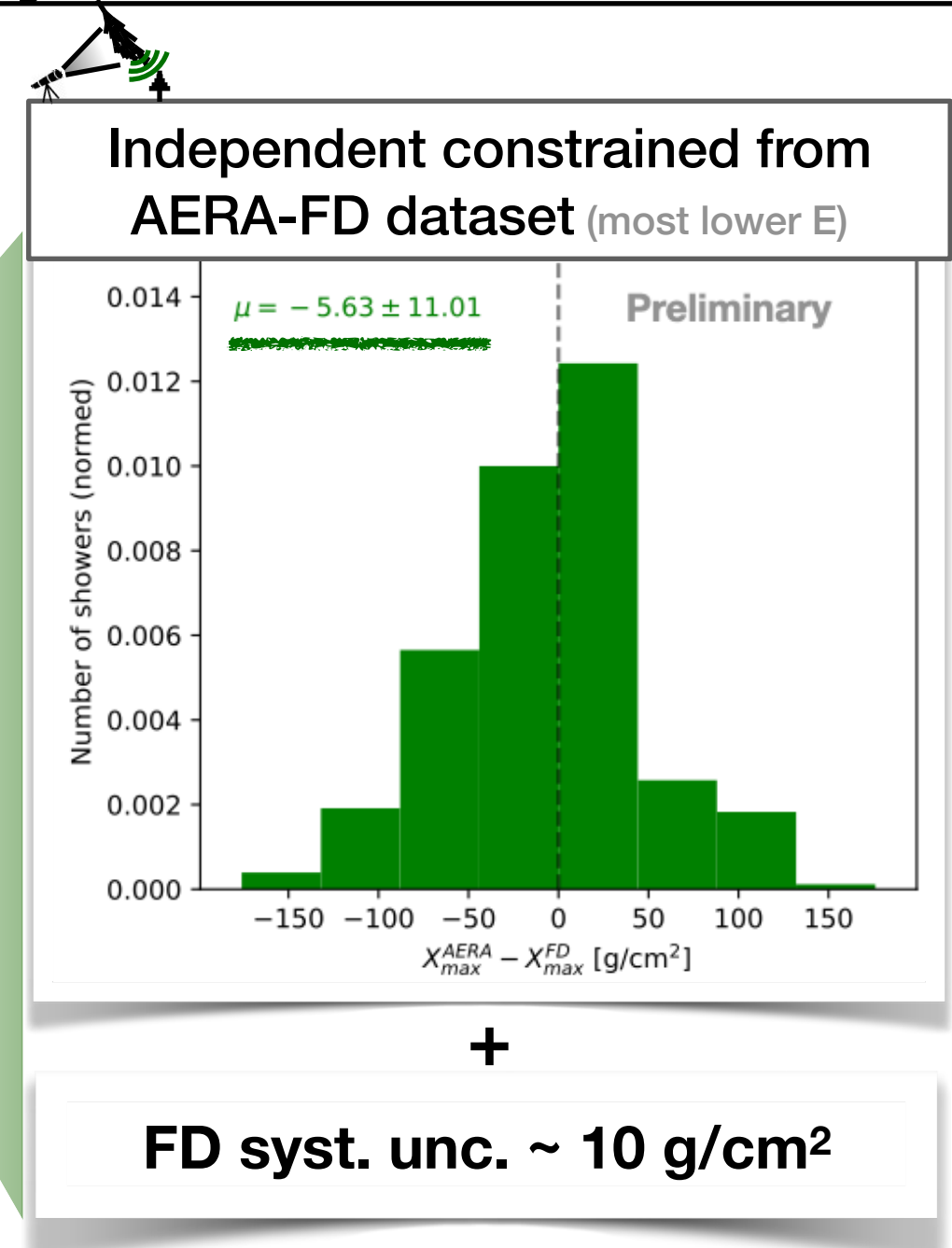
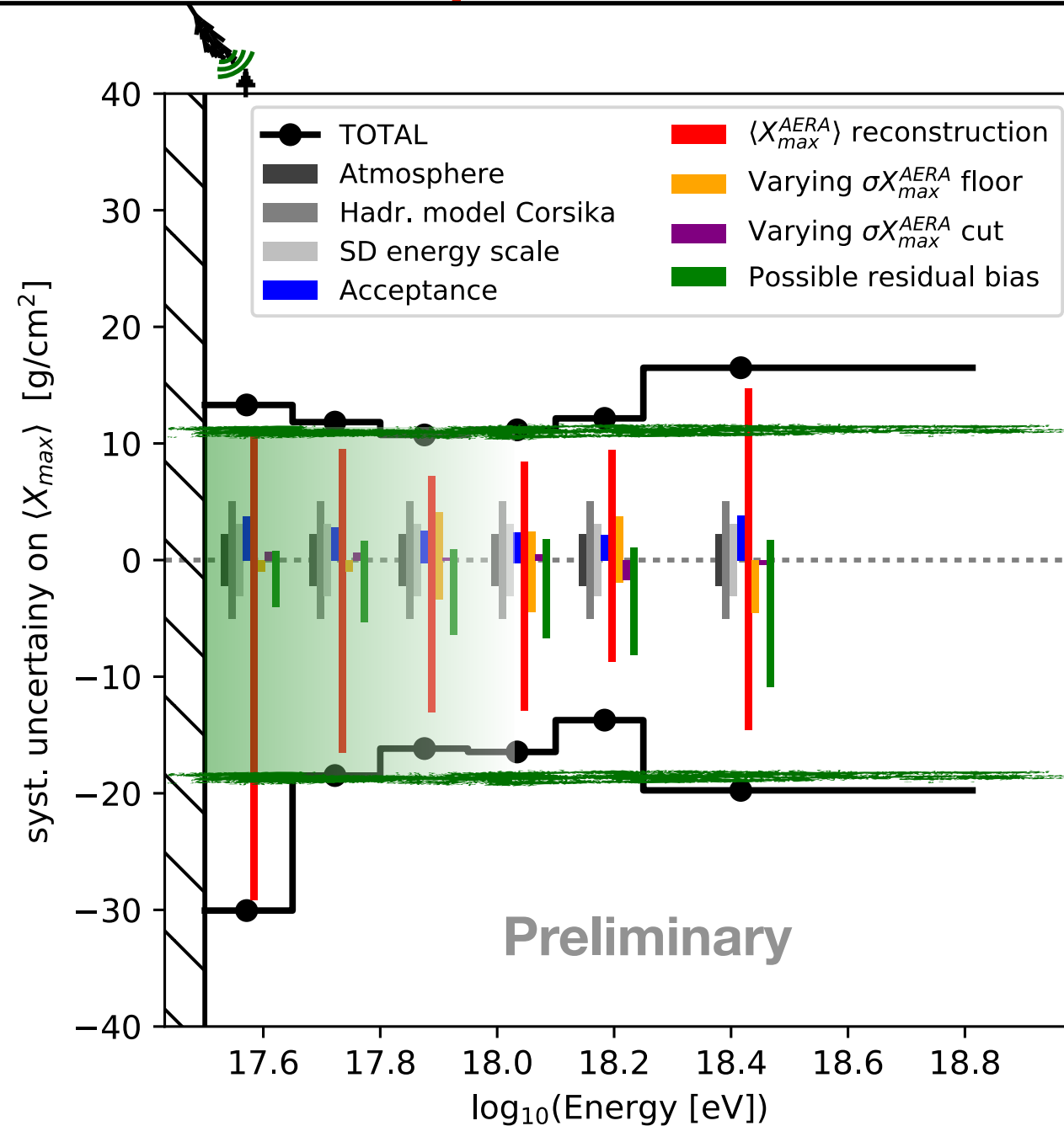


- No general radio-bias w.r.t other techniques (within uncertainties).
- Highlights that systematic uncertainties are key to interpret and compare.
- LOFAR-AERA differences are being investigated in a working group

—> come talk to us during coffee and lunch!



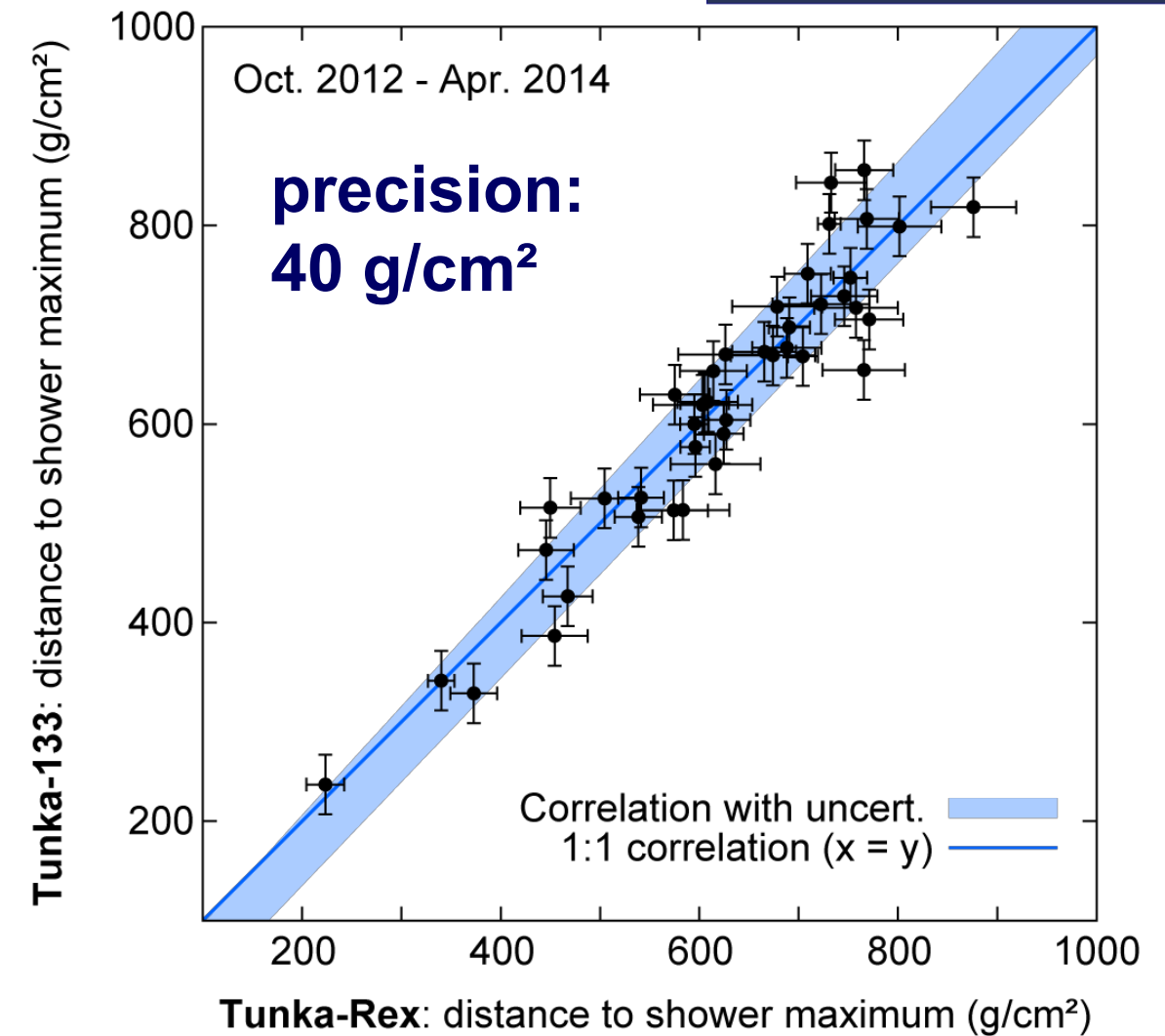
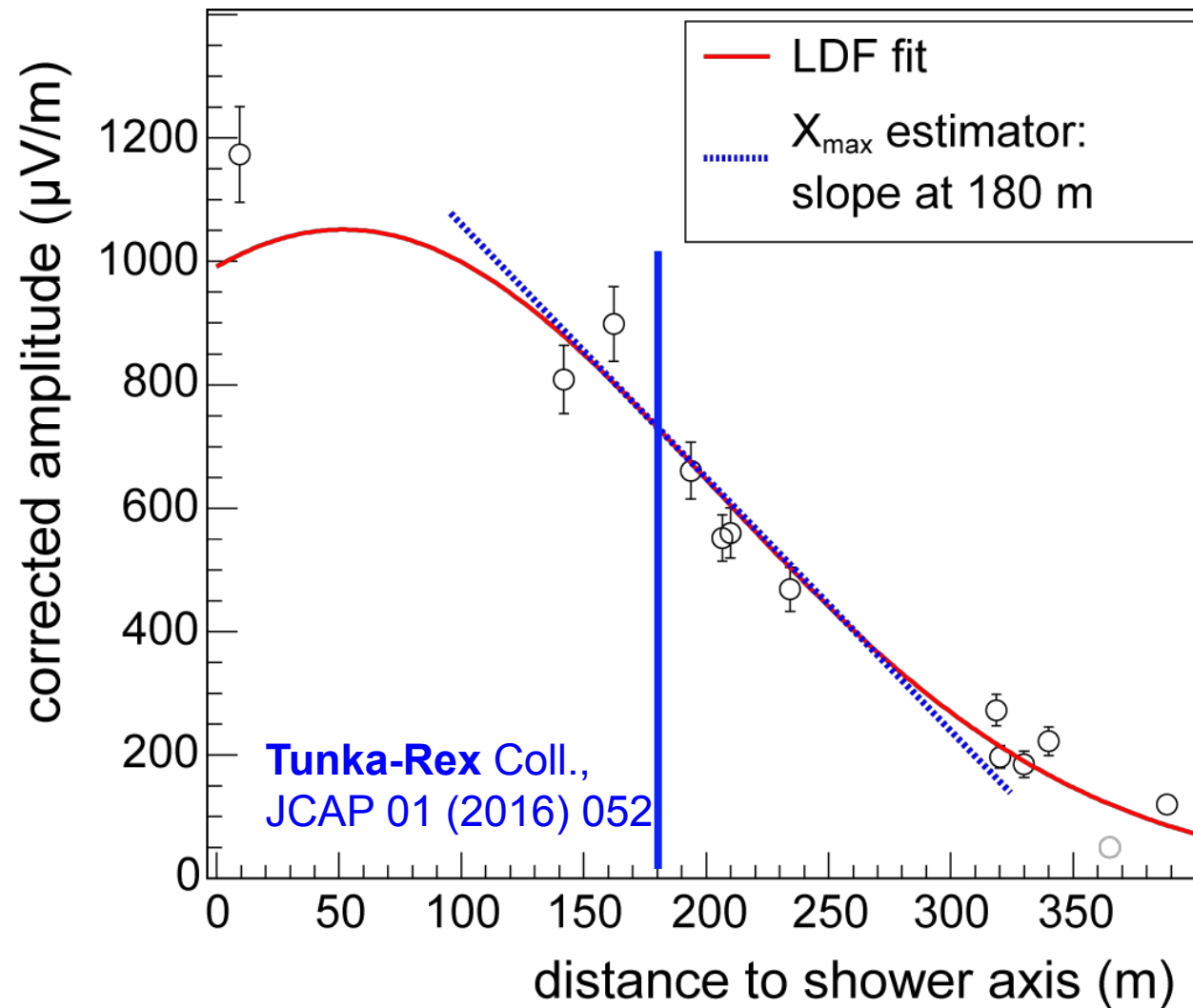
# Two independent estimates of systematic uncertainties



- Cross check:** two independent estimates for total systematic uncertainties are **in agreement**.  
—> suggests systematic uncertainties are **well-understood** and **no significant contribution is missing**.

# Shower maximum: proof by Tunka-Rex

- One of several methods: slope of lateral distribution



# Determine the properties of the incoming particle with the radio technique

- **direction**       $\sim 0.1^\circ - 0.5^\circ$
- **energy**       $\sim 15\% - 30\%$
- **type ( $X_{\max}$ )**  $\sim 20 - 30 \text{ g/cm}^2$

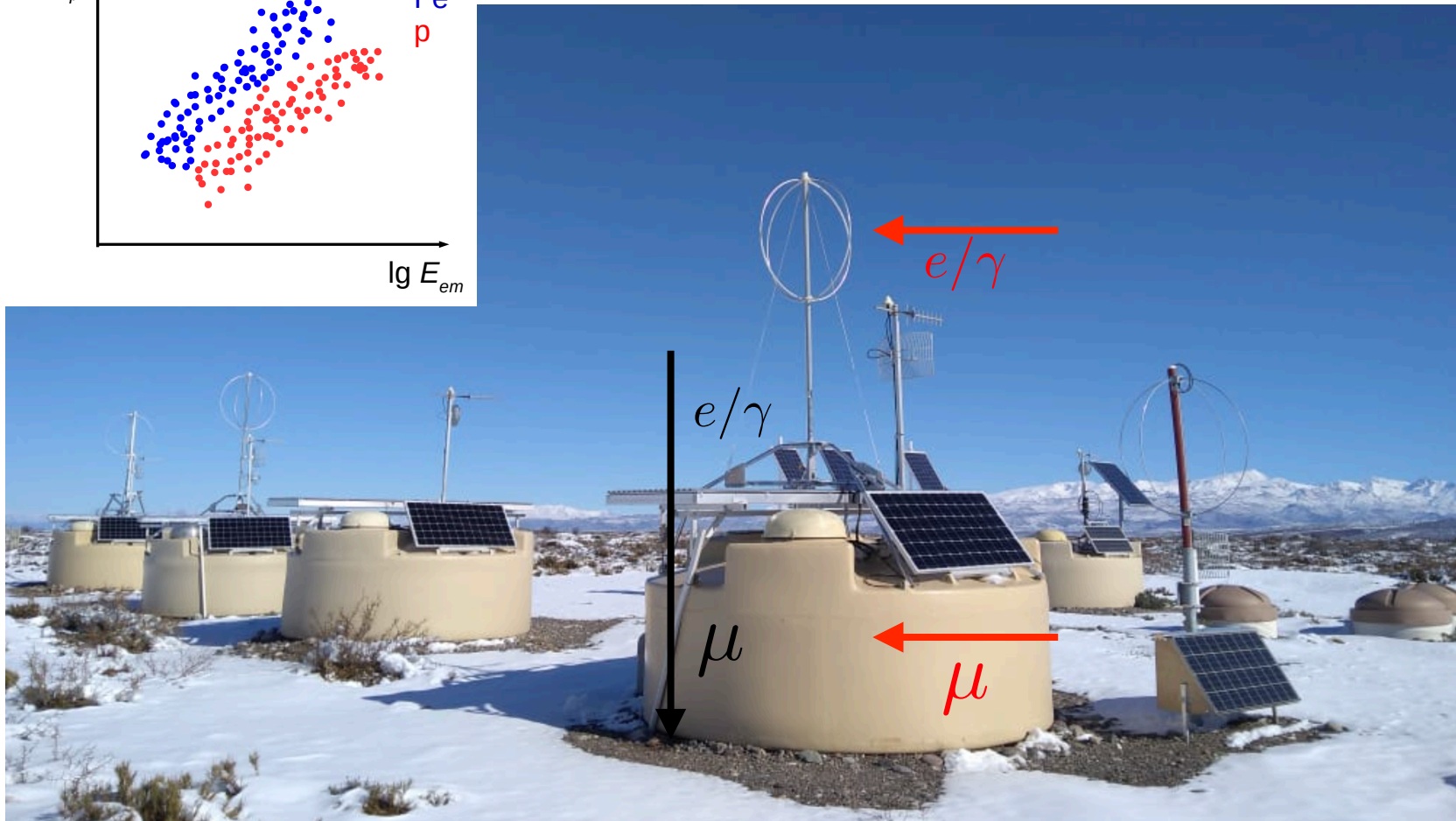
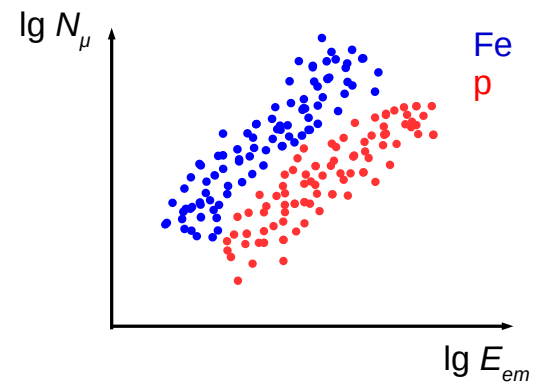
(depending on energy, detector spacing, ...)

—> **radio technique is routinely used to measure properties of cosmic rays**





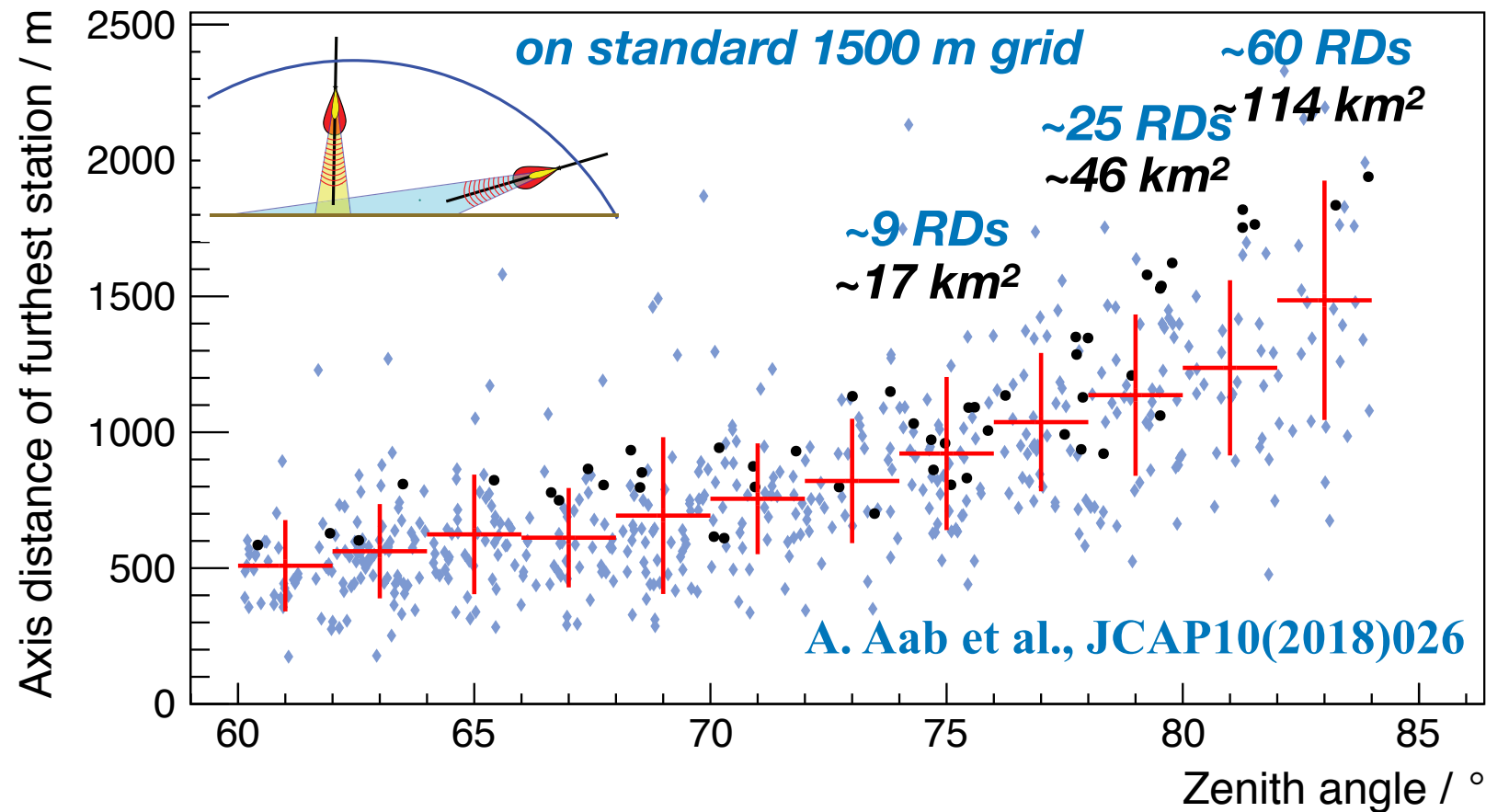
# The Radio Detector of the Pierre Auger Observatory



## Key science questions

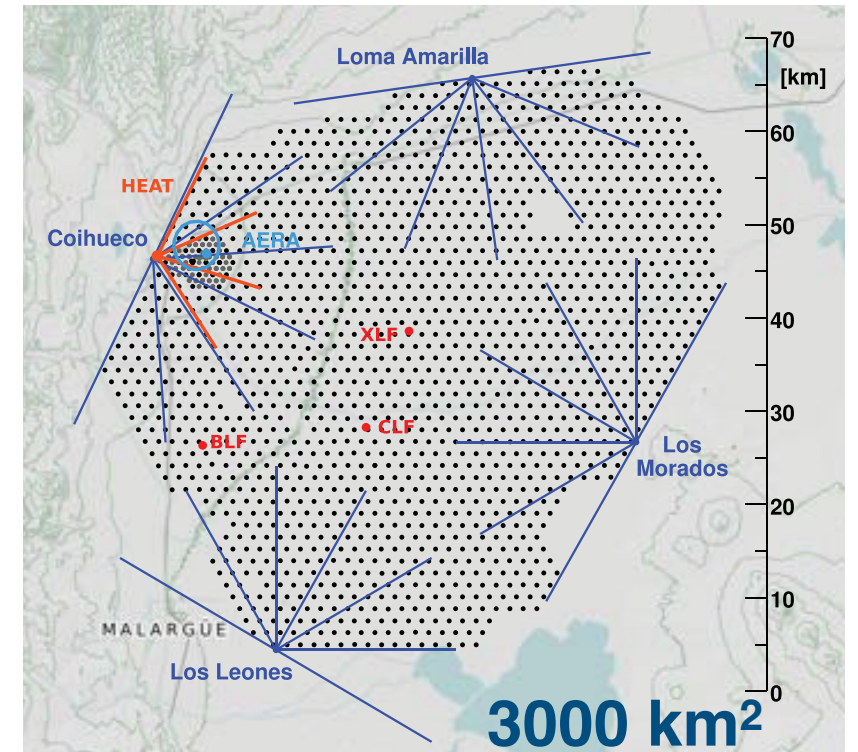
- What are the **sources** and **acceleration** mechanisms of ultra-high-energy cosmic rays (UHECRs)?
- Do we understand **particle** acceleration and **physics** at energies well beyond the LHC (Large Hadron Collider) scale?
- What is the fraction of **protons**, **photons**, and **neutrinos** in cosmic rays at the highest energies?

# Horizontal air showers have large footprints in radio emission



this is MEASURED with the *small* 17km<sup>2</sup> AERA

## Pierre Auger Observatory



**Surface Detector array:**  
 Water Cherenkov Detector,  
 Surface Scintillator Detector,  
 Radio Detector  
 1600 stations on 1500 m grid  
 61 stations on 750 m grid



# Expected Performance

## End-to-end simulation

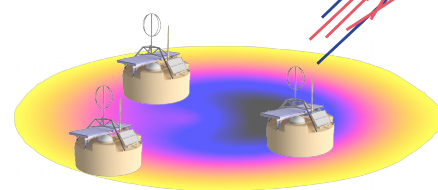
8000 CoREAS showers

$10^{18.4} - 10^{20.1}$  eV

p, He, N, Fe

$65^\circ - 85^\circ$

1.5km grid

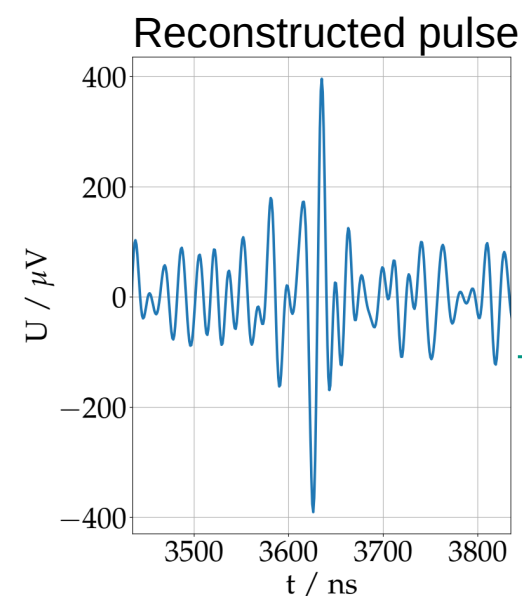
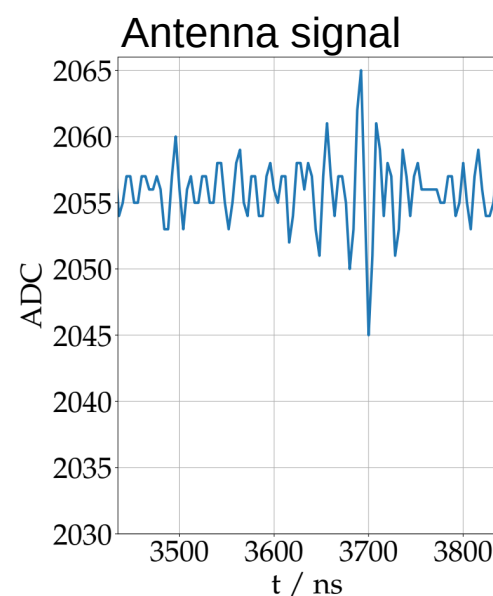
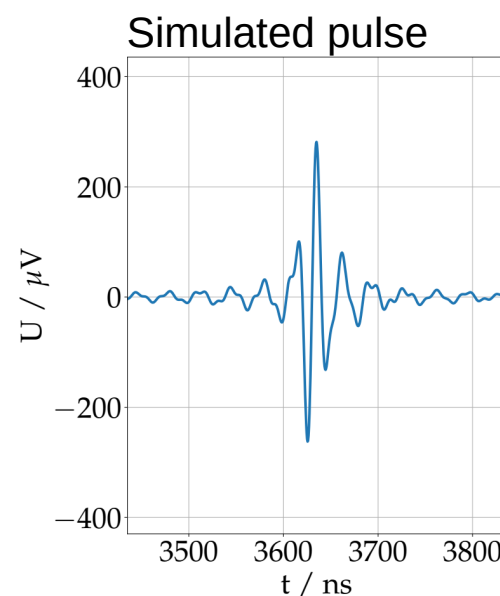


WCD triggers!

Simulate instrumental response

(directional response, analog gain, digitization, .....

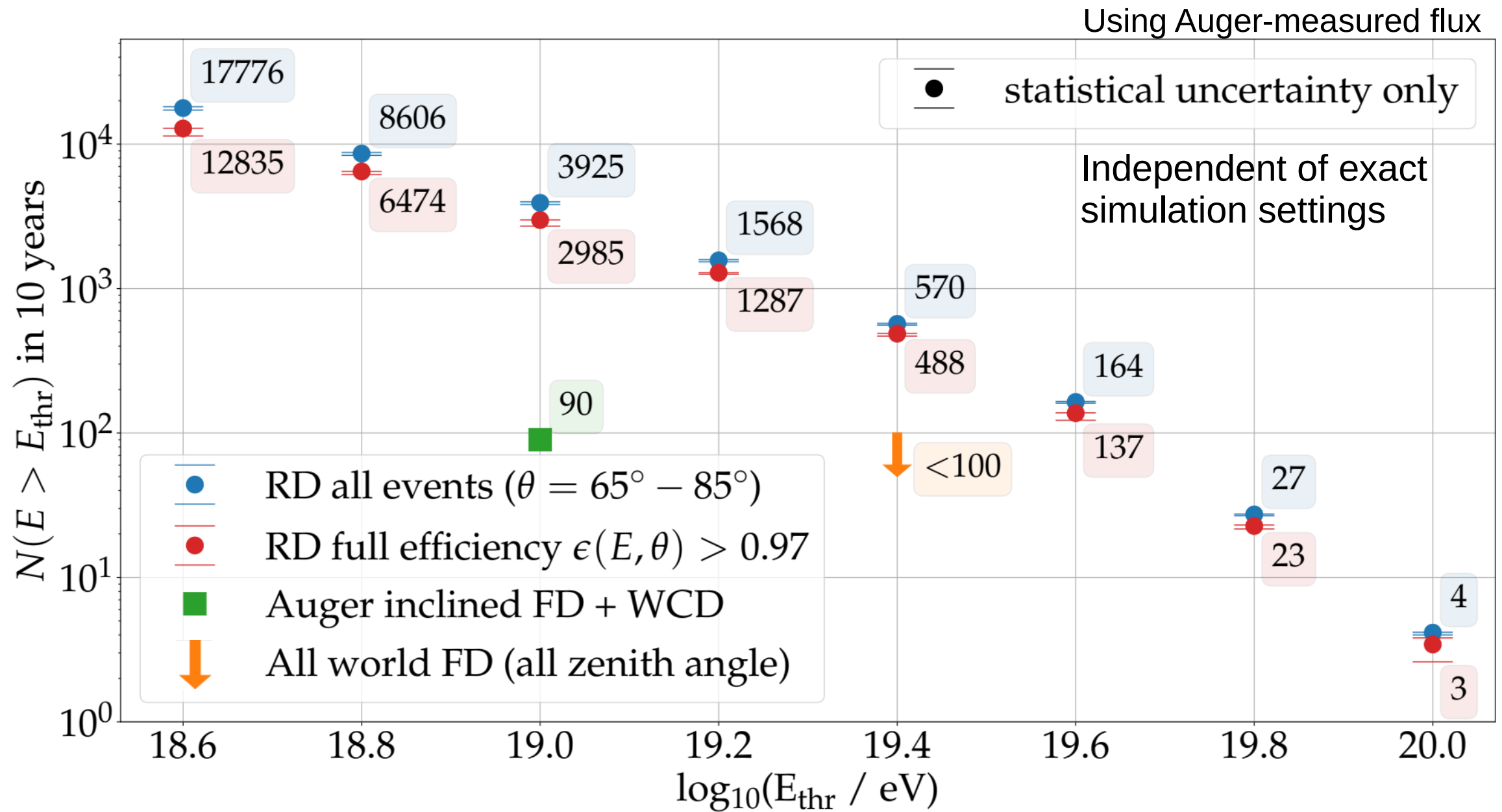
- Including uncertainties ( $\sigma_A = 5\%$ )
- Measured noise



see Felix Schlüter, ARENA 2022

*see talk by Felix Schlüter on Thursday*

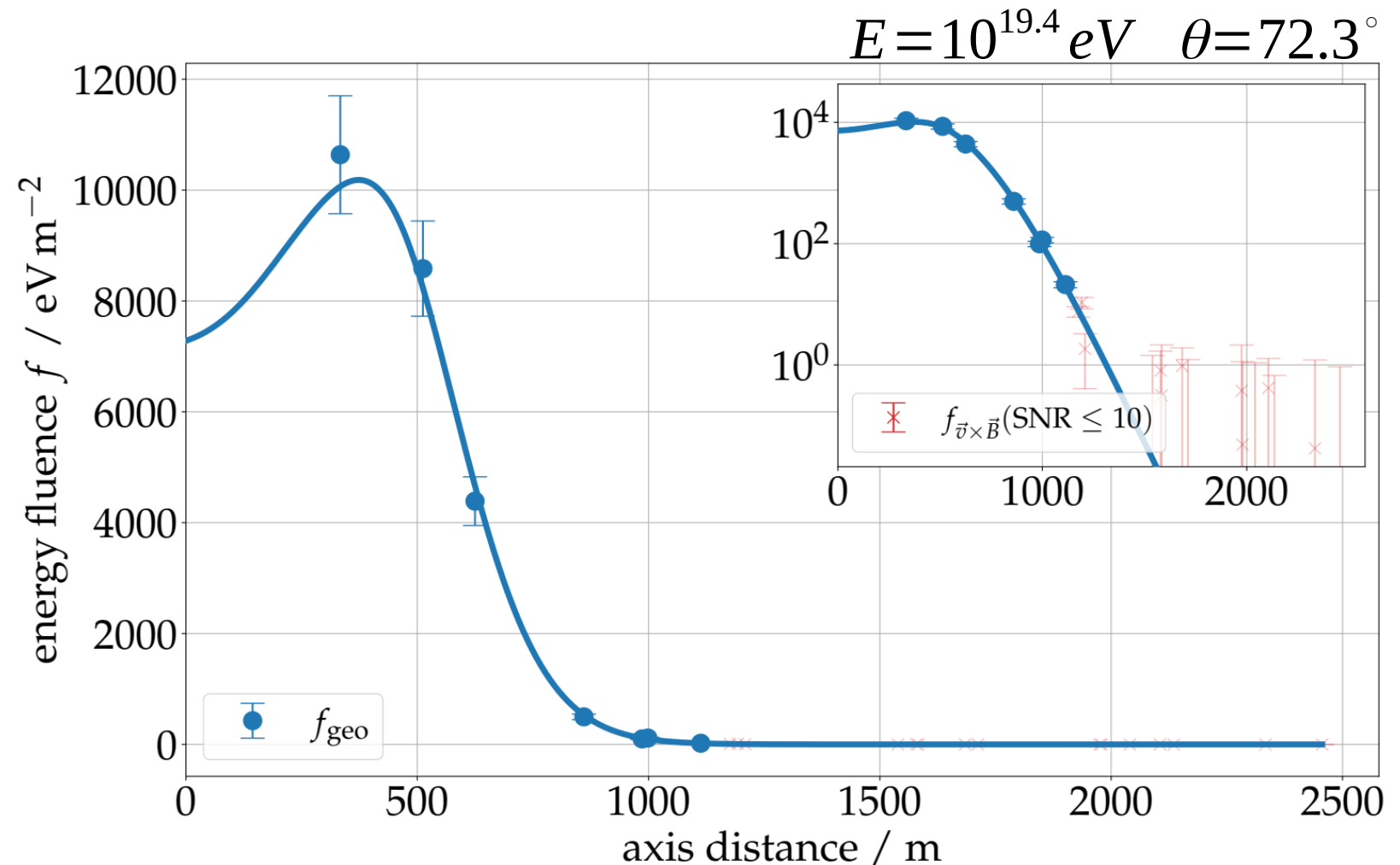
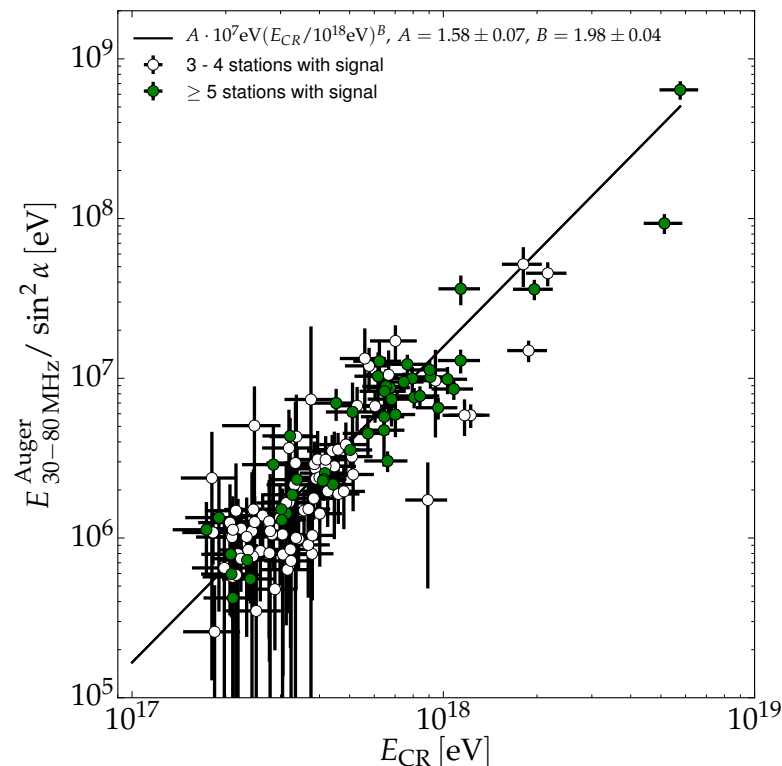
# Expected number of cosmic rays after 10 years



# Lateral signal distribution

## new model for LDF

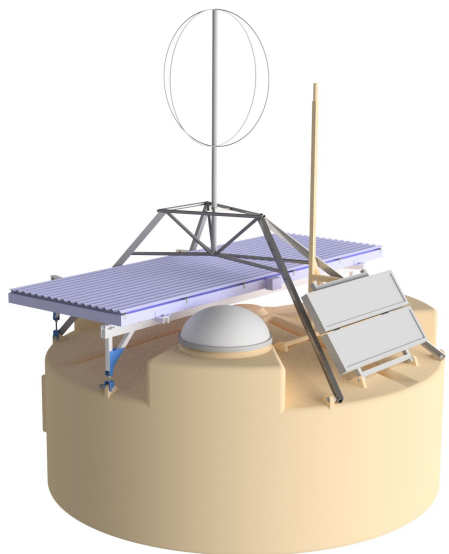
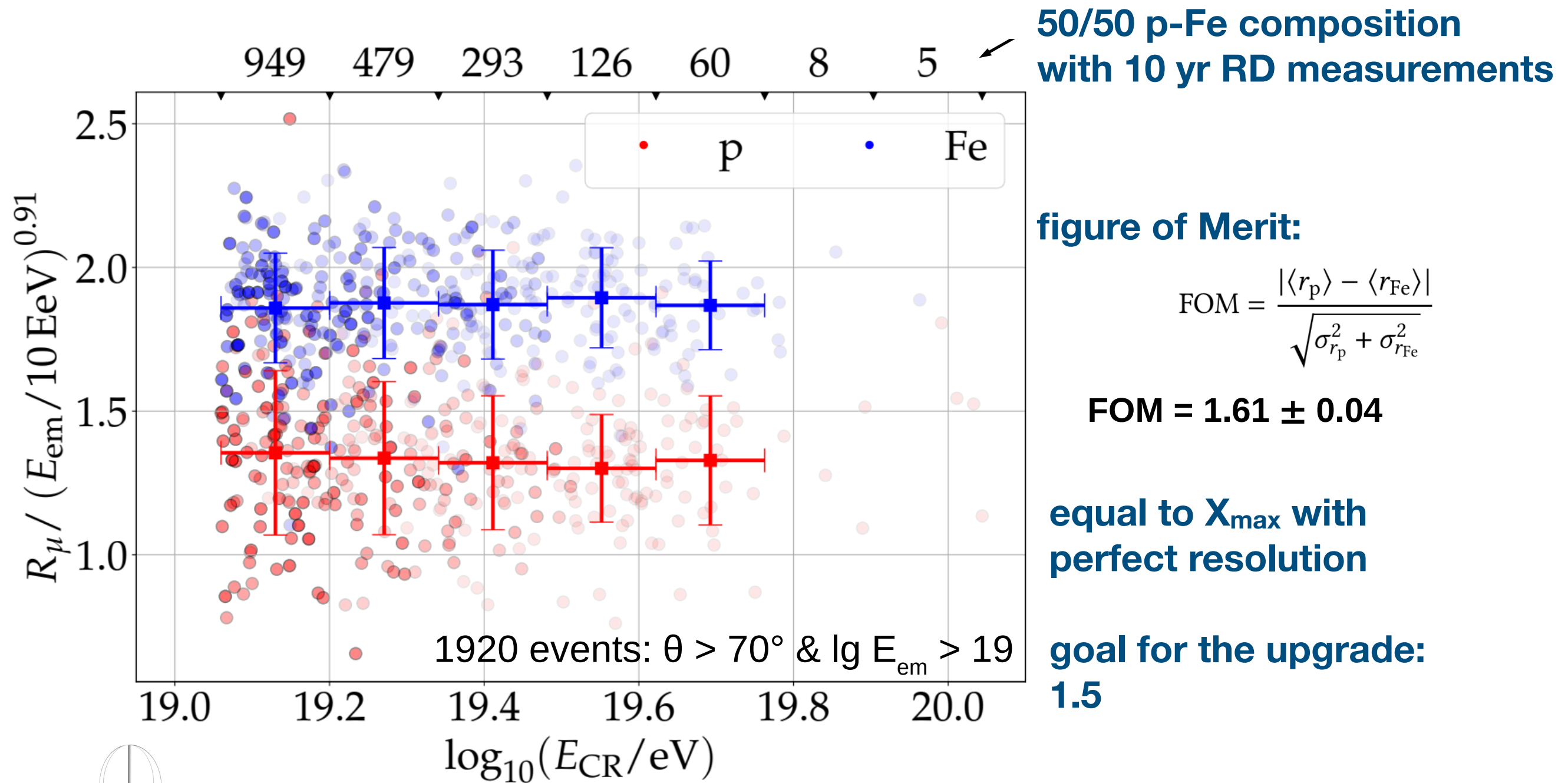
- 2 parameter + core coordinates
- derive start values from WCD (use RD arrival direction)
- integral -> energy estimator



see Felix Schlüter, ARENA 2022

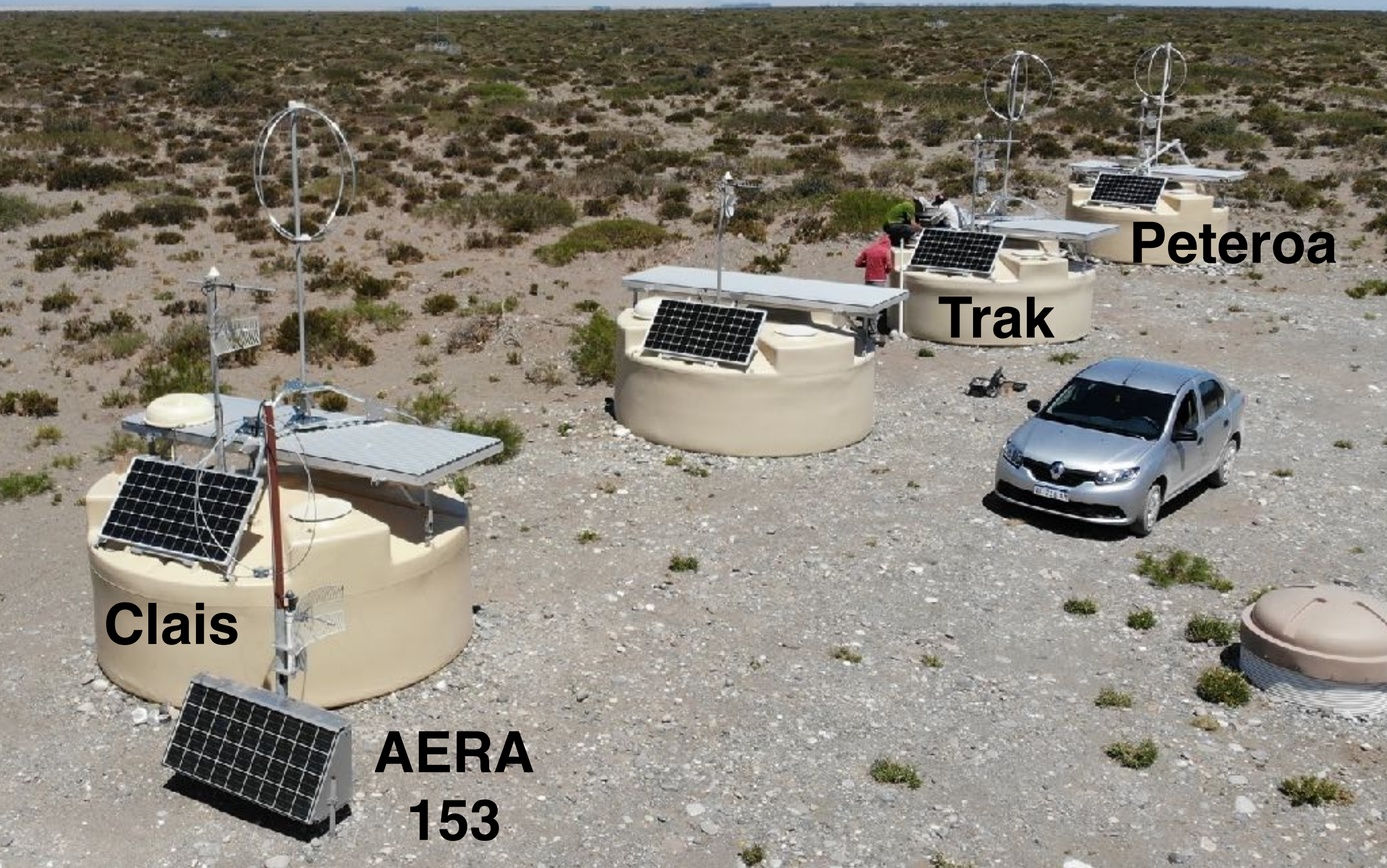


# Particle type for each cosmic ray





since November 2019  
10 prototype stations installed

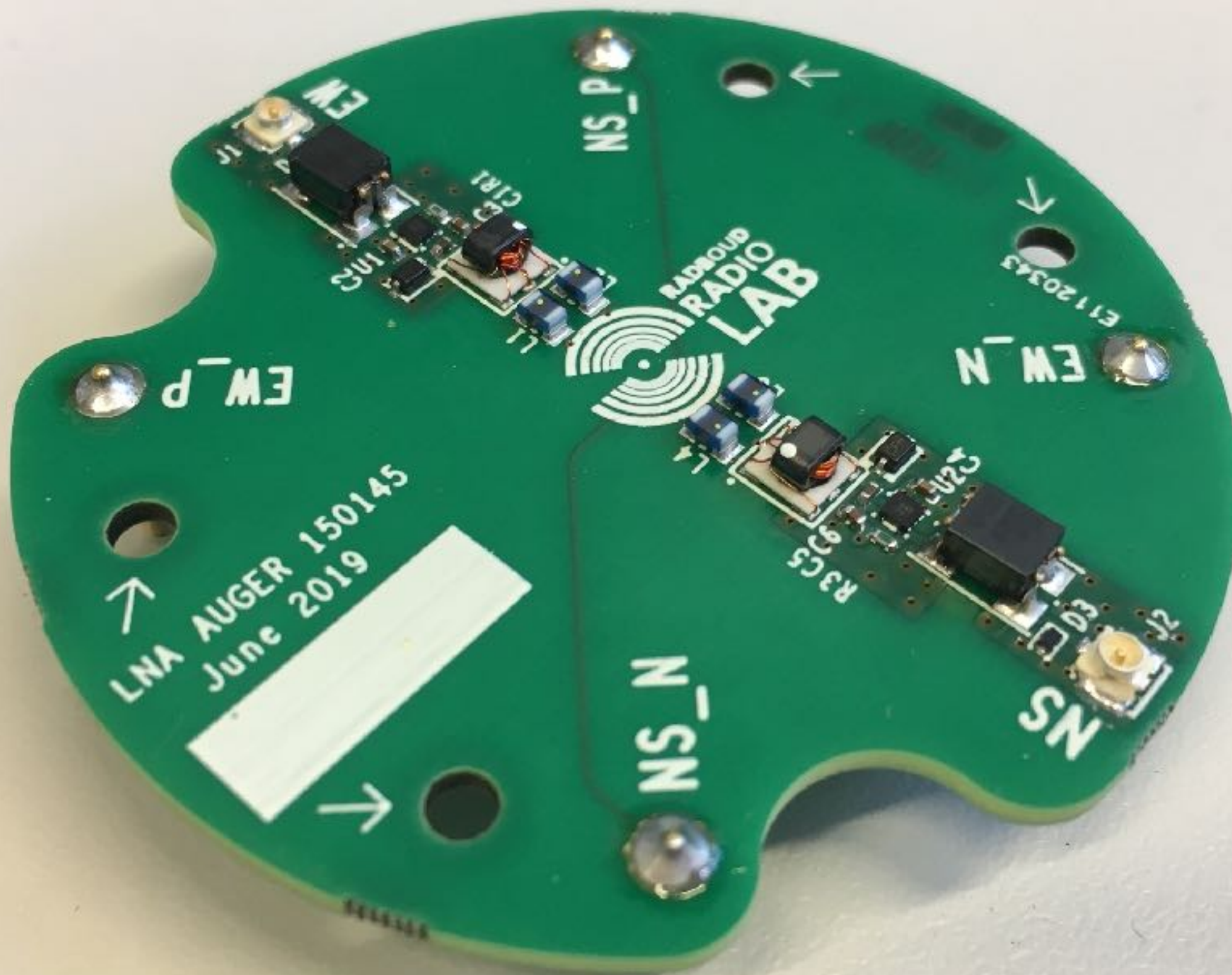




# radio digitizer

**developed at RU Nijmegen**



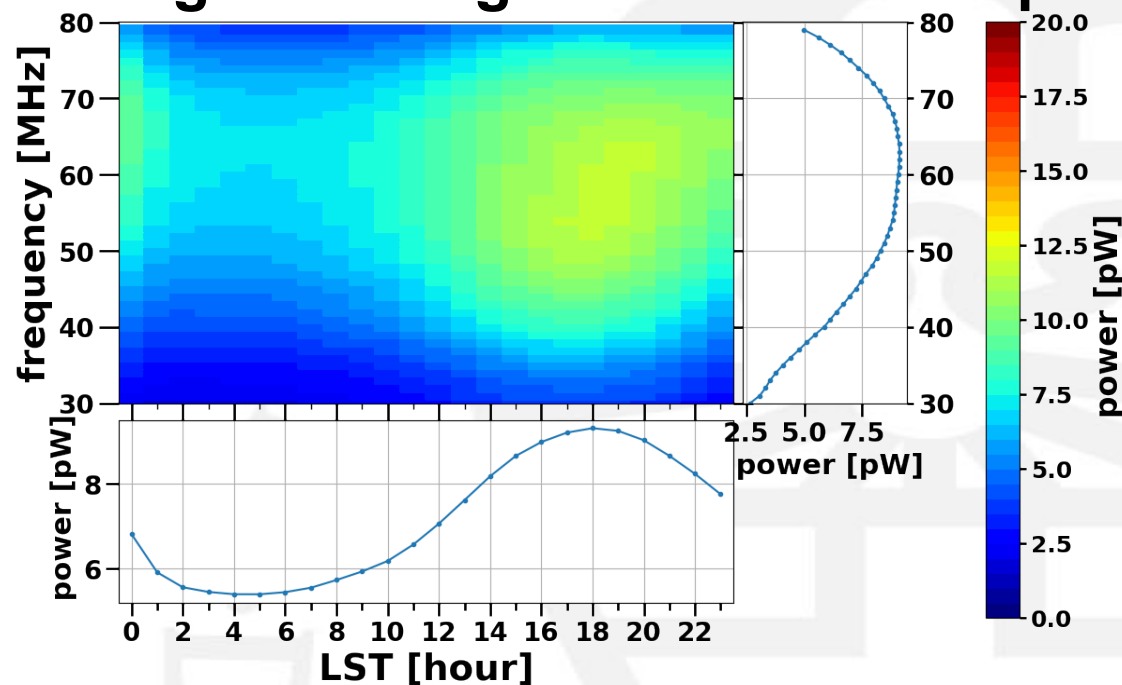


**final version of LNA, RU Nijmegen, June 2019**

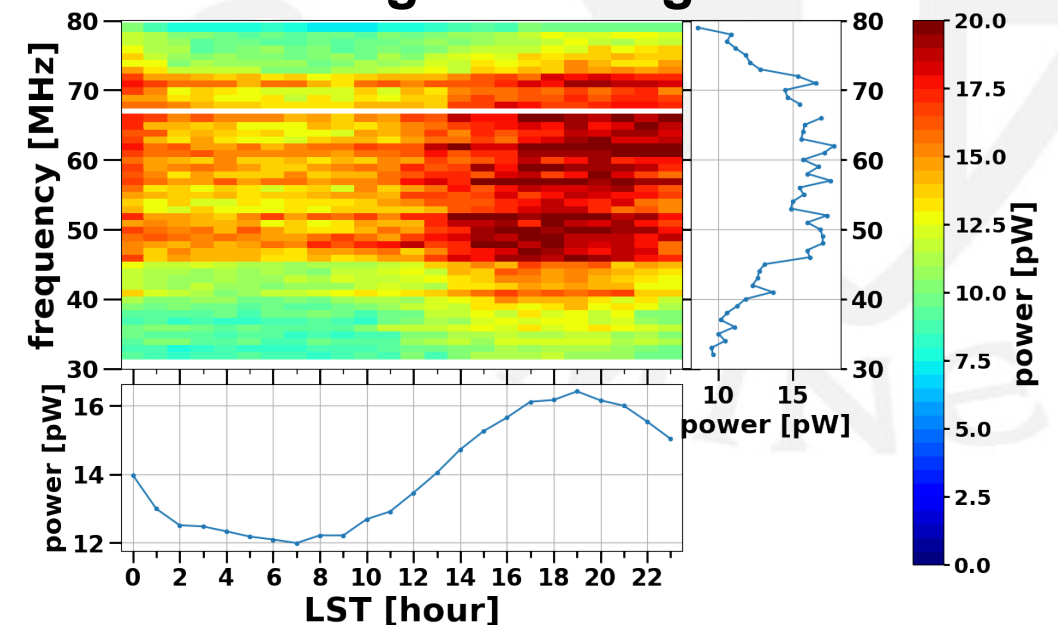
# Calibration with Galactic signal

## sidereal modulation of Galactic signal

Simulated galactic signal in the EW loop



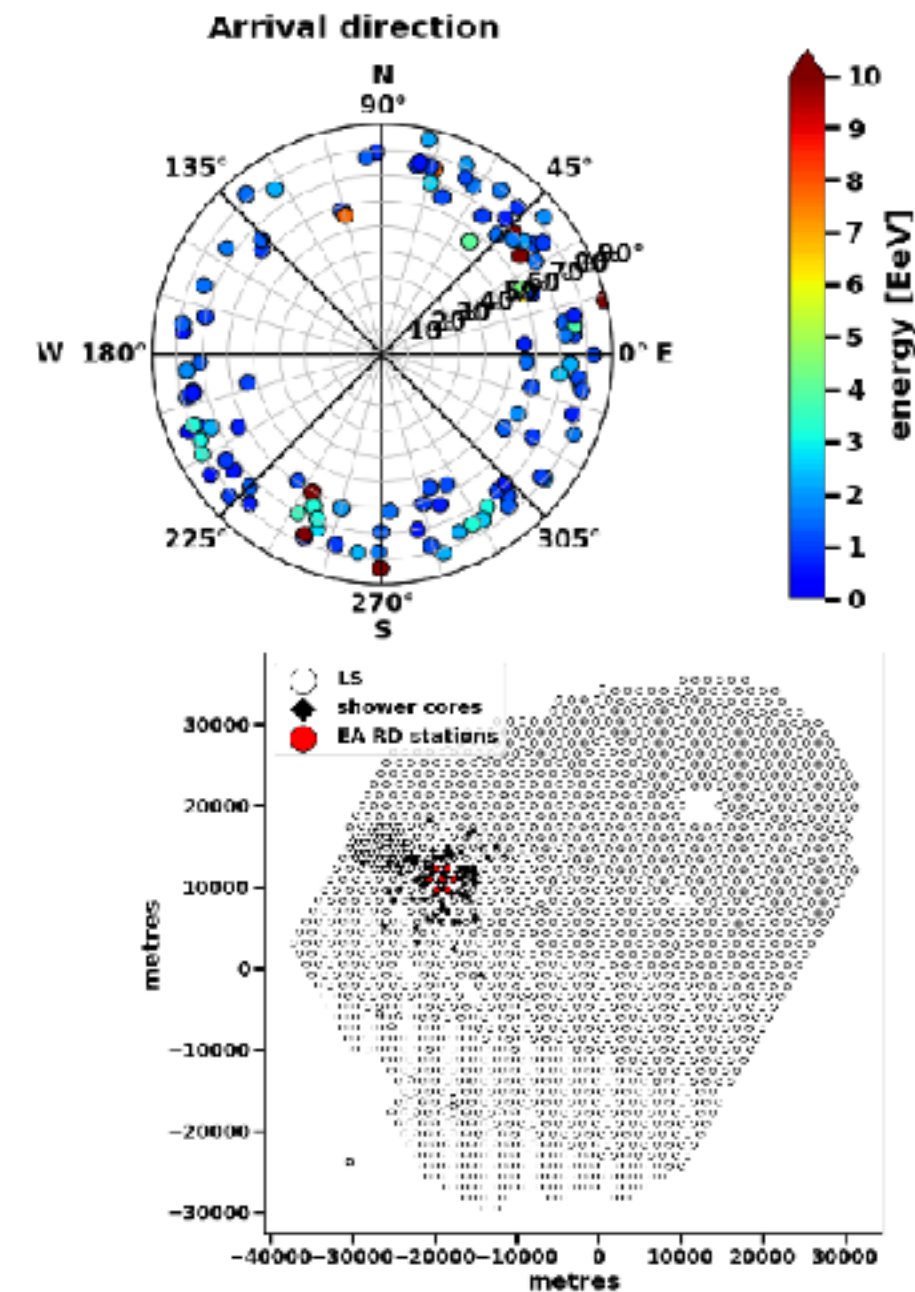
Measured noise & galactic signal in the EW loop



- EW calibration constant:  $1.03 \pm 9.6\% \pm 2\%$
- NS calibration constant:  $0.96 \pm 9.7\% \pm 2\%$
- Uncertainty caused by the Antenna model: max 1.5%
- For more details see this proceeding: <https://pos.sissa.it/395/>

# Air showers measured with engineering array

## Nice 3-fold event above $\lg(18.4/\text{eV})$



**Event 67742721 :-)**  
Time (UTC): 2022/4/19 18:14:47  
Time (GPS): 1334427305 s 414520000 ns  
Trigger: 4C1: 6T5 T5Has  
Stations: 18 (Acc: 3, Bad: 41)

**Global reconstruction (LDF + axis) (5)**  
 $E = (7.74 \pm 1.10) \times 10^{18} \text{ eV}$   
 $(\theta, \phi) = (75.4 \pm 0.1, 74.1 \pm 0.1) \text{ deg}$   
 $(x, y) = (-19.10 \pm 0.10, 9.82 \pm 0.27) \text{ km}$   
 $N19 = 1.4 \pm 0.2$   
radius =  $46.75 \pm 0.27 \text{ km}$

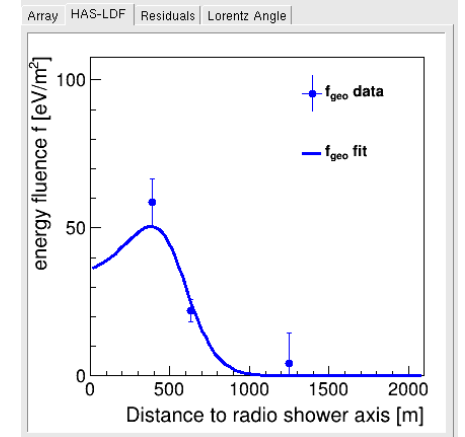
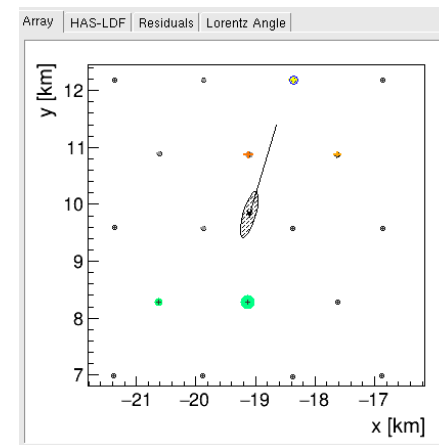
**Monitoring**  
average stations age: 15.7 yr  
T = 6.0°C; T (day) = 6.0°C

Event Info MC Info HAS LDF Info

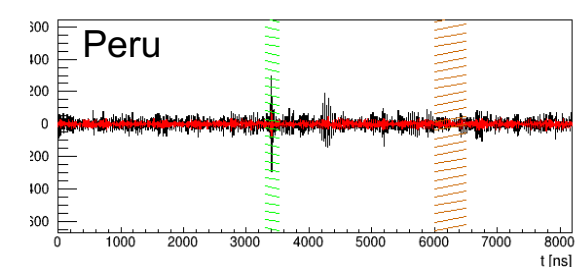
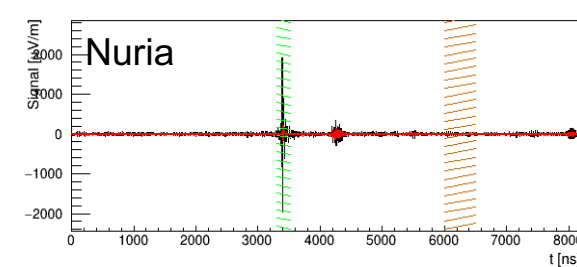
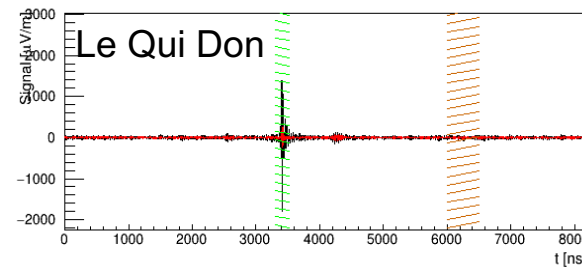
**Run: 0, Event: 67742721**  
GPS Time 1334427305 s 414520000 ns  
UTC Date: 2022/04/19 - 18:14:47  
Signal stations: 3 (3 with pulse)

**Wavefront: (sphere)**  
 $(\theta, \phi) = (76.49 \pm 3.3, 74.08 \pm 10.49) \text{ deg}$   
geomagnetic angle  $\alpha = 114.1^\circ$   
 $\chi^2 / \text{ndf} = (< 0.01) / 1$   
radius =  $30 \pm 334 \text{ km}$

**LDF: (HAS)**  
Emag energy =  $(3.96 \pm 0.43) \times 10^{18} \text{ eV}$   
Core (x, y) =  $(-19.10, 9.82) \text{ km}$

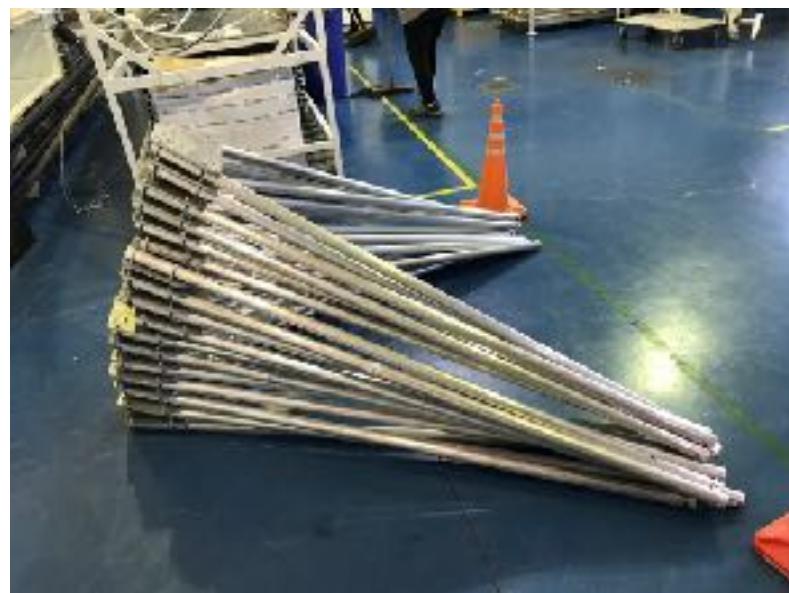


| Station List  | Options |
|---|---------|
| Le Qui Don: fluence = $2397.0 \pm 272.5 \text{ eV/m}^2$ , SNR = 3798.2, d = 583 m |         |
| Nuria Jr.: fluence = $2274.0 \pm 258.9 \text{ eV/m}^2$ , SNR = 3418.4, d = 375 m  |         |
| Peru: fluence = $120.8 \pm 19.1 \text{ eV/m}^2$ , SNR = 134.6, d = 1196 m         |         |
| Granada: fluence = $-0.5 \pm 7.3 \text{ eV/m}^2$ , SNR = 2.2, d = 1749 m          |         |
| Ruca Malen: fluence = $0.4 \pm 3.2 \text{ eV/m}^2$ , SNR = 1.8, d = 677 m         |         |
| Jaco: fluence = $-0.3 \pm 4.3 \text{ eV/m}^2$ , SNR = 1.8, d = 1448 m             |         |





# Mass production of RD started at Observatory





# Radio detection of extensive air showers

## Precision measurements of the properties of cosmic rays

The radio technique is now able to characterize cosmic rays:

-direction ✓

-energy ✓

-mass ✓

@100% duty cycle

—> application on largest scales at Pierre Auger observatory

